Uncertainty in Wind Energy Forecasting

Corinna Möhrlen

A Thesis Submitted in Partial Fulfillment
of the Requirements for the Degree of
Doctor of Philosophy
in
Civil & Environmental Engineering

May 2004

Contents

Summary

Wind energy is the energy source that contributes most to the renewable energy mix of European countries. While there are good wind resources throughout Europe, the intermittency of the wind represents a major problem for the deployment of wind energy into the electricity networks. To ensure grid security a Transmission System Operator needs today for each kilowatt of wind energy either an equal amount of spinning reserve or a forecasting system that can predict the amount of energy that will be produced from wind over a period of 1 to 48 hours. In the range from 5m/s to 15m/s a wind turbine's production increases with a power of three. For this reason, a Transmission System Operator requires an accuracy for wind speed forecasts of 1m/s in this wind speed range.

Forecasting wind energy with a numerical weather prediction model in this context builds the background of this work. The author's goal was to present a pragmatic solution to this specific problem in the "real world". This work therefore has to be seen in a technical context and hence does not provide nor intends to provide a general overview of the benefits and drawbacks of wind energy as a renewable energy source.

In the first part of this work the accuracy requirements of the energy sector for wind speed predictions from numerical weather prediction models are described and analysed. A unique set of numerical experiments has been carried out in collaboration with the Danish Meteorological Institute to investigate the forecast quality of an operational numerical weather prediction model for this purpose.

The results of this investigation revealed that the accuracy requirements for wind speed

and wind power forecasts from today's numerical weather prediction models can only be met at certain times. This means that the uncertainty of the forecast quality becomes a parameter that is as important as the wind speed and wind power itself. To quantify the uncertainty of a forecast valid for tomorrow requires an ensemble of forecasts.

In the second part of this work such an ensemble of forecasts was designed and verified for its ability to quantify the forecast error. This was accomplished by correlating the measured error and the forecasted uncertainty on area integrated wind speed and wind power in Denmark and Ireland. A correlation of 93% was achieved in these areas.

This method cannot solve the accuracy requirements of the energy sector. By knowing the uncertainty of the forecasts, the focus can however be put on the accuracy requirements at times when it is possible to accurately predict the weather. Thus, this result presents a major step forward in making wind energy a compatible energy source in the future.

Acknowledgements

This work is a result of my research activities in the Sustainable Energy Research Group, Department of Civil & Environmental Engineering, National University of Ireland, Cork.

I would like to thank all of those that contibuted to this work. Thanks to my supervisors (Dr. Eamon McKeogh, UCC and Jess U. Jørgensen, DMI) and examiners (Prof. Philip O'Kane, UCC and Prof. Dara Entekhabi, MIT) for their input to this work.

Thanks to the SERG group and many other colleagues around UCC for good discussions and technical support.

Thanks to the people in the DMI-FM section at the Danish Meteorological Institute for providing the DMI-Hirlam system, data for the *Irish Study* and for hosting me several times throughout this project. Special thanks to Jess Jørgensen, Kai Sattler, Claus Petersen, Bent Hansen and Maryanne Kmit for their support and many discussions. Without Jess Jørgensen's technical and scientific support this work would not have been possible.

I would also like to thank Kilronan Windfarm ltd., South Western Services (SWS), Powergen UK plc., B9 Energy (O&M) Ltd., Saorgus Energy Ltd. for their support in supplying wind farm data.

Thanks to the Higher Education authority for funding the *Irish Study* in the Programme for Research in Third level Institutions 2000-2003.

Thanks to Eltra a.m.b.a. for funding the Multi-Scheme Project, especially to Gitte Agersbæk, Peter Børre Eriksen, Poul Mortensen and Henning Parbo.

Chapter 1

Introduction

Forecasting becomes a requirement for a Transmission System Operator, if wind energy penetration increases above a threshold value. The magnitude of this threshold value depends on a number of factors such as the weather pattern, size and connectivity of the electrical grid, the start up time of the current power plants, the geographical dispersion of the turbines and the amount of alternative energy sources (e.g. hydro energy) available to balance the changes in wind power instantly. The main reason for this requirement is the intermittent nature of wind. Therefore, it is most likely that wind energy will not continue to contribute to reduce the CO_2 emissions in the future without forecasting. The major alternatives to wind energy forecasting are backup storage capacity and a strong interconnectivity between the electrical grids. Both alternatives are associated with technical and economical restrictions, which can be barriers to the installation of larger amounts of wind energy. Forecasting can therefore be considered as a more efficient way to increase the wind energy penetration.

On a global map of electricity grids for the year 2003 showing the installed wind energy relative to the energy consumption on the grid, the western part of Denmark catches attention. The energy production from wind occasionally exceeds the consumption in this area. It is the country with world wide the highest percentage of wind power in terms of installed wind power capacity relative to consumption in the electrical grid. It was also in the western part of Denmark where wind power was recovered in the 1970ies oil crisis and the first modern turbine was developed. A period of 25 years

with strong subsistence from the state for constructing and installing wind turbines has generated a landscape filled with wind turbines. The high concentration of wind power has caused many problems for the electrical grid operator. Nevertheless, the political environment has collectively supported wind power independent of all complains from the local transmission system operator. The result today is that the Danish electrical grid contains 22% of wind power, which is more than twice the target set by the European Union for the year 2010 (Commission of the European Countries, 2000). This area has therefore been chosen as the benchmark area for my theory on how wind energy can be handled in the future.

From a forecasting point of view, the Danish area does not seem to be problematic. The country is very homogeneous, surrounded by other countries and the turbines are geographically dispersed. Ireland was chosen as the second demonstration site. The purpose was to study the impact of inhomogeneous and complex terrain, and also the difference between turbines being placed in wind farms and clusters of wind farms rather than individually. Together the Irish and Danish demonstration sites will hence cover many problems associated with the penetration of wind power. The prediction of offshore wind power is not within the scope of this thesis. Nevertheless, most of the work presented here will also be valid for offshore wind energy.

In the current wind energy forecasting system for the West of Denmark, there are errors in the prediction of wind power on a daily basis (Jackson, 2003). These errors result in surpluses or deficits of electrical power. Surpluses are in the Danish case balanced by supplying electricity to water pumps in Norway, which pump water back into water reservoirs. Because hydro energy is an almost reversible source of energy, it is very suitable for balancing prediction errors, which changes rapidly from surplus to deficit. Deficits of electrical power are balanced with any available energy source. Hydro energy is used to balance deficits, if it is unknown that a deficit occurs shortly before the electrical power is required. Without this option and the interconnectivity to Germany and Sweden, a major part of wind energy in Denmark could not be taken into the grid in a cost effective way. The only local alternative is to balance the prediction

errors with gas and coal fired plants. These plant's startup time is however too long to be a suitable energy source for creating balance on the grid. In other words, in absence of the Norwegian hydro stations and the interconnection to the German electrical grid, a considerable spinning reserve would be required to secure the electrical grid in West Denmark, because only a small number of turbines can be curtailed.

The development of wind energy is country dependent and the development structure seems to be a function of the wind resource, the political environment, the electrical grid and the market. This means that different strategies are required to solve forecasting in different countries. The split between electrical grid responsible parties and suppliers in the liberalised markets also increases the complexity of the problem.

A worst case scenario in the years to come is, if the political targets (e.g. the Kyoto protocols) are met without any reduction of CO_2 emissions. Such a worst case scenario occurs, if too much spinning reserves from *brown energy sources* (e.g. coal fired plants) are required to compensate for the unresolved problems regarding the intermittent nature of wind energy. Then the energy production from wind farms cannot be considered 100% CO_2 free any longer. In other words, the more backup capacity a system operator requires to secure the operation, the less environmentally friendly wind power plants become, regardless of their annual contribution.

In Western Denmark for example a prediction error of 1m/s with an average wind speed of 10m/s corresponds to approximately 320MW in power. This amount is almost the equivalent to the largest single fossil fuel power plant in the system of the Transmission System Operator ELTRA. In this context ELTRA claims (personal communication, 2001) that an increase in accuracy by 1% results in a gain or loss of DKK 2 million. Even though forecasting today reduces the balancing costs for wind energy, so far no prediction system can deal with the variability of wind such that an accuracy of 1m/s is achieved (Jackson, 2003, Knight, 2003).

To summarise, the goal of this work was to analyse the sources of errors in numerical weather prediction models and to find a pragmatic solution for a typical transmission system operator to reduce spinning reserve requirements for wind energy.

I will complete this general introduction by reporting, that there has been a political decision in the European Union (Commission of the European Countries, 2000) that 20% of renewable energy shall be installed by 2010, where the bulk shall come from wind energy. The purpose of this thesis is not to discuss, whether this decision is sensible and what environmental benefits there are, but to suggest a solution on how to deal with the required amount of wind power in a secure way.

The key result of my thesis is that the approach I introduce in this work is capable of predicting how reliable wind power is as an energy source in an electrical grid. This parameter can enhance the environmental value of wind power probably regardless of the amount of installed capacity. A second important parameter, which can be directly derived from my approach, is the risk for surpluses and deficits in electrical power due to deviations between predicted and actual weather that can become dangerous for the security of the electrical grid in the future. Knowledge of these risks can greatly enhance the safety on the operation of electrical grids.

Structure of the thesis

The introduction describes the purpose of wind energy forecasting for a transmission system operator. This is followed by a discussion on the requirements for a weather prediction system to increase the accuracy of wind speed forecasts.

Chapter 2 and 3 deal with the identification of the specific requirements to increase the accuracy of meteorological forecasts from numerical weather prediction models. A unique set of numerical experiments have been carried out in this context in collaboration with the Danish Meteorological Institute in Copenhagen, Denmark. The study focused on various different horizontal resolutions in the numerical weather prediction model. The results from this study are discussed and conclusions for the further development are drawn.

The first investigations on model resolution resulted in the development of a new method

to tackle the problems associated with forecasts errors of wind speeds from the meteorological centre's numerical models. A Multi-Scheme Ensemble Prediction System comprising 50 ensemble members was developed and tested over a 3 months period with particular focus on Denmark and Ireland for this purpose. The study was actively supported and sponsored by the Danish Transmission System Operator ELTRA. A detailed description of the system design, the configuration of the 50-member ensemble and the verification of this ensemble prediction system is presented in Chapter 4.

In Chapter 5 a selection of the most important results for wind power predictions from the Multi-Scheme Ensemble Prediction System project is presented. The emphasis in this chapter is on the specifically developed probability forecast products for wind energy: the uncertainty estimate generated from the ensemble and the mean of the ensemble.

In Chapter 6 the results of the two studies are summarised and conclusions are drawn.

A Glossary of meteorological terms is added in the Appendix F and aims to define the most important meteorological terms found in this work. It attempts to present definitions that might have a different meaning in other scientific areas and to prevent misunderstandings. It should be understandable to the non-meteorologist and a reference for the specialist.

1.1 State-of-the-art models to convert wind speed to wind power

State-of-the-art short-term forecasting of wind energy uses a chain of models to predict wind energy on a 48h-horizon. Existing model systems feed wind speed and direction from the local national meteorological offices' Numerical Weather Prediction (NWP) models into another model, which transforms wind speed to wind power based on either physical or statistical approaches. The localisation of the wind speed takes place either explicitly before or implicitly in the equations that produce the power output. In

most models a number of reference sites are used to compute the wind power, which is then up-scaled or extrapolated to the relevant area. There are several models on the market. The models can be classified either as dynamical, physical, statistical, or as hybrids of any of these. They all require similar input (e.g. wind speed, wind direction, temperature, pressure, density). They provide the same output (wind power) and contain the same limitations; none of the models can repair the errors of the numerical weather prediction model forecasts, which are used as input (e.g. Jackson, 2003).

An example of a physical flow model to convert wind to power including a correction model to count for shadowing effects in a wind park is *Predictor*, developed by Risø National Laboratory in Denmark (Landberg et al. 1999, 2000). This model also used MOS (model output statistics) on the output of the numerical weather prediction model.

An example of a statistical model using advanced time series analysis techniques to cover any systematic mismatch of the NWP model and the turbine measurements is *WPPT* (Madsen, 1995, 1996 and Nielsen et al., 1999 and 2000). Other models of this type use neural networks and adaptive statistics together with observations. Two examples are ISET's prediction model in Germany (Rohrig, 2000) or MORE CARE, a model developed under a 5th Framework project (Hatziargyriou, 2001).

The numerical weather prediction (NWP) models fall into the category of dynamical models. These models are computationally more demanding and mainly used for providing the input data to the physical, statistical or hybrid models. No other publication has been found until now of a NWP model where power predictions are produced inside the three dimensional numerical model than the author's own publications (Moehrlen et al., 2001, 2001a, 2002 and Jørgensen et al. 2001, 2002)

1.2 Core problem for current wind power models

The forecasts from the Met Centres are not tailored towards sufficient accurate forecasts of wind speeds near the surface and in the range of 6-15m/s. This range is most critical in the production of wind power, because it is the range, where a wind turbine's power

production increases or decreases with a power of three (Mengelkamp, 1988). The lack of accuracy, especially of surface winds from NWP models, has its background in the structure of these models. The worst errors are usually found near the surface, which is parameterised [1] in a NWP model. The errors from the met centre's NWP models has therefore been identified as the core problem for current wind power models in various proceedings of meetings and conferences of the wind energy community. Some examples are the IEA Meeting on Wind Forecasting (2000), EWEA conferences (Copenhagen (2001), Brussels (2001), Paris (2002) etc.), and other publications (Jackson, 2003, Knight, 2003, McGovern, 2003, Giebel, 2001, Landberg, 2000).

The errors from NWP models can be split into local errors and non-local errors. Local errors are constant over the prediction horizon and are mostly a result of the inaccurate surface representation in the model system. The accuracy of the model's surface representation depends mostly on the horizontal resolution of the NWP model and on the lowest surface level. The local error can be classified as the model's bias, and can be corrected with longterm statistics of the output paramters of the model (also known as *model output statistics* or MOS).

Non-local or meteorological errors have a meteorological origin and can be considered as the limits to predictability of the atmosphere. These can be due to deficiencies in the NWP system that result in a unrealistic error growth. An insufficient amount of observations that are available to adjust the initial model state before the prediction is carried out are also considered non-local errors. In fact, most of the NWP model's error sources are non-local (Haltinger, 1971). Thus, a local statistical or physical correction model cannot compensate in the wind power predictions for the wind speed errors used as input to such a model. It also cannot account for the error in the wind speed predictions from the NWP models.

From a meteorological point of view, the error sources in fact differ from day to day depending on the general flow pattern of the atmosphere. Figure 1.1 illustrates the daily error of a 24 hour wind speed forecast during one month. Forecasts with a small

[1] The specification of physical processes in a necessarily simplified manner (Physick, 1988).

error are marked with a dotted black circle and forecasts with a large error are marked with a grey circle. This illustration shows the variability of the forecast quality. It is important to note, that the mean error of the forecasts is relatively small, whereas the daily absolute error has a high variability, which can for example result in significant errors for a transmission system operator, if if lies within the range of 6-15m/s.

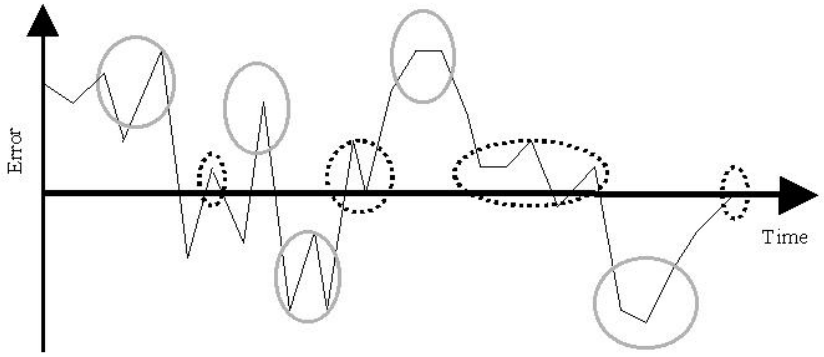

Figure 1.1: Illustration of the daily error of a 24 hour forecast during one month. The dotted circles are times where the model has a small error, whereas solid line circles denote times where the model error is high. The dotted circles are in contrast to meteorological interpretation in wind energy equally or more important than the solid circles, because of the increased accuracy requirements and the need to identify times where the forecasts can be trusted (ie.e low uncertainty).

In fact, the most significant errors on a daily basis are often a factor of 2 or 3 greater than the monthly averaged error. Phase errors in the prediction of low pressure systems and frontal systems on a synoptic scale contribute most to the total error as either over-predictions or under-predictions. The total error can therefore be reduced significantly, if the prediction quality of these phenomena can be improved. This is especially the case for wind energy predictions, because the synoptic scale weather in Western Europe mostly causes changes in the wind speed range, which has most impact on the power production of a typical wind turbine (6-15m/s). Thus, a small error of for example

parameter	Met Service (over land)	Met Service (over sea)	Transmission System Operators Requirement
Forecast Range	0-24h	0-24h	1-6h & 12-48h
Speed Accuracy	$5m/s$	$5m/s$	$1m/s$
Range of interest	$> 10m/s$	$> 13m/s$	$5 - 15m/s$
Direction Accuracy	$0.45°$	$0.45°$	$0.15°$
Turbulence	Gusts $> 20m/s$	-	$> 10m/s$
Target Area	1000 x 1000km	3000 x 3000km	300 x 300km
Local Effects	-	-	+
Observation Delay	105min	105min	-
Compute Time requ.	30min	30min	3h
Forecast Frequency	6h	6h	3h

Table 1.1: Comparison of Wind Specific Requirements of Met Services and Utilities

1 m/s in the predicted wind speed can cause an error of 20% of installed capacity in predicted wind power (Moehrlen, 2001a, Jackson, 2003).

Table 1.1 gives an overview of the differences between met centres deterministic systems and utilities requirements. The different requirements in meteorology and wind energy shown in the table demonstrate that an improvement of the quality of the forecasts for a meteorological centre means something else than for a utility.

The experiments in the *Irish Study* focused on the quality of forecasts seen from a transmission system operator's point of view and are therefore the first experiments of this kind.

1.3 Wind power computation

The computation of wind power is by tradition done by using a power curve from a turbine manufacturer on predicted wind speed. This is a simplification, which can be justified by the lack of accuracy of the predicted wind speed. A numerical weather prediction model provides other variables that may enhance the computation of wind power.

To move the power prediction inside a NWP system provides new opportunities to

compute the wind power more accurately. Especially on the very short range prediction horizon (1 to 6 hours ahead), where the NWP model has the highest degree of accuracy, the need for detailed power prediction with respect to grid security demands highest quality (Jackson, 2003). On longer time horizons (12h-60h) statistical corrections are required to reduce the non-local errors. In that case, the advantage lies more in the flexibility of including second order parameters in the wind to power conversion such as wind shear, cloud water, turbulent kinetic energy, stability of the boundary layer.
The wind power conversion from wind speed to wind power in this work has taken place inside the NWP model. A simplified power computation module was implemented into the numerical model in collaboration with staff from the Danish Meteorological Institute. Parameters such as air density or vertical wind shear and the turbulence intensity have not been taken into account within this work. Nevertheless, the power computation were moved into the NWP model such that the details of the model state are available in a time resolution of a few minutes. This strategy automatically eliminates one of the deficiencies of using a mean wind speed in the power computation. Because of the complex dependency between wind speed and wind power, it is during windy, unstable weather conditions important to operate with very short time averages of the wind speed (Moehrlen, 2001a). Accumulating wind power using a short time step for the wind speed will represent the actual power better than averaging the wind speed over a number of time steps before using it as input to the power curve. This effect was already discussed by Mengelkamp in 1988, who also concluded that the time averaging of the wind speed can affect the power computation significantly.

1.4 The prediction time horizon

For an transmission system operator it is important to separate the power prediction into three categories (Jackson, 2003, Knight, 2003, McGovern, 2003).

1. The *ultra short range prediction* (0-9 hours ahead). This forecast range is often also referred as *nowcasting* and is in the present context important for the security

of the electricity grid and for electricity trading on the spot-market. The NWP forecast error is relatively low in this forecast range and most effort should be put into computing the wind power as accurately as possible.

2. The *short range prediction* (10-48 hours ahead). This forecast range is required, if wind energy should become a substitute for other energy sources, for example coal or gas. The accuracy requirements are not as high as for the ultra short range and are dependent on the electricity trading mechanisms. Forecasts on this time horizon are dominated by NWP forecast errors in the wind speed that last over more than six hours. In this case it is important to either reduce this error or alternatively predict this error.

3. The *medium range prediction* (3-5 days ahead). This forecast horizon is important in periods of high wind speeds, where wind energy can replace brown energy sources (e.g. coal fired plants). In fact this forecast horizon is particular important at days, where the prediction indicates a sustainable wind power contribution for the following 2-3 days. If this forecasting horizon can be further improved to for example another 2 days, it would be possible to replace more and more brown energy sources with wind energy. Another example of the importance of this forecasting horizon are maintenance related works on the electricity grids or wind turbines. In both cases the possibility of planing a few days ahead has economic value. Electricity grid repairs or maintenance should not take place in times with a lot of incoming wind power. Wind park erections, maintenance or repairs also require calm conditions (less than 10m/s).

A major problem for utilities at present is that different meteorological data sources are required to cover all forecast ranges (Jackson, 2003, Knight, 2003, McGovern, 2003).
In this work two of the described time horizons have been researched thoroughly. The third time horizon (3-5 days) is going beyond the scope of this thesis. Note that at present only large centres such as the European Center for Medium Range Weather

Forecasting (ECMWF) in the United Kingdom or the National Centre for Environmental Prediction (NCEP) in the United States of America cover this time horizon in operational mode.

The time horizons that have been researched in this work can be summarised as follows:

1. The *ultra short range* is researched by configuring the NWP model HIRLAM in high resolution over a small area that covers the thesis' target areas (Ireland and Denmark).

2. The *short range* is under investigation by creating an ensemble of NWP models in coarser resolution. These ensemble forecasts cover a large area such that the largest errors in the wind power predictions become predictable. The goal is to configure an ensemble of forecasts such that a high correlation between predicted uncertainty and actual forecast error is achieved

1.5 The motivation behind this work

The focus of the present work was to verify a NWP model system and adopt the system in such a way that the described problems or part of the problems can be solved. The focus when adapting the NWP model DMI-HIRLAM from the Danish Meteorological Institute was on the requirements of end-users that are dealing with wind energy such as the transmission system operator ELTRA. This adaptation includes the configuration of the model system for the specified purpose and the development and implementation of a wind power module inside the NWP model.

The motivation behind this work was to create a sustainable framework by providing the ground work for an actual implementation of a NWP model that predicts wind power together with all standard meteorological parameters for the wind energy community.

Chapter 2

Resolution Experiments with a Numerical Weather Prediction Model

The following describes the work performed with a numerical weather prediction model, which aimed at providing a better understanding of the requirements to such models when used to forecast wind energy production. The modelling area was centred around the British Isles and in particular Ireland. The project is therefore referred to as the *Irish Study* in the following. Many recently developed approaches to forecast power production from wind experienced major limitations with respect to accuracy of the predictions as a result of imperfect input wind speeds from the met centre's NWP models (e.g. Madsen, 1996, Nielsen, 1999, Mönnich, 2000, Landberg, 2000).

This prompted an investigation of the sources of errors from these models. Additionally, it was intended to find solutions to minimise these errors and to find appropriate ways of handling the requirements of wind energy in NWP models in the future. This is the background of the experimental campaign, which was technically supported by the Danish Meteorological Institute (DMI).

Using a NWP model for wind energy forecasting demands high accuracy of the surface parameters. Therefore, the demands for the precision of land cover data and small grid spacing in the domain is also high. On the other hand, the size of the domain must be

large enough to include not only all terrain features, which may influence the meso-scale flow, but also the large scale weather. This was the reason for testing a NWP model in different horizontal resolutions.

2.1 Experiments in various horizontal Resolutions

Various resolutions were investigated in this experimental campaign with respect to wind power predictions and the need for more accurate land cover data when modelling in complex terrain and in high resolution. A selection of five wind farms in Ireland was chosen for the evaluation of the experiments. As mentioned above, these preliminary experiments aimed to address the deficiencies of existing models.

Apart from the evaluation and verification of the NWP models' capability to model wind speeds, the experiments were also used to develop wind power computations inside the numerical model.

Throughout the experiments, it was found that there is an advantage in having the power calculations inside the numerical model. Major physical properties like direction dependent roughness, actual air density, the stratification of the atmospheric boundary layer, momentum fluxes, wind shear, gusts and turbulence can then also be used in the calculations.

2.2 Model Description

The hydrostatic NWP model Hirlam from the Danish Meteorological Institute (DMI) was used in this study. The Hirlam System was developed by the Hirlam Project group, a co-operative Project of the national weather services in Denmark, Finland, Iceland, Ireland, the Netherlands, Norway, Spain and Sweden (Machenhauer, 1988, Gustafsson, 1993, Källén, 1996). Hirlam stands for HIgh resolution Limited Area Model. The HIRLAM project started in 1983, when the model system was first programmed. The first operational implementation of the model was run in the Finish Meteorological

Institute (FNMI) in 1989.
A so-called reference system has been maintained in the European Centre for Medium range Weather Forecasting (ECMWF) ever since, although most of the 8 countries involved have a modified version of the reference system in their daily operation. This is due to differences in computer facilities and technical strategies within the met centres. There are more than fifty scientists involved in improving and maintaining the Hirlam system.
A brief description of the implementation of the DMI-HIRLAM system and its configuration is given hereafter. A more detailed description of the model system can be found in Jørgensen (1999) and Saas et al. (2000).

2.2.1 Model Equations

Atmospheric models used in meteorology are based on the equations of fluid mechanics discretized in space and time, with geophysical parameters appropriate to the Earth's atmosphere. These equations are conservation laws applied to individual parcels of air. In the DMI-HIRLAM model, these so called *primitive equations* (PE) are used to describe the hydrodynamical flow on a sphere under the assumptions that vertical motion is much smaller than horizontal motion (hydrostasis) and that the fluid layer depth is small compared to the radius of the sphere.
The precise form of the primitive equations depends on:

1. *the vertical coordinate system* The hydrostatic approximation allows transformation of the primitive equations to alternative vertical coordinates, such as pressure, normalised pressure, normalised height, potential temperature or combinations of these. This transformation is used to make the numerical implementation of the equations more accurate.

2. *the horizontal representation* The equations of motion involve many partial derivatives in space. Partial derivatives of wave fields are used in spectral models and

can be calculated exactly, or they can be calculated by means of a finite difference approach or finite element approach, which is used in grid models.

3. *the formulation of the advection process* The numerical description of the advection process is split into two branches: the Eulerian and the Semi-Lagrangian.

When the primitive equations are used in numerical weather prediction models, the equations are of prognostic character and describe the evolution of the wind components u and v , temperature T, surface pressure p_s and humidity q over time. The solution of these equations contain however some approximations. These are:

- gravity is constant
- the Earth is a sphere and curvature terms are neglected
- the vertical Coriolis force is neglected
- the vertical accelerations are ignored in the vertical momentum equation (hydrostatic approximation)

In general the primitive equations describe for example how the momentum of an air parcel changes due to pressure gradients and the Coriolis force. They also describe vertical movement and changes in surface pressure of an air parcel by keeping the mass conserved. The temperature changes of an air parcel by adiabatic cooling or warming due to vertical displacement is also featured. Processes and effects of turbulent transport and drag, gravity wave breaking, condensation, evaporation and radiative effects are also included in these equations. The moisture of an air parcel is assumed to be constant except for losses or gains from precipitation, evaporation and condensation from and off the continents, oceans and clouds. To solve the primitive equations, some diagnostic equations are required. These are for example:

- The Ideal Gas Law

$$p = \rho RT \tag{2.1}$$

where p is pressure in (Pa), ρ is the density in (kg/m^3), R is the universal gas constant (287 J/kg K) and T is the temperature in (K).

and

- The Hydrostatic Equation

$$\frac{\partial \phi}{\partial p} = \frac{-RT}{p} \tag{2.2}$$

where p is pressure, ϕ is the geopotential, R is the universal gas constant, T is the temperature.

The ideal gas law describes the relationship between pressure, density and temperature. The hydrostatic equation describes the relationship between the density of air and the changes of pressure with height and states that whenever there is no vertical motion, the difference in pressure (∂p) between two levels (∂Z) is caused by the weight of the layer of the air. It is used as a simplification of the complete form of the vertical equation of motion (the non-hydrostatic equation). It assumes that the vertical acceleration in the non-hydrostatic equation is negligible.

The complicated discrete form of the model equations used in DMI-HIRLAM are described in Saas et al. (2000). More in depth descriptions and general derivations of the primitive equations (PE) can be found for example in Lorenz (1960), Haltiner (1971), Physick (1988), Krishnamurti (1996) or White (2000).

2.2.2 Model Grid

The vertical resolution in the model is irregularly divided into a specified number of levels. In this study 32 levels were used. The computational cost is dependent on the model's horizontal resolution, but also it's vertical coordinate system. This number of levels was chosen, because 32 levels are computationally relatively efficient without compromising much on the number of levels near the surface. The distance between these levels is lowest in the Planetary Boundary Layer (PBL) and highest in the Stratosphere (approx. 10km to 50km) and lower Mesosphere (approx. 50km to 85km). The finer resolution in the boundary layer is especially needed to parameterise turbulent processes. The pressure and geopotential are computed in the middle points of the levels, the so called *half levels*, to satisfy the conservation law at the *full* levels.

For example, when computing the temperature of an air parcel in a model level, the pressure above and below that air parcel needs to be known. Therefore, some model variables are computed at the *full levels* and others at the *half levels*. The discrete version of the primitive equation is developed such that pressure, geopotential and vertical advection terms are defined at half levels and the remaining variables only on the full levels. The vertical coordinate Equation 2.3 defines the pressure on the discrete levels. These *half level coordinate surfaces* for the pressure computations are computed as:

$$p_{k+\frac{1}{2}} = A_{k+\frac{1}{2}} + B_{k+\frac{1}{2}} \cdot p_s \tag{2.3}$$

where $A_{k+\frac{1}{2}}$ and $B_{k+\frac{1}{2}}$ are predefined coefficients, k is the number of levels (1...N). $B_{k+\frac{1}{2}} = 0$ at the uppermost levels (pressure coordinate surfaces) and $A_{k+\frac{1}{2}} = 0$ near the surface (terrain following coordinates) (Källén, 1996, Saas et al. 2000).

Table 2.1 shows the vertical coordinate surfaces for geopotential and pressure and includes the coefficients A and B at *half levels* and *full levels* for the model configuration used in this study. The values for A and B at the *full levels* are linearly interpolated. The pressure is computed according to Equation 2.3.

The height above ground (geopotential) is calculated for each level by combining the ideal gas law (Equation 2.1) and the hydrostatic equation (Equation 2.2). Note, that these values are only valid for one specific surface pressure and one specific temperature profile. These values change when the pressure and temperature are updated throughout the forecast according to

$$\frac{\partial \phi}{\partial \eta} = -\frac{RT}{p \cdot \frac{\partial p}{\partial \eta}} \tag{2.4}$$

where ϕ is the geopotential height, R is the Universal Gas Constant, T is temperature.

level	$A_{k+1/2}$	$B_{k+1/2}$	A_k	B_k	$p_k[Pa]$	z[m]
32	0.000	0.997	0.000	0.998	101187.8	11.1
31	0.000	0.993	0.000	0.995	100864.7	37.3
30	0.000	0.989	0.000	0.991	100471.4	69.3
29	13.449	0.981	6.724	0.985	99867.2	118.8
28	29.207	0.972	21.328	0.977	99019.5	188.6
27	65.672	0.958	47.439	0.965	97885.9	283.1
26	109.381	0.942	87.526	0.950	96425.2	406.3
25	177.335	0.922	143.358	0.932	94624.2	560.9
24	259.195	0.898	218.265	0.910	92443.4	752.1
23	366.695	0.869	312.945	0.884	89895.1	981.4
22	495.699	0.837	431.197	0.853	86952.3	1254.4
21	650.567	0.801	573.133	0.819	83647.7	1572.2
20	834.681	0.762	742.624	0.781	79976.1	1940.4
19	1044.629	0.719	939.655	0.740	75984.3	2360.4
18	1290.792	0.672	1167.710	0.696	71694.4	2837.2
17	1563.592	0.624	1427.192	0.648	67160.1	3373.1
16	1877.765	0.573	1720.679	0.599	62431.8	3972.1
15	2222.023	0.521	2049.894	0.547	57561.9	4638.4
14	2609.347	0.469	2415.685	0.495	52622.8	5374.4
13	3036.083	0.415	2822.715	0.442	47658.4	6187.5
12	3500.043	0.363	3268.063	0.389	42750.4	7078.9
11	4024.616	0.310	3762.330	0.337	37929.6	8061.0
10	4560.539	0.260	4292.577	0.285	33268.9	9136.1
9	5200.480	0.210	4880.509	0.235	28785.6	10325.1
8	5762.078	0.165	5481.279	0.187	24525.7	11638.2
7	6504.598	0.118	6133.337	0.141	20497.6	13114.1
6	6847.548	0.079	6676.073	0.099	16708.3	14791.7
5	7436.982	0.039	7142.265	0.059	13166.5	16757.7
4	6512.910	0.017	6974.946	0.028	9841.0	19160.0
3	5253.873	0.000	5883.391	0.008	6754.7	22299.8
2	2500.000	0.000	3876.936	0.000	3876.9	27029.3
1	0.000	0.000	1250.000	0.000	1250.0	38130.3

Table 2.1: Example of a vertical coordinate table for the experiments in the *Irish Study*

The hydrostatic DMI-HIRLAM uses the general pressure based and terrain following vertical coordinate system, which is called $\eta(p, p_s)$ coordinate system, where p is pressure and p_s is surface pressure. The function η itself however is unknown, because there is no requirement for having explicit knowledge about η. Equation 2.4 is sufficient to

close the primitive equations, because it defines the vertical velocity in each layer once the surface pressure tendency is computed by vertical integration of the continuity equation. Note, that a terrain following vertical coordinate system is one with the lowest coordinate surfaces that follow the terrain.

For flow over complex terrain a vertical sigma-coordinate in which pressure is normalised by the surface pressure is often employed instead of general pressure coordinates (Physick, 1988). The sigma coordinate system defines the vertical position of a point in the atmosphere as a ratio of the pressure difference between that point and the top of the domain to that of the pressure difference between a fundamental base below the point and the top of the domain.

Both sigma and eta coordinate systems are pressure based and normalized and are easy to mathematically cast the governing equations of the atmosphere into a relatively simple form. The η models have however some advantages over the σ models:

- η models do not need to perform the vertical interpolations that are necessary to calculate the pressure gradient force (PGF) in sigma models (Mesinger and Janji, 1985). This reduces the error in PGF calculation and improves the forecast of wind and temperature and moisture changes in areas of steeply sloping terrain.

- Although the numerical formulation near the surface is more complex, the low-level convergence in areas of steep terrain are far more representative of real atmospheric conditions than in the simpler formulations in sigma models (Black 1994). The improved forecasts of low-level convergence result in better precipitation forecasts in these areas. The improved predictable flow detail compared to a comparable sigma model more than compensates for the slightly increased computer run time

- Compared with sigma models, eta models can often improve forecasts of cold air outbreaks, damming events, and leeside cyclogenesis For example, in cold-air damming events, the inversion in the real atmosphere above the cold air mass on the east side of a mountain are preserved almost exactly in an eta model.

Figure 2.1 shows the vertical structure of the model including these terrain following η levels from the surface and up to 850hPa. One dot denotes one grid point in the model. Figure 2.2 shows the vertical structure from 850hPa to the uppermost level at 10hPa. It can be seen in this plot that the η levels become flat relative to the underlying orography in the stratosphere (above 200HPa). The vertical scale of Figure 2.1 is only 1500m, whereas Figure 2.2 covers 25km of the models atmosphere. Therefore, the underlying orography on Figure 2.2 cannot be seen. The horizontal grid is a staggered Arakawa C grid, where the grid points are the mass points (T, q, p_s) and the velocity terms are moved northward (u) and eastward (v) (Mesinger (1978), Arakawa, 1972) .

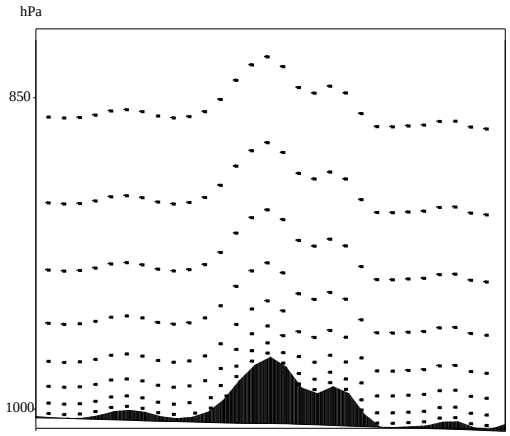

Figure 2.1: Vertical structure of the model: 1013hPa to 850hPa

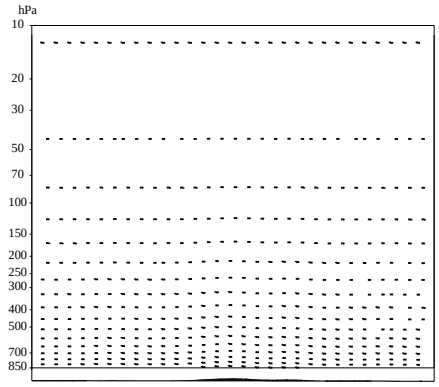

Figure 2.2: Vertical structure of the model: 850hPa to 10hPa

The coordinate system in the model is expanded to spherical coordinates, so that the surface of the earth corresponds to a coordinate surface. The spherical coordinate axes are (λ, θ), where λ is longitude, θ is latitude. The coordinates in the model grid are spherically rotated (Saas et al, 2000).

$$\delta X = a \cdot cos\theta \cdot \delta\lambda \tag{2.5}$$

and

$$\delta Y = a \cdot \delta\theta \tag{2.6}$$

The reason for using spherically rotated coordinates is to position the equator (latitude 0) into the centre of the model domain. With this approach an almost uniform resolution is achieved and the meridians do not converge too much.

The distance between the two points for which the model equations are solved define the resolution of the model grid. This grid distance should be chosen in such a way that topographic features that influence processes of one's interest are properly resolved. If this minimum grid distance is impractical because of computational expense, then all smaller scale processes need to be parameterised.

2.2.3 The Adiabatic and Diabatic Part of the Model

The adiabatic part of the model is computed in the full 3-dimensional model grid. For numerical stability the dynamical equations are solved by a semi-implicit time scheme in nearly all models. These semi-implicite time schemes handle the gravity wave terms with linearised equations. The semi-implicit time scheme allows for at least three times longer time stepping than a pure explicit time scheme. The reason is that in the explicit scheme the fastest perturbation propagates with the external gravity wave at approximately 300m/s. In the semi-implicit solution the advection term is the fastest explicitly handled propagation term with approximately 100m/s. Whereas the external and internal gravity waves are handled implicitly (e.g. Haltiner, (1980), Holton, (1979)). The time step in a semi-implicit scheme is

$$\Delta t = \frac{\Delta x}{v_c} \tag{2.7}$$

where v_c is the phase speed of the fastest propagating perturbation, which is approximately 100m/s for the implicit scheme and 300m/s in the explicit schemes. The Speed of the fastest winds in a model must therefore be less than or equal to the grid spacing divided by the time step. The three mathematicians named Courant, Friedrichs, and

Lewy discovered a criterion (CFL) that, if violated, leads to the *blowing up* of a finite-difference weather prediction model (Courant, R., 1928). Because of the CFL criterion, a modeller cannot arbitrarily choose a horizontal grid spacing without also taking into account the time step of the model.

The diabatic part of the model is computed in a 1-dimensional vertical column. It is described by using parameterisation schemes. The so-called "physics" comprises the processes of latent heat release (condensation, evaporation, sublimation and precipitation), radiation, sub-grid-scale transport of momentum, temperature and moisture variables down to small scales associated with turbulence. The DMI-Hirlam uses the CBR Turbulence Scheme for vertical diffusion (Cuxardt et al., 2000), the Soft TRAnsition COndensation (STRACO) scheme for convection and condensation (Saas, 1997) and an adopted Savijärvi-Radiation scheme (Saas et al. 1994). The surface fluxes (momentum, heat and moisture) are computed with a detailed boundary layer formulation using the Monin-Obukhov Similarity relationship in the traditional way (see e.g. Garratt, 1992).

2.2.4 Hydrostatic versus Non-Hydrostatic Modelling

Because of the approximations in the hydrostatic models, it is often believed that they are unsuitable for modelling in high spatial resolution. Because of the accuracy requirements (see Chapter 1), it is most likely that modelling wind parameters for wind energy purposes will require high resolution under certain circumstances. The following is a discussion on the use of a hydrostatic model with a horizontal grid resolution as small as 0.014° for that purpose.

Physick (1988) states that the hydrostatic assumption is applicable as long as the horizontal length scale of the phenomena modelled is greater than the density-scaled height of the atmosphere ($(\rho\partial\rho/\partial z)^{-1}$). In other words, the vertical acceleration is negligible compared to other terms in the non-hydrostatic equation. Because the density-scaled

height of the atmosphere (troposphere) is about 8km and the smallest resolvable features in a NWP model is $4\Delta x$, the hydrostatic assumption always holds for a horizontal grid distance Δx of approximately 2km (Physick,1988).

The physical parameterisation in the model is computed in a vertical column at each horizontal grid point. Each column is independent of the other columns. The horizontal coupling of the model variables takes place via the dynamical computations. The effective resolution is therefore a combination of $4\Delta x$ in the model's dynamical part and $1\Delta x$ in the model's physical part. In practise, this means that for example wind and temperature profiles are computed with a $1\Delta x$ resolution.

Higher resolution in the grid distance by neglecting the non-hydrostatic residual (total pressure minus hydrostatic pressure perturbations) can be justified under certain circumstances. The criterion for neglecting the non-hydrostatic residual then becomes a function of the horizontal grid distance, the large-scale stability, sub-grid scale heating and friction (Physick, 1988).

For example, when modelling sea breezes, it has been reported that there is little difference between hydrostatic and quasi non-hydrostatic simulations at horizontal resolutions of 1km (Pielke, 1972 and Orlanski, 1981) down to 300m (Fast and Takle, 1988). This is because a sea breeze is a slowly developing process without vertical acceleration.

2.2.5 Boundary Conditions

The upper, lower and lateral boundary conditions have to be specified in a hydrostatic model. Upper boundary conditions should be designed to minimise the reflection of vertical propagating waves. Therefore, the upper boundary should reach far higher than the area of interest. The DMI-Hirlam system is a limited area model and has the upper boundary at 10hPa, whereas in ECMWF's global model it is at 0.1hPa.

Lower boundary conditions depend strongly on the detail required at the surface. In general, the model surface is divided into land, sea and sea-ice in each grid point. This is done through a so-called land-sea mask. Grid points are defined through fractions of

land and sea/sea-ice or through fixed definitions of pure land or sea, e.g. if more than a certain percentage of the actual surface in the grid box is land it is defined as land and vice versa. The benefit of using fractions is that it resembles the reality more accurately. The disadvantage is that the distribution of land and sea within the grid-box is unknown and hence can lead to errors in the surface parameterisations. Unless the horizontal resolution is very high in order to keep the model's coast line zone narrow, the lowest model level should be at a height of at least 30m. Sea surface temperature is always kept constant throughout the forecast and updated from observed values. Roughness parameters, albedo, thermal properties of snow and ice, land cover and orography are described in the physiographic input data. Surface fluxes and humidity at the surface are parameterised.

Lateral boundary conditions to force the atmospheric forecast variables are supplied from a boundary generating model. Dependent on the application, this can be for example a global model such as that from the European Centre for Medium Range Weather Forecasts (ECMWF). For downscaling purposes however the boundary generating model can be any NWP model that covers a larger area than the area of interest. In this study the DMI-HIRLAM-E model, which covers the area of Europe was used and downscaled to an area covering Ireland and parts of the UK.

In addition, DMI's large scale model (DMI-HIRLAM-G) and ECMWF's model were used and downscaled to the same area. At the time of the experiments (2001), Hirlam-G was run operationally in 0.45° horizontal resolution and used lateral boundary values from ECMWF. Hirlam-E was run operationally with a horizontal resolution of 0.15° and used lateral boundary values from the G-model. The kernel of the models is the same. A boundary relaxation technique is also applied to interpolate the boundary generating models' variables to the limited area model variables linearly in time. The boundary update frequency depends on the output frequency of the boundary generating model. Met Centres usually have an update frequency of 6h. In this the boundary frequency varied from 1h to 6h.

2.2.6 Analysis Techniques

The forcing of the models in this study took place with 3 different analysis techniques. In the analysis the real state of the atmosphere is adjusted to the model space. In fact, the analysis is performed by comparing observations from the global network for atmospheric data (GTS) with a very short forecast. A correction to the 'first guess' field of the analysis model is then made from the difference of the observed variables and the forecasted variables. In this study forecasts from the following analysis techniques were used:

1. optimal interpolation (OI) - Hirlam-E - observations have effect on a local scale (circular around the observation)

2. 3-dimensional variational data assimilation (3DVAR) - Hirlam-G - a broader range of observations can be used and these have effect on the global state of the atmosphere in the 3 dimensional space

3. 4-dimensional variational data assimilation (4DVAR) - ECMWF - a larger time window of observations can be used that have effect on the global state of the atmosphere because of the fourth dimension being time

The optimal interpolation approach was developed in the mid 1970's as the first analysis technique in numerical weather prediction models (e.g. Lorenc, (1981), Källen (1996), Lönnberg and Shaw (1987)). This analysis technique was however restricted to conventional observations from synoptic stations, ship, aircraft and drifting buoys etc.. The 3DVAR was developed with the purpose of incorporating a broader range of observation types such as satellite data or radio sounding (e.g. Järvinen et al. (1997), Gustafsson et al. 2001). The 4DVAR was developed due to an increase in satellite data and a reduction of radio sounding networks in the late 80's. The 4DVAR uses a continuous feedback between observations and model, based on the so called Kalman-filter technique (e.g. Courtier et al. 1994, Bouttier et al. 1998, Rabier et al. 2000, Klinker et al., 2000, Mahfouf et al., 2000).

In ECMWF for example approximately 500.000 observational data pieces are considered for the analysis, but only a fraction of this is used (Persson, 2001). For example pressure observations are used between 50%-90% of availability, whereas satellite observations or scatteometer winds are used less than 15%. The selection of the relevance of the observations is the first part. After that, the analysis model undergoes a quality control and deselects those observations that seem erroneous according to its own state of the atmosphere. This quality control however also incorporates a danger, namely that the rejection or acceptance of certain data can also lead to errors in the initial conditions (i.e. the analysis), that influence the forecast very badly. In ECMWF's user guide (Persson,2000) this phenomena is described as "No analysis is perfect". In this documentation five reasons for a *bad* analysis are given:

1. No data over considerable times and areas
2. Bad data have been accepted
3. Good, but unrepresentative data have been accepted
4. Good data have been rejected
5. Good data have influenced the analysis in a wrong way

The last point is due to non-linear interactions in the analysis techniques that can lead to unexpected results. These reasons do not necessarily lead to a failure or a bad forecast, but they can. They can also explain why forecasts can fail to predict certain weather situations. This happens especially, if these phenomena are not included in the initial conditions of the model, because the relevant observational data have been rejected. A well known example of such a failure was the sailing competition *Fastnet Race* in 1979, where a hurricane with gale force 10 was not predicted. Five boats sank and seventeen competitors died in that storm. A more recent example was the 1999 French storm, where an observation from a ship in the Biscay was rejected that indicated the development of the hurricane. Both events were not forecasted timely.

It has been a discussion among meteorologist over years what the cause of the failed simulations of these hurricanes was (personal communication with DMI, 2001). The discussion also concentrated on the above mentioned 5 reasons, which suggests that it is obviously not a trivial task to find the sources of errors in a weather forecast.
In the case of Ireland, the most relevant observations are those from ships and aircraft over the Atlantic and synoptic stations and Radio-sounding stations in the model area. Because of the exposure to the Atlantic, modelling the Irish area accurately is very much dependent on a sparse net of observations over the Atlantic and can be subject to imperfect analysis much more than continental areas.
In this study the OI technique was used in the Hirlam-E model, the 3DVAR technique was used in the G-model and the 4DVAR technique was used in the ECMWF model. Note, that the OI technique used in the Hirlam-E model was based on year 2001 and is no longer used operationally in DMI.

2.3 Wind Power Prediction inside the NWP model

As mentioned in the beginning of this chapter, the experiments have also been used for the development of power computations inside the numerical model. In fact, a simplified power production module has been coupled to the NWP model used for this study.
The first version of the power prediction module is rather simple. It uses power curves from the turbine manufacturers or from available long-term databases to convert wind speed into power. The wind speed in the computations is the vertically interpolated wind speed at turbine height in the model level space. This means that the turbine height is consistent with the model's orography and errors that occur as a result of unrealistic representation of the model's orography are filtered away. This simplification has most effect in hilly terrain, where the model's orography can differ significantly from the real orography. In such cases, the real wind profile is effected by local effects that might not be present in the model system. Such effects can then lead to misinterpretation of

the results from the numerical model.

The assumption is that the turbine manufacturer's power curves are valid for a density of $1.2kg/m^3$. So far, wake effects are disregarded.

The module that computes energy output E in Joules of a wind turbine from wind speed u in a particular time period T can be described with

$$E = \int_0^T pwr(u)dt \tag{2.8}$$

where the power function $pwr(u)$ is a tabulated function E in unit [J/s].

The assumption is that there is no trivial analytical expression for $pwr(u)$. Hence, it is not possible to calculate its values at an arbitrary point. Instead a piecewise linear interpolation with equally spaced intervals is used. To smooth the curve between the velocities (u), a second piecewise linear interpolation is conducted.

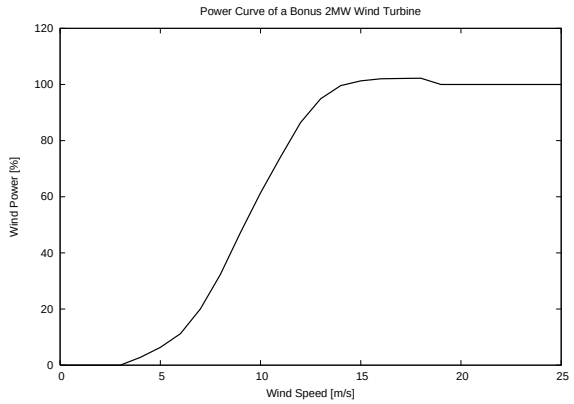

Figure 2.3: Power Curve of a 2MW Bonus Wind Turbine

The variability over time of the wind speed can be significant in hilly terrain for example, where wind speed changes of 3-15m/s can easily occur over one hour. This variability is taken into account when converting wind velocity to power output by also interpolating the inner term. The background for this averaging is to account for the asymmetry in power output due to increases and decreases in wind speed. This asymmetry can be

best described by a typical power curve as shown in Figure 2.3. If the wind speed increases from 3m/s to 5m/s, the power output increases by approximately 6%. If the wind speed however increases from 7m/s to 9m/s, the power increases by approximately 27%. In this example the power in the range from 7m/s to 12m/s increases with a factor of 4.5 compared to the range 0m/s to 7m/s.

The tabulated power function that was implemented into the model system can be written as:

$$pwr(u) = \frac{1}{2}[\widetilde{pwr}(u_{vel} + \Delta u_{vel}) + \widetilde{pwr}(u_{vel} - \Delta u_{vel})] \tag{2.9}$$

with $\widetilde{pwr}(u_{vel})$ being the power output values of the velocity term u_{vel} plus and minus Δu_{vel}. Δu_{vel} is a tunable parameter to account for turbulence and eddies on a larger scale. The power function is then defined as

$$\widetilde{pwr}(u_{vel} + \Delta u_{vel}) = c_+ \cdot pc_y(i_+ + 1) + (1.0 - c_+) \cdot pc_y(i_+) \tag{2.10}$$

and

$$\widetilde{pwr}(u_{vel} - \Delta u_{vel}) = c_- \cdot pc_y(i_- + 1) + (1.0 - c_-) \cdot pc_y(i_-) \tag{2.11}$$

where pc_y are the y-values in the power curve table, i_- and i_+ reflect the different power values involved in the interpolation of $\widetilde{pwr}(u_{vel} + \Delta u_{vel})$ and $\widetilde{pwr}(u_{vel} - \Delta u_{vel})$. The velocity u_{vel} is vertically interpolated over two levels and is defined as:

$$u_{vel} = c \cdot \rho_{k+1}\sqrt{u_{k+1}^2 + v_{k+1}^2} + (1.0 - c) \cdot \rho_k \cdot \sqrt{u_k^2 + v_k^2} \tag{2.12}$$

with ρ being the density at hub height, k and $(k+1)$ are the vertical levels in the model, c is the vertical interpolation coefficient.

$$c = \frac{z_{hubheight} - z_k}{z_{k+1} - z_k} \tag{2.13}$$

The coefficients c_- and c_+ are defined to

$$c_- = \frac{(u - \Delta u) - pc_x(i_-)}{pc_x(i_- + 1) - pc_x(i_-)} \tag{2.14}$$

$$c_+ = \frac{(u + \Delta u) - pc_x(i_+)}{pc_x(i_+ + 1) - pc_x(i_+)} \tag{2.15}$$

where pc_x is the x-value in the power curve table, i_- and i_+ are the indices of pc_x for $(u+\Delta u)$ and $(u-\Delta u)$, respectively. They can differ from each other and depend on the size of Δu_{vel}, which is solved implicit as a tunable parameter. A reasonable lower limit of Δu_{vel} is 0.5 m/s. This corresponds to the variations of wind on the time scale of one minute. In fact Δu_{vel} is related to the so-called gust factor, which can be parameterised from the wind speed and stability. Two effects increase the value of Δu_{vel}:

- length of the model's time stepping
- turbulence intensity

2.4 Diagram of the Model System

The following diagram shows the model system as it was constructed for the first part of the experiments.

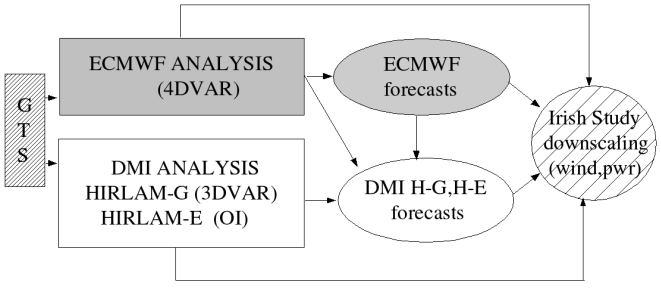

Figure 2.4: Diagram of the Model System used for the Experiments

The squares boxes in the diagram are the operational analysis systems in ECMWF and DMI, the elliptic boxes are the operational forecasting system in DMI and ECMWF. The circular box denotes the research experiments carried out in the Irish Study in delayed mode as hindcasts. Observations only entered the experiments via the operationally generated analysis fields from the squared boxes.

Chapter 3

The Quality of Wind Power Predictions from a NWP model

A set of experiments was designed to verify the quality of a typical numerical weather prediction model when used to predict wind power. The experiment campaign had to be split into categories and the design kept flexible, because this was the first time such experiments have been undertaken in this area.

The first experiments were conducted to investigate what kind of errors are most significant and on which time horizon are these errors found. The basis for an evaluation of forecasts is the size of the initial error and the growth rate of the forecast error. Figure 3.1 is an illustration of these two main error sources in a weather forecast. The y-axis shows the root mean square error (rms) and the x-axis shows the forecast length. The first type of error source in a weather forecast can be identified, if a forecast starts with a relative high root mean square error. This type of error reflects the model's bias and is called a *local error* and is illustrated by the hatched area. If the forecast starts with a relatively small root mean square error and increases linearly with the forecast length, the dominating error is referred to as a *non-local* error. In this case the smaller local error is illustrated with grey color. It can be seen that the error functions can cross each other, if the non-local error has a high growth rate.

The structure of the experiment campaign was therefore dependent on the outcome of initial experiments that focused on these two types of error sources. These experiments

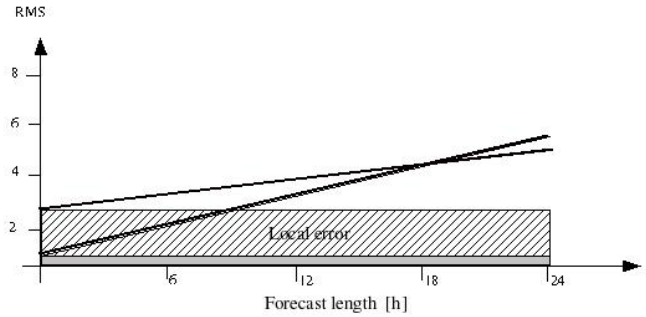

Figure 3.1: Schematic example of forecast error growth as a function of forecast length

were run with a forecast length of 24h and horizontal grid resolutions of 0.15° and 0.05°. The outcome from these initial runs was that both error sources had significant impact on the forecast quality. Not only a linear error growth rate with forecast length was observed, but also a forecast length independent error was observed.

3.1 Experiments to address the Local Error

The initial two experiments suggested that it is necessary that the first part of the experiments are constructed to address this *local error*. This set of experiments was named *Irish Study*, because the verification of the experiments took place with observational data from Irish wind farms and wind masts. The error growth of the *non-local error* was dealt with in a second part of the experiment campaign and is described in chapter 4 and 5.

Exp Name -	Model Resol. [deg]	Adv. scheme [deg]/m	Bnd forcing [h]	Bnd upd -	Model area -	FC length [h]	Time [days]	Integration period [2001]
e300	0.300	Euler	HIR-E	3	A	24	59	01.08-03.08
se300	0.300	SemiL	HIR-G	3	A	24	59	01.08-03.08
e150	0.150	Euler	HIR-E	3	A	24+6	201	10.01-04.19*
sg150	0.150	SemiL	HIR-G	3	A	24	59	01.08-03.08
e075	0.075	Euler	HIR-E	3	A	24	59	01.08-03.08
e050	0.050	Euler	HIR-E	3	A	24	201	10.01-04.19*
g050	0.050	Euler	HIR-G	3	A	24	59	01.08-03.08
sg050	0.050	SemiL	HIR-G	3	A	24	59	01.08-03.08
ec050	0.050	SemiL	ECMWF	6	A	24+6	59	01.08-03.08
e014	0.014	Euler	HIR-E	3	B	24	59	01.08-03.08
g014	0.014	Euler	HIR-G	3	B	24	59	01.08-03.08
sg014	0.014	SemiL	HIR-G	3	B	24	59	01.08-03.08
n014	0.05 to 0.014	Euler	HIR-G	3 to1	A toB	6	201	10.01-04.19*
g050p	0.050	Euler	HIR-G	3	A	6	201	10.01-04.19*
n150	0.150	Euler	HIR-E	3	C	6	379	07.01-07.15*

Table 3.1: List of Experiments conducted in the *Irish Study*. The name of the experiments is based on the used resolution (col. 2) and advection scheme (col. 3). Col. 4 describes the Boundary forcing model (HIR = HIRLAM). Boundary update (col. 6) was every 3h. forecast length (col 7) was 24h and 6h for e150 and ec050.

To address the *local error*, the focus of the experiments was on the ultra short range (1-6h). This meant that the *best possible forecast* was chosen to be evaluated and verified. The boundary update was every 3 hours (see Section 2.2.5). Only one case had boundary update every 6h. The reason for this was that the downscaling of the forecasts took place from ECMWF analysis data, which are only available at a time

resolution of 6h.

To summarise, the *Irish Study* comprised 15 model runs. The different model setups are shown in Table 3.1. The experiment names give an indication of the setup and resolution. That is, "e" stands for Eulerian dynamics, "s" stands for Semi-Lagrangian dynamics, "g" stands for Hirlam-G and "ec" stands for ECMWF, which indicate that the downscaling took place from either the Hirlam-G model or ECMWF analysis. The default was downscaling from Hirlam-E. Most of the experiments covered a two month period (January to March 2001). Three experiments however covered a 7 month period from October 2000 to April 2001 (e150, e050, n014). One experiment (n150) covered a 12 month period from July 2000 to June 2001. The experiments with longer periods than the three months are indicated with a " $*$ " after the date.

3.2 Model Areas

Figure 3.2 to Figure 3.4 show the model areas used in this study. All three areas are formulated in rotated latitude/longitude coordinates. The south pole is located near India at coordinate (80,0) in this model domain, because of the rotated coordinate system. The Area A model domain consisted of 79 longitudinal and 31 latitudinal grid points for the grid spacing of 0.30°. It consisted of 158 longitudinal and 62 latitudinal grid points for the grid spacing of 0.15°. It consisted of 474 longitudinal and 186 latitudinal grid points with the grid spacing of 0.05°.

The Area B model domain was only used for the very high resolution experiments and covers Ireland only. The model domain consisted of 302 longitudinal and 300 latitudinal grid points for the grid spacing of 0.014°.

Area C is covering Europe and Greenland and was only used for the one-year experiment n150 in 0.15° horizontal resolution. The area consists of 362 longitudinal grid points and 366 latitudinal grid points.

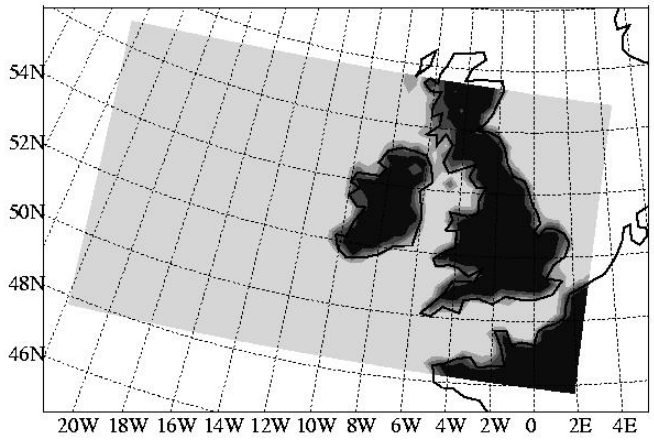

Figure 3.2: Model Area A covering Ireland and most of the UK.

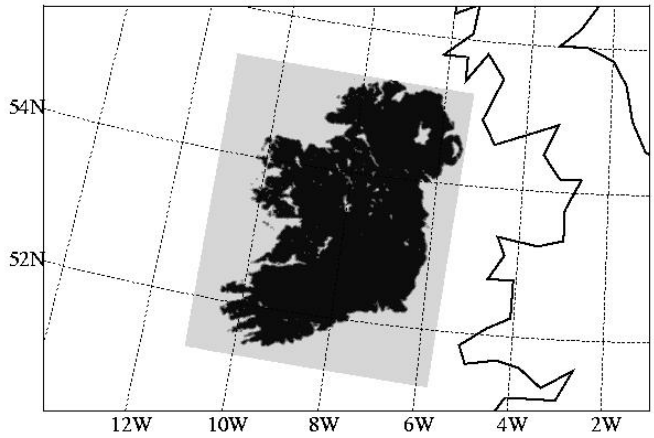

Figure 3.3: Model Area B for high resolution runs over Ireland

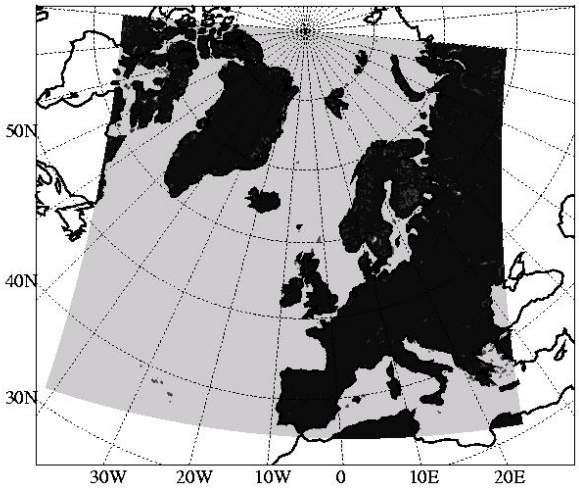

Figure 3.4: Model Area C

3.3 Model Configuration

In the previous section the experiment structure and some technical details of the run schedules of the 15 experiments was described. In this section details about the model configuration and input data is described and discussed. The experiments were all conducted with the same model (DMI-Hirlam). The configuration of the model varied in the choice of two different numerical formulations for solving the advection term (dynamic schemes) and in the horizontal resolution of the model grid.

3.3.1 Applied Dynamics Schemes in the Experiments

Two schemes have been applied in the model dynamics:

1. The Semi-implicit Eulerian scheme

2. The Semi-implicit Lagrangian scheme

For both schemes nested model runs of 0.3°, 0.15°, 0.05°, and 0.014° horizontal resolution have been undertaken and compared to observational data. A discussion and details of the methodology of these approaches will follow in the next section.

3.3.2 Vertical and Horizontal Resolution

All model runs in this study used 32 vertical levels. The approximate height of the relevant model levels (28,29,30,31) for the verification above ground is shown in Table 2.1. The different horizontal resolutions varied from grid spacing of 0.3°, 0.15°, 0.05°, and 0.014°. Details of these are shown in Table 3.1.

Case studies also included horizontal grid sizes of 0.075°, 0.028°, and 0.019°. In fact the case studies were applied mostly at extreme events (e.g. wind speeds reaching 25m/s) and had the purpose to better understand the effects of resolution in such cases. Because of their non-statistical character these experiments were not recorded explicitly. They are mentioned here, because they added value to the overall understanding of the problem, especially to the predictability of extreme events.

3.3.3 Surface Treatment

The earth's surface is a source and sink for the quantities momentum, heat and moisture. Any parameterisation of these quantities must simulate the transfer processes within the atmospheric boundary layer and the ground. In numerical weather prediction models, the turbulent fluxes are traditionally computed from drag formulae relating the surface fluxes to the mean states of the surface and the atmosphere at the observation height, which is typically the lowest model level (Saas, 2000).

Surface Fluxes and Roughness

In the HIRLAM model, the formulation of the surface fluxes follows the Monin Obukhov similarity theory, which is widely used in numerical weather prediction models. The

formulations can be found in Saas (2000), such that only the variable with most effect on the surface winds is discussed here.

The roughness lengths for heat, moisture and momentum are taken to be equal. According to the theory of the planetary boundary layer, the actual values of roughness depend strongly on the land surface type (Garratt, 1977). The effect of subgrid scale orography in the model is significant, such that the values of aerodynamic roughness to describe surface drag in a formulation based on roughness length often need to be adjusted.

The aerodynamic roughness length z_0 is a prognostic variable. For example over water, Charnock (1955) has hound, that z_0 is a function of friction velocity u_* and gravity:

$$z_0 = \frac{0.032 \cdot u_*^2}{g} \tag{3.1}$$

where u_* is the friction velocity and g is gravity and z_0 is assumed to be ¿ 0.0015cm. As mentioned above, the roughness length over land is therefore a specified variable. In the model, it remains constant throughout an integration, even though it is not necessarily constant throughout the domain (Physick, 1988). There are comprehensive lists of values for various surfaces, (e.g. Pielke, 1984). The friction velocity u_* is computed from the boundary layer parameterisation scheme. The sensitivity of the friction velocity to the accuracy of the surface winds is difficult to quantify when modelling with a NWP model. This is due to the complexity of the model and its governing equations, but also because of the horizontal grid size in the model, as this defines the ability of the model to resolve a given phenomenon. Even though the physical parameterisation is done in one dimensional columns for each grid box, it is difficult to estimate the impact of changes in the roughness fields. In the HIRLAM model, an algorithm is used, that makes the aerodynamic roughness proportional to the variance of subgrid scale orography. The actual values are then computed in the climate field generation (see next section on physiographic data). This ensures an optimisation of the modelling of subgrid scale phenomena according to the resolution of the model.

The sensitivity of different parameterisation schemes (as a whole) on the accuracy of the surface winds has been investigated and will be discussed in chapter 4 and chapter 5.

Physiographic data

The physiographic data used for describing the lower boundary originates from different sources. The orography is taken from the GTOPO30 data (1998) and land cover is based on GLCC (1997), version 2. In the model the aerodynamic roughness z_0 is aggregated from these databases. It is a combination of roughness due to sub grid orographic influence and vegetation roughness. The aggregation cycle creates monthly roughness fields, which are utilised with a smooth transition. Over Ireland, the original land cover data is mainly classified as a blend of fields and woods. This classification is acceptable when modelling with relatively coarse horizontal resolution, even though not optimal. For wind energy predictions however, a horizontal resolution of 0.15° is too coarse.
At a resolution of 0.15° or more, the non-separability of surface types results in large uncertainties in the aggregated roughness fields. It was therefore necessary to update the current land cover data with new local high-resolution land surface fields that do not contain blended classifications.
Additionally, the topography had to be adjusted, because the mountains were too smooth in the model space. Large differences of up to 150m were found at several wind farm locations. These differences can result in large local errors of the wind flow. The fact that most wind farms in Ireland are located at the top of mountains of 300-500m above sea level, made it therefore necessary to update the topography of these mountainous areas.

3.4 Observations

The simulations are verified against observations from 5 wind farms in Ireland. Two farms are located in Northern Ireland (BessyBell and Lendrum) and two are located in

the South West of Ireland (Milane and Tursillagh). Initial verification has been done with a site located in the North West of Ireland (Kilronan). The turbines at this site are placed on a mountain top at 352m above sea level, with lakes to the north and south. At all other sites hills and mountains at an elevation of approximately 300-400m above sea level surround the wind farms.

The vegetation at all sites is characterised by grassland with bushes and few trees.

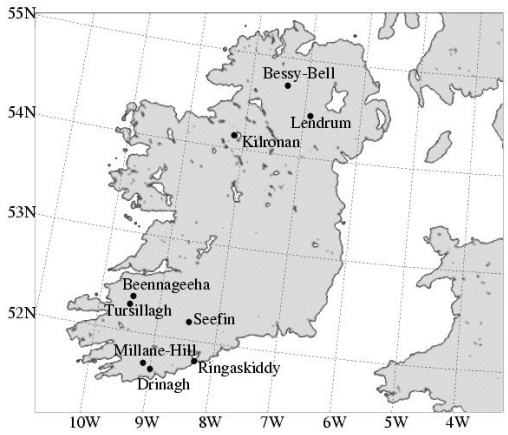

Figure 3.5: Verification Sites in Ireland

In Figure 3.5 the location of the wind farms is included together with other observational sites used later in this work. The model output that was verified and analysed in this study comprised wind speed, direction and wind power for the wind farm sites on 5 vertical levels, 4 times a day (0h, 6h, 12h, 18h) with output in half hourly intervals.

3.5 Observation Verification

The statistical tests used for objective analysis of the model runs versus observations were chosen from standard statistics. The following statistical parameter have been computed for wind speed and wind power for each wind farm over the period described in Table 3.1. The following only lists the parameters used in the statistical test. Details on sample size, location etc. are included in the tables in the result section of the study

(Section 3.6.3) .

* correlation between modelled and observed parameters (cor)

* variance (var) (also referred to as *standard deviation of the mean*)

* mean absolute error (mae)

* bias

* root mean square (rms)

* standard deviation (bias corrected) (stdev)

* minima and maxima (min, max)

The formulae of these tests can be found in Appendix A. A discussion of the verification strategy follows in the next section.

3.6 Methodology of the Applied Approaches

This section gives a more detailed look on the applied approaches and discusses the methodology and chosen strategy in the context of the work carried out.

3.6.1 Model Dynamics

The semi-implicit Eulerian scheme and semi-implicit Lagrangian scheme were used in the dynamics of the model. Details of the equations and numerical solutions of these approaches are well documented and are only discussed qualitatively in the context of their usage in this work. The Hirlam System's dynamics is described e.g. in Saas et al. (2000) or Källén (1996). General details and characteristics of these schemes can be found in e.g. Krishnamurti et al. (1996), Mathur (1970).

The fundamental difference between an Eulerian scheme and a Semi-Lagrangian scheme is that the Semi-Lagrangian dynamics is computed by interpolation, whereas the Eulerian scheme uses finite differencing techniques. In the Semi-Lagrangian scheme mass and wind field is used to compute where a parcel of air originated.

Because the wind flow is not constant and hence air parcels originate from irregular

grids, the Semi-Lagrangian scheme's space differencing is done by interpolation along trajectories of the past at each grid point. The time differencing in the Semi-Lagrangian scheme is a central differencing from $x_{i-\frac{1}{2}}$ to $x_{i+\frac{1}{2}}$. The interpolation in time and space causes a damping. Therefore, the Semi Lagrangian scheme is said to have an inherent damping.

In general, the Semi-Lagrangian scheme is more parameterised than the Eulerian scheme. It however incorporates a more economic dynamic scheme, especially in the advection. This is because it can use much longer time stepping in comparison to the Euler schemes. The accuracy of the scheme is determined by the time-step. Or in other words, the time step is only limited by the accuracy requirements.

The Eulerian scheme describes the flow in and out of a grid box. No matter how strong the flow is, only the nearest neighbours are taken into account in the equations of a particular grid box. The Eulerian scheme is therefore more suited for a local prediction than the Semi-Lagrangian scheme. It is however a problem that the derivatives are computed discrete and often in first order accuracy. Thus, a local gradient might not always be accurate in an Eulerian scheme.

On the other hand, if there is a strong rotation of the flow (e.g. in the centre of a low) the finite differences of an Eulerian scheme are solved much more accurately than in an interpolating scheme. In contrast to the Semi-Lagrangian Scheme, a parcel of air must not be advected further than one grid point in an Eulerian scheme. The Eulerian schemes are also restricted in their time stepping, due to considerations of computational stability set by the CFL criterion (see Section 2.2.3).

3.6.2 Orographic considerations

Figure 3.6 gives an overview of the differences in the model's surface representation. Cross sections at resolution of 0.30°, 0.15°, 0.05°, and 0.014° are displayed. The cross sections represent a longitudinal section of approximately 200km and are at latitude 53° North and from longitude 9.25° West to 6.50° West. One of the wind farms used

in the verification is located in that area. The differences in the 4 resolutions are quite dramatic.

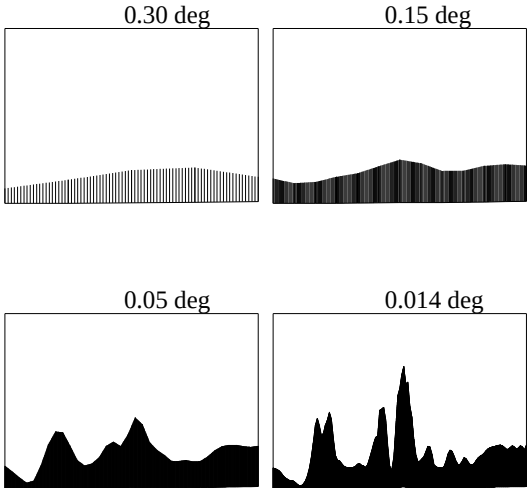

Figure 3.6: Cross sections at different horizontal resolutions of 0.30° (top left), 0.15° (top right), 0.05° (bottom left), 0.014° (bottom right). The area covered is in the North of Ireland and relates to an east-west line of approximately 200km at $53°N$ and $9.25°W$ to $6.50°W$. The vertical scale is approximately 530m above sea level for the 0.014°plot, 350m a.s.l for the 0.05°, 200m a.s.l for the 0.15° and 180m a.s.l. for the 0.30°.

Note, that the steepness of the orography in the lower right plot is slightly distorted, because the cross section covers around 143 grid points. Nevertheless, each mountain in the plot contains about 10 to 15 grid points of approximately 1.4km. Note, that in the high resolution 0.014°, the two highest peaks in the center of the plot merge to form one peak in the 0.05° resolution. In the 0.30° plot the peaks are also smoothed out, such that the mean peak is reshaped and found at a different location as in the high resolution plots. This shows that only the large scale weather is taken into account when modelling at such a resolution. Whereas already in the 0.15° model the mountains are at the correct location and the lack of orographic features can be partly solved by increasing the roughness and using model levels that reflect the height of interest.

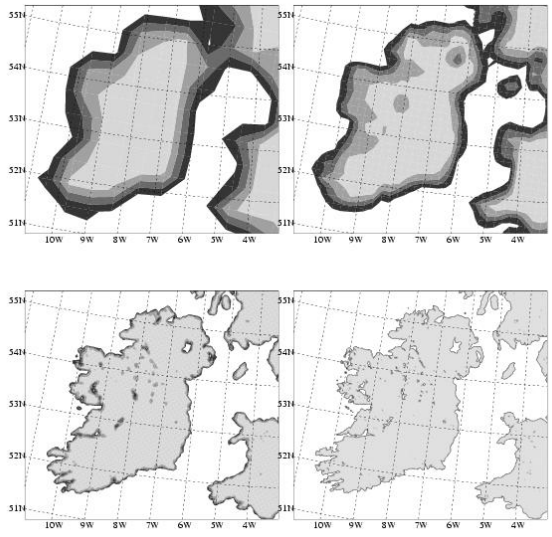

Figure 3.7: Fraction of Land and Sea in different Model Resolutions. Left upper plot is with a horizontal Resolution of 30km, right upper plot is at 15km, left lower plot is at 5km and right lower plot is at 1.4km

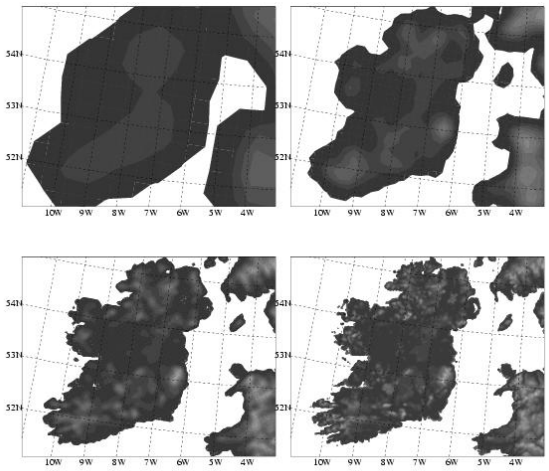

Figure 3.8: Surface Geopotential in different Model Resolutions. Left upper plot is with a horizontal Resolution of 30km, right upper plot is at 15km, left lower plot is at 5km and right lower plot is at 1.4km

Figure 3.7 and Figure 3.8 show fraction of land and sea and surface geopotential for Ireland in the same horizontal grid spacing as Figure 3.6. The left upper plot shows 0.30° ($30km$), the right upper plot shows 0.15° ($15km$), left lower plot shows 0.05° ($5km$), and the right lower plot shows 0.014° ($1.4km$).

Most significant is the difference between 15km and 5km, whereas the difference between 5km and 1.4km is not so significant. It is also worth noting that in the coarser resolutions (30km and 15km), Ireland is merged with Scotland in the North. The Shannon estuary in the Mid West of Ireland for example is also invisible in the coarse resolution. Lough Neagh in Northern Ireland only appears as partly land and sea in the 15km resolution and not at all in the 30km.

Naturally, the question arises whether it would not be beneficial to also use increased resolution in the climate files (physiographic data) when modelling in the coarse resolution and thereby resolving the surface features better.

The problem with such an approach is that a numerical model cannot resolve sharp vertical changes without causing instabilities for two reasons:

Physically: gradients that are build at the top of the mountain with their surrounding become very inaccurate because of the downhill slopes.

Numerically: two-grid waves cannot be solved with less than 2 grid points and in mountainous regions, the orography changes need to be proportional to the grid size.

A smaller grid spacing could therefore be necessary in areas with complex terrain and in mountainous regions. Especially, if the tendency in the future is to build larger wind farms, it is most important to be able to accurately capture these small scale phenomena in the short forecasts of 1 to 6h.

Since the orography in the coarse resolution cannot be increased over a certain limit, the future naturally points toward modelling in as high resolution as possible. The drawback of such an approach is the computational cost. In fact, the difference between running a model with 1.4km and 5km grid spacing is an increase in CPU-time by 20. If this is scaled for 15km and 5km grid spacing, the computational costs of modelling with 1.4km in comparison to 15km grids is therefore approximately 50 times higher.

The *Irish Study* therefore also aimed to study the requirements for reaching higher accuracy in the modelling of wind speed and to investigate the practical implications for achieving this goal.

3.6.3 Verification Strategy

The interpretation of model results is not trivial. While there are commonly used statistical tests, the interpretation of these is not always straight forward and in some

cases it can even lead to wrong conclusions. Especially, when applying test in an area where there is not much experience. Thus, in any evaluation process care has to be taken in the interpretation of the results. For example when evaluating different resolutions for a specific parameter such as wind speed, the high resolution simulations often do not show any improvement in the statistical tests (e.g. rms) relative to the coarser resolution. In particular peaks of high wind speed, which are significant for the power predictions often produce large errors in the high resolution statistics.

As an example, it was observed in Ireland that only very high resolution models can capture wind peaks of more than 20m/s. But exactly these peaks create large errors in the statistics, if the model has a phase error of one or more hours. This is because the model fails twice, once for not predicting it, when it occurred and once for predicting it when it did not occur.

Hence, the verification of the model output when using a NWP model for wind power prediction is an aspect in the forecasting process that requires the development of new strategies.

In meteorology there are two common methods of objective verification to analyse model output. This is:

1. observation verification
2. field verification

The advantage of field verification versus observation verification is that the local effects do not disturb the verification. Field verification can also take place in areas with few permanent observational sites such as over sea. That means, that computed fields from the initial state (analysis) are verified. The summation of areas also provides a more robust estimate of the forecast quality.

The benefit of field verification becomes clear if areas rather than single sites are of importance, which is often the case for utilities and system operators.

It has also been a tendency in the past that wind power models were "upscaled" from single sites to areas of interest. This happened for various reasons and the smoothing

effect of the upscaling from a finite number of points to an average over an area was one of them.

In the past this was a necessity, because the conversion of wind speed to wind power was handled outside the numerical weather prediction models. Even though the NWP models work in field space, wind speed and other parameters have been extracted for specific sites to be used for upscaling by linear models to larger areas. In such cases, verifying forecasts against observations becomes quite difficult, because the errors are not transparent.

Even though field verification has quite some advantages, traditional observation verification has been carried out in the *Irish Study*. Whereas wind speed and direction would have benefited from the field verification, the verification of wind power and the evaluation of error sources in the wind to power computations was not possible on a field basis, because the observational data at the Irish sites were point specific rather than area integrated.

For this reason the field verification is only suitable for areas, where a large amount of individual turbines are dispersed over areas, like the western part of Denmark or the northern part of Germany.

3.6.4 The Wind Power Prediction approach

The first two experiments in the *Irish Study* suggested to use high horizontal resolution and short boundary update frequency for the power predictions and thereby include as many small scale features as possible. Therefore, the experiments for testing the power predictions inside a NWP model were chosen on a horizontal grid of 0.014° and hourly boundary update frequency was achieved through a two level nested model system with 0.05° resolution in the outer grid. Wind speed, wind direction and wind power were written out at each time integration step. This setup was necessary to also evaluate the effect of using instantaneous values rather than averaged values over half an hour or one hour.

Other approaches (e.g. Mengelkamp,1988) usually compute the energy output with the velocity cubed, a frequency distribution and a power coefficient. These approaches are different to the above approach, where the velocity is interpolated horizontally over grid points, interpolated vertically over levels and then converted directly to energy output with a tabulated power curve. This output is for specific points, i.e. the horizontally interpolated wind velocity is at the wind farm location for which a power curve exists. However, the output does not have to be for single sites. It can also be used for areas/fields, because the energy output is computed from a tabulated function of the power curve. That means, if an area integrated power curve exists, the power computations can also be conducted with area integrated wind velocity. The idea behind it is that the power curve itself takes care of the non-linearity in the conversion from wind velocity to power.

Another advantage is that any improvement to the power curve, such as statistical corrections can easily be added without recoding the module. Efficiency in the computations is also ensured, because the *table lookup procedure* of the energy output by piecewise linear interpolation of the wind velocities is computational efficient and statistical improvements do not need to be computed inside the numerical model. Thus, the overhead for the power computations in the model is bearable.

3.6.5 Statistics for and in Power Curves

The idea of a simple power module inside the NWP model is to build a skeleton that can be complemented with other modules and improved over time and thereby offers a sustainable solution. The goal was to create a module that is simple and independent of observations or statistical corrections in the event that these are not available. It should also focus on a physical description wherever possible. In that way the power prediction tool becomes more flexible, easier to implement into other models and areas, easier to maintain and less dependent on local observations.

In fact, the basic idea should be followed by the development of a more sophisticated

description of the power curves. As described above, in this first approach, standard power curves from the manufacturers have been used. A better parameterisation of the power curves is to develop an efficiency parameterisation for the turbines, using the most relevant secondary effects on the power production such as wind shear, cloud water, turbulent kinetic energy, stability of the atmospheric boundary layer etc. The HONEYMOON project (A High resOlution Numerical wind EnergY Model for On- and Offshore using eNsemble predictions) is in fact following this idea in a 2 year project (2003 to 2005) funded by the EU fifth Framework Program (Contract No. ENK5-CT-2002-00606).

Measured power curves always show an uncertainty. This is because air density, turbulence, vertical wind shear, a wet rotor or a difference in the direction between the rotor and the wind affects the efficiency of the turbine. The mean wind speed is however the most important parameter for power predictions. The other parameters are also not more difficult to predict than the mean wind speed in the NWP model. In fact, density and vertical wind shear are modelled more accurately than wind speed in current NWP models. Thus, it is suggested to include these parameters in the future prediction of power, because they can explain up to 15% of the power prediction for stronger wind speeds.

Mean wind speed with density correction is in the future referred to as a primary effect and all remaining effects that have impact on the power production as secondary effects. Secondary effects are for example a sudden change in the wind direction due to a frontal passage. The preliminary studies of the observations of power and wind used in this work indicated that the effect is not negligible. In some cases the secondary effects also require a significantly higher time resolution than one hour. That is, a sudden change in the wind direction requires a time resolution of the order of minutes to allow for a proper parameterisation of the turbine efficiency. Inclusion of all the secondary effects with one hour NWP data time resolution is however impractical. The required time resolution for the primary effects is less critical than for the secondary effects. Therefore, the focus on in this study was on the primary effects.

3.6.6 Time resolution in the Wind Power Prediction

Theoretically high time resolution is a requirement for accuracy and consistency in the wind energy forecasting. From a prediction point of view, it also seems most beneficial to use high time resolution of the NWP data in the power prediction. This means that energy output is computed every time step and written out in accumulated form every hour. Then, these calculations can be used to take primary and secondary effects into account in the power production. Improvements in the NWP model system will in this way also improve the wind power computations.

Preliminary experiments showed that there is a significant difference between the power from hourly averaged wind speeds and instantaneous wind speeds for certain weather pattern. It was also visible that linear interpolation over one hour under certain weather patterns is a very poor approximation. Predicted primary power contribution can differ up to +/- 700KW for a 5000KW farm, although the predicted average and instantaneous wind speed differ only +/- 1 m/s (Moehrlen et al., 2001). If an accuracy of 10% or more is required, these effects have to be taken into account by computing instantaneous as well as averaged wind speed. Only then can the power predictions benefit from the high time resolution and further improvements in the NWP models.

3.6.7 Advantages of computing Wind Power inside the NWP model

The strategy of having the prediction of power inside a NWP model ensures a gradual improvement in time on both wind speed and energy output. Such a strategy provides the basis for longterm developments. The main advantages of this approach are:

- the possibility of modelling with high time resolution
- to parameterise the energy output and turbine efficiency on a physical basis
- to have a sustainable development and test-bed for wind power predictions

- improvements in the NWP model have also positive impact on the wind energy predictions

3.6.8 A Note on the Relationship of Synoptic Scale Forcing and Wind Power Generation

The challenge of this work was to determine an optimal combination of the required resolution to simulate local effects and the required model domain to capture large scale flow.

Another way of formulating this is that it is important to forecast atmospheric fronts accurately to reduce situations where a front arrives earlier than predicted. In such a case, an excess of electricity would occur that could have technical and market implications in the period from the actual arrival to the predicted arrival. A delayed arrival of a front (relative to the forecasts) would lead to a deficit of electricity, high prices for balancing power or even instabilities in the grid. Applied to areas like Ireland this means that the more directly a low hits an area, the narrower and sharper the fronts are, and the more sensitive the wind energy forecasts.

The goal was therefore to understand the sources of errors that cause phase errors, to find methods to solve the problems associated with the errors and possibly to reduce phase errors to an acceptable limit for wind energy. However, it should be pointed out that in conventional weather prediction an acceptance limit of phase errors of at least three hours exists in todays weather forecasting of more than 6h ahead. Whereas a phase error of thirty minutes in wind energy forecasting can already be problematic.

In Ireland for example, the governing forces of the wind are large scale pressure gradients due to highs and lows propagating eastward in the Atlantic. The Irish area is also characterised by a weak diurnal cycle. The background of the weak diurnal cycle is a combination of high average wind speed, a high coverage of grass with a high roughness length and the fact that Ireland is surrounded by deep water with a moderate temperature. As a consequence, related atmospheric phenomena, such as sea breezes,

also play a minor role. This does not mean that there are no local weather effects. On the contrary, the orography triggers meso-scale weather particularly under unstable conditions. But, even though these processes are important for wind energy in an area like Ireland, the effects are a consequence of large scale weather forcing. Therefore, both the large scale and small scale effects have to be simulated with the same model. This means that the model area must be large enough to simulate the large scale forces and also have sufficient resolution to incorporate the orography with a relatively high accuracy.

To summarise, an optimal prediction system should be able to forecast the development of lows and fronts on a scale of several thousand kilometres. On the other hand the required area grows with required forecast length and the resolution is a function of the complexity of the terrain. This combination makes forecasting difficult, computationally demanding and sets restrictions on the applicability of certain combinations.

3.7 Observation Verification at Wind Farms

In this section and the following sections, the results of the *Irish Study* are presented. In the first section one reference wind farm is verified and analysed. In the next section the results of four other wind farms are compared with those from the reference farm. The accuracy with which certain weather parameters can be predicted from a NWP model is strongly related to the large scale flow patterns and the terrain features that influence the flow. The complexity of the terrain, the model's resolution and domain size thus have direct influence on the accuracy of the forecasts. The results are for this reason interpreted in form of a discussion of the error sources in the prediction of wind velocity and wind power.

Exp	model level	mean [m/s]	variab [m/s]	max [m/s]	bias [m/s]	mae [m/s]	rms [m/s]	cor [m/s]	sample size
obs	-	8.07	3.94	25.07	-	-	-	-	1440
e300	29	8.27	3.79	24.00	-0.244	1.727	2.418	0.805	1422
s300	29	-	-	-	-	-	-	-	-
e150	29	8.12	4.01	23.00	-0.320	1.788	2.471	0.808	1416
g150	29	8.35	3.79	22.30	-0.040	1.623	2.319	0.820	1434
e075	30	8.26	4.05	22.10	-0.402	1.881	2.525	0.800	1422
e050	30	7.85	3.75	21.90	0.052	1.914	2.599	0.771	1434
ec050	30	8.16	3.88	20.70	-0.337	1.681	2.356	0.820	1326
g050	30	8.02	3.75	21.20	-0.091	1.602	2.267	0.828	1440
s050	30	7.52	3.87	22.50	0.383	2.207	3.132	0.682	2868
sg050	30	7.93	3.77	21.00	-0.066	1.616	2.286	0.824	1422
e014	30	8.29	4.16	22.30	-0.432	1.858	2.508	0.812	1417
g014	31	7.98	4.24	24.10	0.114	1.749	2.396	0.825	1434
sg014	30	8.61	3.91	23.40	-0.848	1.854	2.487	0.804	1248

Table 3.2: Wind Velocity Statistics from the forecasts started at 00h.

3.7.1 Verification of Wind Speed at a Reference Wind Farm

The verification focused first on the detailed verification of wind velocity for one reference wind farm. The statistics comprised 24-hour forecasts started every 6 hours. Thus, there are always four forecasts valid for any fixed point in time.

In Ireland most of the wind farms are located near the West coast or in hilly regions of 300m to 600m above sea level. Due to the complexity of the terrain at the location of the reference wind farm, the verification of 24h forecasts showed that it is necessary to first focus on and verify the capability of the model to simulation the weather at specific sites rather than evaluating the predictability over a long time horizon. Therefore, the second part of the verification was carried out on the very short range (1-6h) for four additional sites.

Impact of Model Levels and Forecast Times

A summary of statistical tests carried out for the 15 experiments at the reference wind farm Kilronan is given in Table 3.2, Table 3.3 and Table 3.4. All tables refer to wind velocity in unit [m/s]. Note, that what is referred to as variability (variab) in this

work is often also referred to as "standard deviation of the mean". The equations of all statistical parameters can be found in Appendix B. The short names in the column "Exp" are defined according to the experiment description in the previous chapter and Table 3.1. The statistical tests were analysed on 5 vertical levels (28,29,30,31,32) and at four different forecast lengths (00h, 06h, 12h and 18h) (see Table 2.1). Measurement information of the observational data can be found in Appendix C.

In Table 3.2 the results from a conventional set of statistical parameters is shown from the 00h forecast at the level that corresponds to the hub height of the turbines. As discussed in the previous chapter this height can be different from the actual hub height of the turbine and varies with model resolution and location of the wind farm. The mean, variability and maximum are also shown for the observations in unit [m/s]. The results in the table show that there is no significant difference between the coarse resolutions (0.3°) and the high resolutions. The mean differs only approximately 6%-7% from the observed mean. The same applies to the variability (variab), mean absolute error (mae), bias, root mean square error (rms) and correlation (cor). The maximum values are consistently higher in the high resolution 0.014° runs than in the 0.5° and 0.15° runs, but not so for the 0.3°. The lack of a clear pattern suggested that more statistical tests needed to be carried out. If it is true that there is no difference between the forecasts with a grid size of 0.3° and 0.014°, the main error sources would be a result of large scale errors. To investigate this statement further, the statistical analysis was extended to compare the results at all forecast lengths (0h,06h,12h,18h) and all 5 relevant vertical levels (28,29,30,31,32).

This graph has no statistical significance, but gives a qualitative impression of the difficulty in the interpretation of the statistical results. It is based on the results from Table 3.3 and Table 3.4. In fact, it averages the results from the best error statistics over each forecast length. Table 3.3 then shows the results from the comparison of different forecast lengths when using an average over the five lowest vertical levels. It was felt that applying a smoothing effect by averaging over the vertical levels could be used to further investigate the dependence of the model on the horizontal resolution.

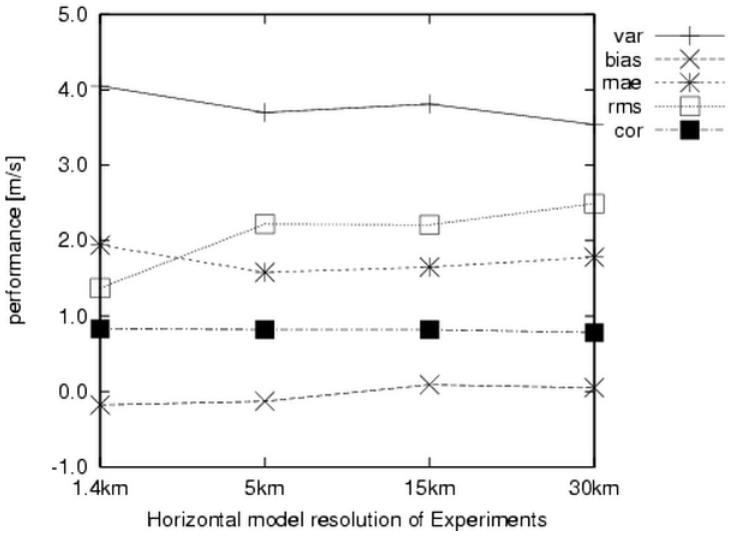

Figure 3.9: Graphical Summary of the statistics for the Kilronan wind farm. The results from Tables 3.3 and 3.4 are averaged over the different horizontal model resolution of the experiments, such that each point in this graph is an average over 2 x the number of experiments with the same resolution.

Figure 3.9 gives a graphical overview of this investigation.
The first column shows the forecast length where the models performed best in average in the statistical tests consisting of mean, variability (variab), minimum (min), maximum (max), mean absolute error (mae). This column is referred to as "stat". In the two columns following, the forecast lengths with best results in mean average error (denoted as mae^*) and correlation (cor^*) are given, where "all" indicates that there is no difference in any. The column "fclen" indicates the forecast length for which the results in the remaining columns are displayed. The results show little difference to the previous table and confirm the hypothesis that there is little dependence on the resolution in the long term statistics. It is interesting to note that column five (fclen) shows that half of the 18h-forecasts performed better than the shorter forecast lengths. This is an indication that the models needed time to adapt to the analysis increments (initial conditions) before being in balance again. Especially in higher resolution, the large scale analysis can have a negative effect on the model's balance and thereby also

Exp.	stats	*mae**	*cor**	fclen	mean [m/s]	variab [m/s]	max [m/s]	bias [m/s]	mae [m/s]	rms [m/s]	cor [m/s]
obs	-	-	-	-	8.07	3.94	25.07	-	-	-	-
e300	0	0	6+12/18	0	7.63	3.60	21.34	-0.40	1.58	2.26	0.81
se300	6	6+18	6	0	7.18	3.45	18.77	-0.78	1.56	2.26	0.82
e150	0	0	6+12/18	0	7.86	3.82	22.26	-0.43	1.63	2.22	0.82
sg150	18	6+18	all	18	7.65	3.78	20.00	-0.36	1.58	2.16	0.83
e075	6	18	6+18	18	8.05	3.96	20.44	0.29	1.83	2.30	0.80
e050	0	0	all	0	8.03	3.76	22.02	-0.05	1.91	2.50	0.78
g050	18	0	18	18	8.12	3.86	19.72	0.11	1.57	2.13	0.84
sg050	all	0+18	18	18	8.03	3.85	19.88	0.08	1.54	2.11	0.84
ec050	12+18	18	18	18	7.92	3.90	20.90	0.21	1.57	2.12	0.83
g050p	all	all	all	all	7.77	3.73	20.31	-0.09	3.52	4.53	0.84
e014	12	12+18	0-12	12	8.20	4.20	22.20	0.21	1.88	2.30	0.81
g014	0+18	12+18	all	12	8.46	4.22	23.32	0.44	1.79	2.19	0.83
sg014	6	0+6	all	6	8.07	4.11	22.00	0.24	1.85	2.32	0.80
m014	-	-	-	-	-	-	-	-	-	-	-
n014	0-18	0-18	0-18	0-18	7.62	3.90	20.02	-0.40	1.63	2.27	0.74

Table 3.3: Statistics from time horizon (h) with best results using an average over model levels

Exp	stats	*mae**	*cor**	fclen	mean [m/s]	variab [m/s]	max [m/s]	bias [m/s]	mae [m/s]	rms [m/s]	cor [m/s]
obs	-	-	-	-	8.07	3.94	25.07	-	-	-	-
e300	29	29	29	29	7.95	3.62	20.95	-0.07	1.67	2.36	0.80
se300	28	28	30-32	28	7.82	3.46	18.56	0.18	1.88	2.61	0.76
e150	29	29	29	29	8.11	3.85	21.92	0.08	1.62	2.18	0.83
g150	29	29	29-32	29	8.12	3.76	20.40	0.04	1.56	2.16	0.83
e075	29/30	31	30	30	7.99	3.82	19.65	0.14	1.77	2.29	0.80
e050	29/30	29/30	30-32	30	7.75	3.51	19.45	-0.32	1.73	2.35	0.80
g050	30	30-32	30-32	30	8.01	3.73	20.20	-0.07	1.50	2.11	0.84
sg050	30	30/32	29-32	30	7.91	3.74	20.17	-0.12	1.47	2.08	0.84
ec050	28/30	30	29-32	30	7.98	3.72	20.90	-0.00	1.60	2.31	0.80
g050p	-	-	-	-	-	-	-	-	-	-	-
e014	30	30	30	30	8.11	4.11	22.00	0.08	1.78	2.24	0.82
g014	30/31	30/31	29-32	31	7.87	4.06	22.17	-0.21	1.71	2.17	0.83
sg014	30	30	30	30	7.87	3.96	21.90	-0.05	1.85	2.41	0.79
m014	30	30	29	30	8.22	4.10	25.10	-0.20	2.05	-	0.87
n014	29	30	30	29	8.58	4.00	23.00	-0.50	2.29	-	0.83

Table 3.4: Statistics from levels with best result using an average over time horizons

on the quality of the small scale features taken into account in the high resolution.

Table 3.4 shows results for different levels using an averaging over the forecast length. The structure of the table is the same as for Table 3.3, except that the column refers to levels, where the models performed best in average. In Meteorology the averaging over forecast lengths is often referred to as a *lagged time average poormans ensemble approach*. The advantage of such ensembles is that part of the uncertainty in the initial conditions is eliminated because of the smoothing effect.

It can be observed in Table 3.4 that there is a pattern in the different resolutions for the levels that fit best to the observations. For the 0.30° and 0.15° grid sizes the best results are obtained at level 28 and 29, which is at heights of approximately 190m and 120m, respectively. It indicates that the orography is too smooth and the location of the turbines is too low in the model space. This changes with higher resolution. When using 0.05° horizontal grid spacing the highest correlation and lowest mean absolute errors are found in level 30 (approximate height above ground of 69m). And similar when using 0.014° horizontal grid spacing, the highest correlations and lowest mean absolute errors are found at levels 30 and 31 (see Table 2.1).

Hence, in the higher resolution, the height above ground resembles the actual height of the turbines. In the coarser resolution this is not the case. Heights above ground in a NWP model depend on the pressure and the orographic representation. In the model space the height of a hill or mountain can therefore be quite different from reality. This means that the height (above ground level) of a turbine can also differ significantly from the corresponding geopotential at a model level. For that reason, care has to be taken when applying wind speeds from NWP models for external wind power models at specific heights (e.g. turbine hub height). For example in the case of the Kilronan wind farm the model level that corresponds to the turbine hub height was found to differ up to 30% from the actual hub height of the turbines. If this is known, an orographic correction to the input data should be computed.

It has also been observed that in most cases the correlation is insensitive to the height of the model levels. It only determines the extent to which values of two variables

are "proportional" to each other. The variability is a much better measure for the *goodness-of-fit* and confirms that forecasts modelled with higher resolutions are more closely related to the observations. The variability of the wind speed is about 10% lower in 0.3° resolution than in 0.14° resolution.

The difference between Table 3.2 and Table 3.4 is that the latter is averaged over 4 different forecast lengths. The differences turned out to be rather small. There was almost no parameter that benefited from averaging the forecasts over time. A small improvement was found in the error statistics (mae, rms). There was no difference found however in the mean, variability or correlations by using this approach.

To summarise, the highest correlation between observations and model output was found in the downscaled 0.5° resolution runs and the 0.014° resolution run with boundaries from the G-model. On average the coarse resolution models perform as well as the high resolution models in the bias, rms and mae error statistics. For example the downscaled g150 runs from the G-model and the downscaled Eulerian e150 runs are superior to all high resolution runs (e014,g014,sg014) . Only the g050 downscaled from the G-model is superior to the coarser resolution runs.

3.7.2 Verification of Wind Speed at Wind Farms

This section deals with the results of the statistics from five Irish wind farms. The statistical tests were conducted for wind velocity in units [m/s] and wind power in units [kW]. These included mean, variance, maximum and minimum, mean absolute error (mae), bias, variability (variab), root mean square (rms) error and correlation. The statistical tests have been conducted to verify the forecast quality of the numerical weather prediction model and not to compare selected sites with each other. This is the reason for using the largest possible set of data for each wind farm and not a small period where data is available for each individual wind farms. The results for each individual wind farm that was verified are also placed in Appendix D for that reason. Hence, the following evaluation of the wind farms will focus on the consequences of the

results for the prediction accuracy rather than comparing the "weather" at different locations. In fact, the result of a direct comparison of individual wind farms would be that the "weather" is different at the different sites.

The purpose of this evaluation is however to investigate the error sources of the numerical weather prediction model at different sites by comparing observational data with forecasts. It was important to find a pattern for the *local error* as described in the introduction of this chapter (see Figure 3.1) and to ensure that errors are not coincidental errors that arise under the specific local conditions of a site.

It was observed at all sites that the modelled mean wind velocity and mean wind power are lower than the observations mean velocity or mean power. Except in Lendrum, where the g014 and n014 modelled mean wind power was slightly higher than the observed mean. This is also true for the variance of the variables (wind power and wind speed). In Lendrum and Bessy Bell the variability of wind speed and wind power is closest to the observations for the experiments se300 and s300. At Milan Hill and Tursillagh there is higher variability in the forecasts from the n014 and g014 experiments than in the observations, whereas all other experiments show lower variability than the observations. The correlation of modelled wind speed to observed wind speed was found to be highest (0.87) for the e300 and se300 experiments at all farms (Bessy Bell, Kilronan, Lendrum, Milan Hill and Tursillagh). In wind power space the correlation of modelled wind power to observed wind power is higher in the higher resolution runs for all wind farms except the Tursillagh wind farm. The analysis of the reference farm is confirmed by the analysis of these four wind farms. That is, the high-resolution experiments do not show a consistent statistical improvement in comparison to the forecasts in coarser resolutions. This result is consistent for all five wind farms for both wind velocity and wind power. A subjective analysis however showed in all cases that only the forecasts in higher resolution can capture terrain features correctly.

3.7.3 Summary of the Statistics at the Wind Farms

- The results indicate strong sensitivity to the models horizontal grid spacing, the surface representation and model area
- Long term error statistics (rms and mae) show almost the same results for all model resolutions, but only the high resolution model can capture the small scale weather phenomena
- The physical height of the model levels that represent the hub height of the turbine depend on the model resolution. When modelling at coarse resolution the effective hub height of the turbine in the model needs to be calculated.
- The *lagged average poormans ensemble forecasts* did not improve the forecasts, i.e. there was no significant benefit in averaging the forecasts with different forecast lengths
- In complex terrain peaks of high wind speed ($> 20m/s$) can only be simulated reliable with model resolutions of $0.05°$ or higher
- The models bias and maxima can only be evaluated in the high resolution. In the coarse resolution (e.g. $0.30°$) large biases can be due to bad representation of the orography.
- It is questionable whether and when the cost of high-resolution deterministic forecasts can be justified

3.7.4 Frequency Distribution at a Reference Farm

Most of the experiments were carried out over a period of 3 months. For such a short period a Weibull distribution will not provide useful results. Instead, a comparison of the frequency distributions of the different model resolutions has been carried out. Only standard frequency parameters and distributions of the experiments were computed and

observations	e014	g014	g050	ec050	e150	se300
29%	43%	48%	47%	44%	49%	53%

Table 3.5: Frequency distribution of Wind Power for the Reference Farm Kilronan in the range 0-500kW

interpreted by subjective evaluation. These results revealed that the higher resolution runs are much more in line with the observations.

In contrast to the standard statistical test, the frequency parameters and distributions demonstrated a linear deterioration of the goodness-of-fit to the observations from 0.30° to 0.014° resolution. Figure 3.10 shows the frequency distribution at the reference park Kilronan of wind power (on the left) and wind speed (on the right) over the three month period January to March 2001. Six experiments (e014,g014,g050,ec050,e150,se300) with 4 different resolutions (0.014°, 0.05°,0.15°,0.30°) are displayed. The peak production of the wind farm is 5000kW. The distribution of wind power has been enlarged to the range of 0% to 15%. The first range of 0-500kW can therefore not be seen fully. In the 0-500kW range the modelled frequencies differ from the observations. This range seemed to be dominating for the power production of the wind farm. The shape of the wind power distribution is therefore skewed to the left with many values in this lower range. The percentages are displayed in Table 3.5.

Frequency parameters were calculated for 10 resolutions at all 5 wind farms. Because the behaviour and results are similar at all sites, only the reference farm (Kilronan) is presented and discussed hereafter. In Table 3.6 and Table 3.7 the results are listed. The tables in Appendix D contain the results for the four other stations.

The mean of the distribution shows that the forecasts from the coarser resolution runs deviate more from the observations than the forecasts from the high resolution. Thus, the smoothing effect in the coarser resolution becomes apparent in this way.

The *skewness* refers to the symmetry of the distribution. The formula can be found in Appendix B. The skewness parameter confirms that the shape of the wind power

Exp	Mean [kW]	Skewness [-]	Kurtosis [-]	P.25 [kW]	P.50 [kW]	P.75 [kW]
pwr.obs	1834.27	0.54	-0.94	520.00	1508.00	2977.00
e014	1814.73	0.71	-0.67	547.07	1385.03	2801.02
g014	1845.14	0.66	-0.69	607.83	1480.83	2834.08
se014	1734.72	0.79	-0.53	533.05	1287.07	2685.38
ec050	1670.36	0.80	-0.44	417.50	1284.31	2534.19
se050	1632.04	0.77	-0.47	395.07	1269.44	2621.84
g050	1625.40	0.83	-0.41	425.78	1188.18	2597.32
e150	1575.74	0.96	-0.18	412.36	1057.61	2398.43
g150	1495.06	0.89	-0.26	265.07	1093.03	2430.80
e300	1372.68	1.08	0.30	271.13	913.14	2112.91
se300	1201.62	1.05	0.31	218.29	854.46	1848.02

Table 3.6: Statistical Parameters from the Wind Power Frequency Distribution for the Reference Farm Kilronan

Exp	Mean [m/s]	Skewness [-]	Kurtosis [-]	P.25 [m/s]	P.50 [m/s]	P.75 [m/s]
ws.obs	7.92	1.01	1.53	5.27	7.33	9.90
e014	8.07	0.51	-0.22	4.83	7.62	10.75
g014	8.22	0.61	0.18	5.02	7.83	10.88
se014	7.85	0.54	-0.11	4.74	7.45	10.46
ec050	7.93	0.57	-0.09	5.13	7.43	10.37
g050	7.80	0.60	-0.13	4.97	7.12	10.45
sg050	7.73	0.61	-0.11	4.86	7.07	10.27
e150	7.42	0.77	0.22	4.46	6.79	9.75
g150	7.19	0.64	-0.21	4.41	6.38	9.66
e300	7.07	0.68	0.05	4.47	6.42	9.32
se300	6.38	0.61	-0.31	3.91	5.79	8.55

Table 3.7: Statistical Parameters from the Wind speed Frequency Distribution for the Reference Farm Kilronan

probability density function (pdf) is weighted to the left with a long tail toward the larger values (see also Table 3.5). The wind speed pdf is more bell-shaped than that of wind power, but also weighted to the left (see also Figure 3.10).

The difference in shape between wind speed and wind power can be explained by the fact that the highest probability is between 6 to 8 m/s, which is at the more flat part of the power curve. The difference between observation and modelled wind power at the different resolutions is increasing with coarser resolution and reaches almost double the values in the 0.30° resolution. This could be interpreted such that the coarser resolutions are weighted much more toward the smaller values in power space. Hence, there is a negative bias in the wind speed. This negative bias however is not present in the skewness values for wind speed. The modelled wind speeds have a lower density (up to almost 50%) toward the smaller values than the observed wind speeds.

The *kurtosis* values for wind power confirm the hypothesis that the distribution of the coarser resolution forecasts is more peaked than the observations and the higher resolution forecasts. The kurtosis refers to the flatness of the distribution in relation to the normal distribution. The positive values in the 0.3° resolution of wind power therefore indicated an increased peakedness with heavier tails than all other resolutions and the observations. The wind speed values behave similar to the shape parameter, but around the zero value. In general, the observations are relative more peaked.

The percentiles were computed for the quartile (25th percentile), median or middle value (50th percentile), and the 75th percentile. The 25th (50th,75th) percentile defines the number of cases where 25time series can be found. The percentiles confirm that the distributions in the coarser resolution are denser toward smaller values. In both wind speed and wind power the difference to the observation increases from 0.014° linearly to the 0.3° resolution. It is worth noting that the coarser resolutions have much less values in the higher ranges of wind power and wind speed. This gives an indication that the relatively good results in the error statistics are due to lower or smoother values in general.

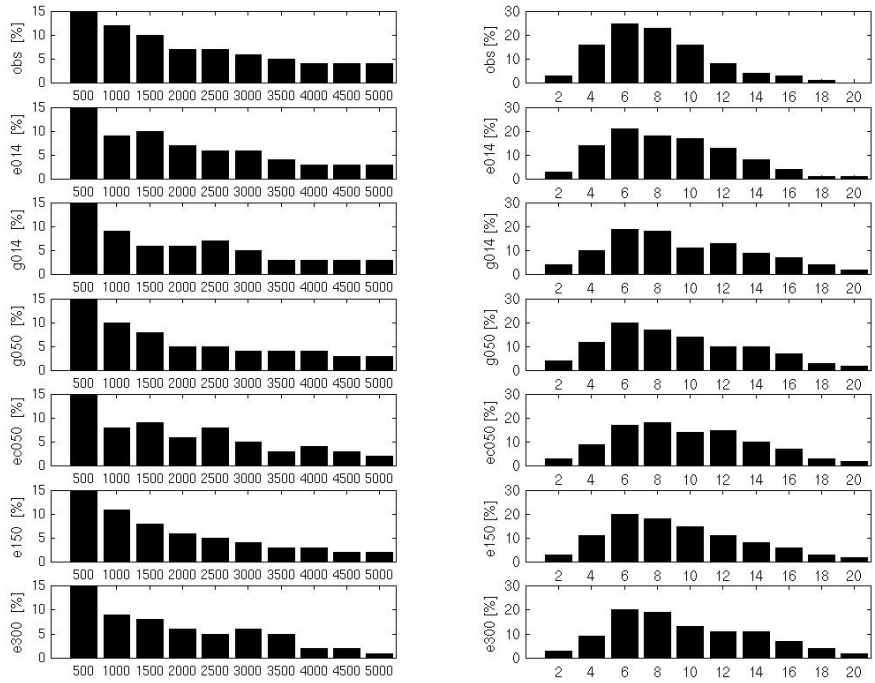

Figure 3.10: Frequency distributions for Kilronan Wind Farm over a 3 months period from January to March 2001. The plots on the left are wind power distributions and the plots on the right are wind speed distributions

The distribution statistics showed that in wind power space the forecasts in the 0.014° resolution are significantly better than in the coarser resolution. In the wind speed space, the 0.05° is equally good as the 0.014°. This confirms the suggestion that 0.05° resolution is necessary under the simulated conditions, but that there is not enough improvement by increasing the resolution to 0.014° to justify the higher computational costs.

3.7.5 Interpretation of the results at a Reference Farm

The statistical tests did not show much improvement when modelling in high resolution (see Table 3.3 and 3.4). At first glance this seems to be a rather surprising result. The subjective analysis of the time series showed however that peaks of high wind speed,

which are significant for power predictions, can only be captured with model resolutions of 0.05° or higher.

Another reason for the relative poor error statistics is the fact that the model area for the high resolution runs was significantly smaller than for the coarser resolution runs. This is due to the high computational demand when modelling in this resolution. For the forecasts this means that the high-resolution runs are slaves of their boundary values. Large-scale effects are only introduced through the non-physical boundary relaxation, which is applied in a very narrow zone. In this case it was applied to a frame surrounding the model domain with a size of approximately 10 grid points.

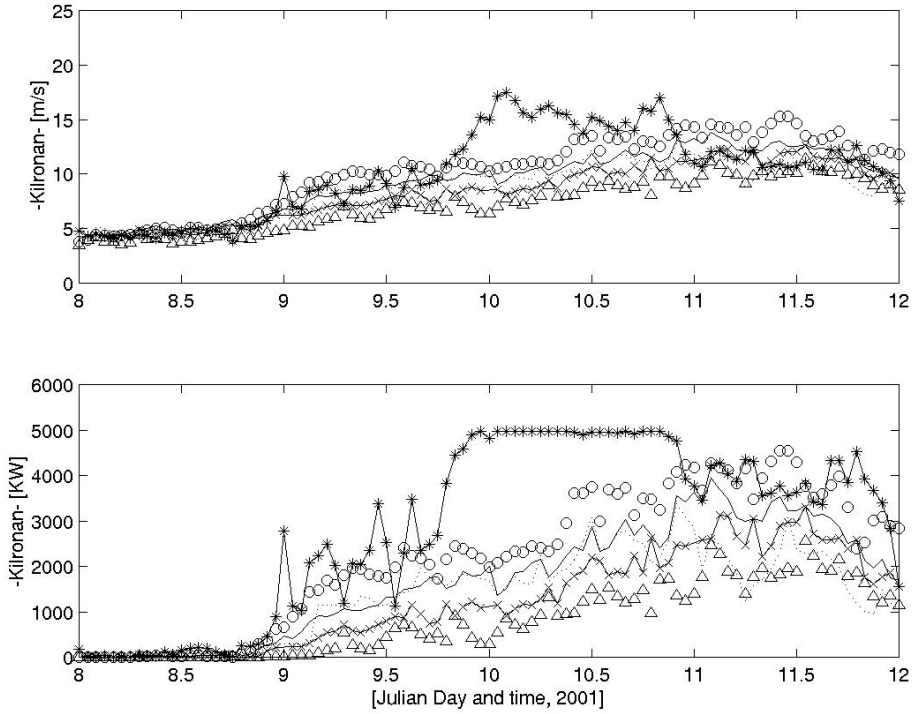

Figure 3.11: Example of predicted wind speed and wind power at Julian Day 10 to 12 at Kilronan Wind Farm. The line with the stars indicate the observations, the dotted line is at 0.014° (e014), the dashed line is also at 0.014° (n014), the solid line is at 0.05° (g050), the dashed line with crosses is at 0.15° (g150) and the dashed line with triangles is also at 0.30° (se300).

Another consequence of modelling on a small model area is that the error that is introduced from noise at the boundaries becomes larger, the closer the points of consideration are to the boundaries. High resolution is also automatically subject to larger rms errors and usually the worst when phase errors arise. In fact, it is most pronounced in extreme events, especially when peak values of more than 15m/s are met. Even though the peaks have the correct magnitude, a phase error creates large absolute errors when the peak wind speed is delayed. In such cases large absolute errors are reported twice, once when the peak event occurs and another time when it is already past. One example of such double errors is the 11th January 2001 in Kilronan.

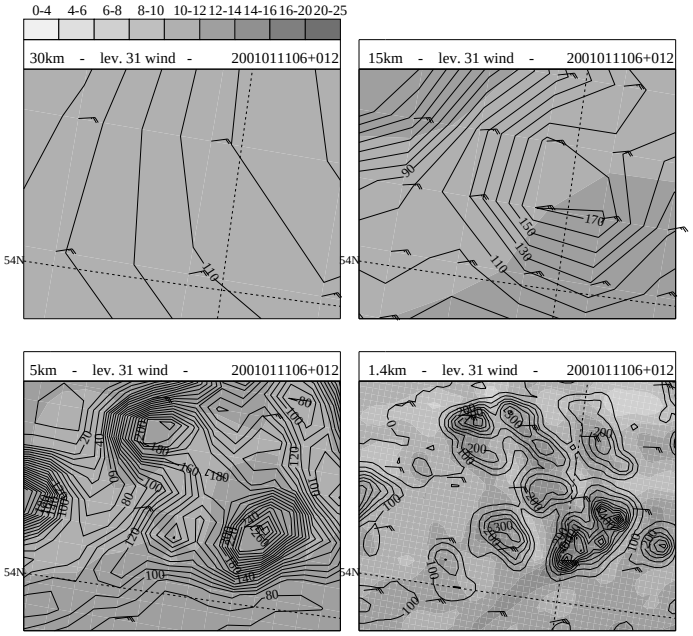

Figure 3.12: Example of predicted wind speed at level 31 (shaded) and geopotential heights (contours with 10m intervals) at Julian Day 11, 18UTC at Kilronan Wind Farm in 0.3° (left upper plot), 0.15° (right upper plot), 0.05° (left lower plot) and 0.014° (right lower plot).

Figure 3.12 shows the difference in the resolutions and also the problem that arises from phase errors in the high resolution. Even though the high resolution seems to

have disadvantages when phase errors arise, the surface representation in the model is a very important parameter for the prediction at specific sites.

It was found that only with a resolution of 0.014° it was possible to capture peak values greater than 15m/s with a high reliability at all wind farms. This can only be seen by subjectively evaluating time series and horizontal plots. Figure 3.12 is the corresponding horizontal plot to Figure 3.11 at Julian Day 11, 2001, where the problem is pronounced. The plot shows 4 different resolutions (0.3°,0.15°,0.05°,0.014°) where the wind speed is shaded and contour lines are the geopotential heights. When analysing these plots, it seems that the statistics is rather misleading with regards to maximum values. Maximum values of 20m/s are achieved by almost every model once in the 3 months period, which means that the parameter does not give an indication about the capability of the model to simulate peak events. The variability in the various resolutions also does not indicate that there are advantages of modelling in higher resolutions. As mentioned above, subjective analysis of the data however revealed some of the important effects of resolution. The 0.30° and 0.15° for example do not have the same orography as the 0.5° and 0.014° resolution. The plot shows that the wind speed at the coarse resolutions is mainly dependent on the large scale flow, because of the smooth orography. In the higher resolution (0.014°), it can be seen that the wind speed follows the terrain features realistically.

The evaluation of the most suitable resolution is not a trivial task. This analysis showed how difficult it is to evaluate whether the higher resolutions are more suitable for predicting wind parameters accurately or not. When averaging over large areas, or accumulating wind power over for example one day, the high resolution outliers might be removed, but the coarse resolution might also be sufficient in such cases. To produce the most reliable results, the *phase error problem* of punishing the high resolution model twice for not having the peak when it occurs and having the peak when it is past has to be attacked.

3.7.6 Interpretation of the results at the Wind Farms

As mentioned in the previous section, the initial conditions can have a negative effect, especially in the high resolution. The reason is that the analysis fields from the global models are usually in rather coarse resolution (approx. 1.0°) . All motion on a scale below 30-60km is then solely generated by the model itself. The weather created by the models is either stationary and locally forced or a function of the motion on a larger scale. If there is no stationary weather with local forcing, the smallest scales represent the statistical behaviour of the model and can differ from the actual local weather condition. If this is the case, the forecasts might be improved by applying a time filter. Such a filter could be useful in the high resolution to take away the shortest waves in time or space and thereby force the model toward the large-scale development.
A detailed study of some selected cases demonstrated that stationary weather with local forcing existed and that the models were able to simulate these scenarios. These situations are however not dominating in areas with complex terrain such as in Ireland. Because weather is mostly very changeable in such areas, stationary weather occurs rather seldom. Applying a time filter on the high-resolution alone will most likely not solve the problem. In contrary, it can also reduce the variability of the forecasts in comparison to the observations, which could have negative effects on the wind to power conversion.

3.8 Error sources in the forecasts

To find the real sources of the error for a given forecast is practically impossible. This is because the model system is setup with approximations, which itself have the potential of being sources of large errors.
It has been demonstrated that one of the most serious sources of error when modelling with a NWP system are phase errors of fronts, which are only in theory separable from other error sources. One way to separate them is to compare model winds with observed

winds at wind parks. This comparison however must include local corrections, which can not be done explicitly in the prediction systems of today. This source of errors has been handled with statistics tools in the past.
Other errors are even more difficult to investigate, because their time dependency is smoother and therefore they are less visible. More over, those errors are often a result of unrealistic approximations of the description of the physical processes or bad representation of the orography that arise on a rather local scale and require special monitoring to be identified or improved.
The following section will provide a summary of the error sources in the NWP models that have been identified in the *Irish Study*.

The Error Sources at a Glance

A detailed discussion and illustration of the error sources in the prediction of wind speed, direction and wind power that were identified in the *Irish Study* follows hereafter. For this purpose a number of time series were selected from the 5 wind farms. A table with information about the measurement of the observational data is given in Appendix C. Figure 3.13, Figure 3.14, Figure 3.15, Figure 3.16, Figure 3.17, Figure 3.18 are used as typical examples of error sources in NWP models for wind energy purposes. The observations and forecasts in these selected cases have been verified against analysed fields to ensure that no misinterpretations are made because of erroneous observation or forecasts. If observations or forecasts had errors they are mentioned explicitly.
It was also not intended to analyse in detail the reason for the failure of the model from a meteorological point of view in these specific cases, but to use examples to illustrate the principles behind the failures. A summary of the findings is provided at the end of the section.
Figure 3.13 shows an example of a peak event that is highly underestimated in power space, even though the wind speeds seem to be predicted relatively well. The peak production of the wind farm is at 5000kW. The wind starts to rise at midday of day

30. In that period all forecasts are in the same range and the maximum error seems to be around 1m/s. However, in power space the observations show already at that point in time higher values than the forecasts. The 0.05° model run (g050) follows closest in power space, even though it is overestimating the wind speed in the range 20-23h on day 30. At midnight there seems to be an observation error, because the observations continue to rise after about one hour. The forecasts of wind speed still follow the observations after midnight, whereas the difference in power space grows up to 2000kW. This is almost half of the wind farms installed capacity.

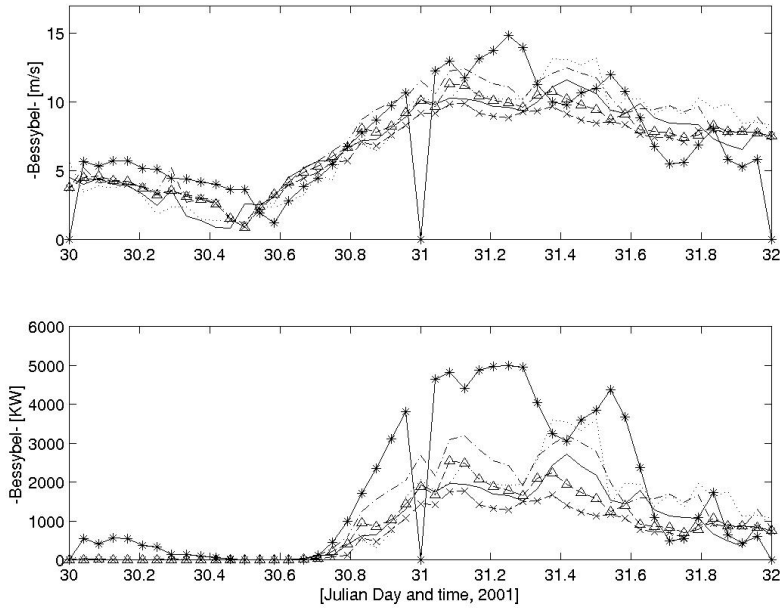

Figure 3.13: Example of predicted wind speed and wind power at Julian Day 30-32 at BessyBell Wind Farm. The line with the stars indicate the observations, the dotted line is at 0.014° (e014), the dashed line is also at 0.014° (n014), the solid line is at 0.05° (g050), the dashed line with crosses is at 0.15° (g150) and the dashed line with triangles is also at 0.30° (se300).

This behaviour indicates that the conversion from wind speed to wind power is not working very well. The simplified model used in this study included power curves from the manufacturer, and suggests that a more sophisticated power curve parameterisation

is required.

The following day (Julian Day 31) shows a typical phase error of around five to six hours, where all forecasts are subject to the error. The errors account for up to two third of installed capacity. These kind of phase errors usually arise when the position of a low is predicted incorrect. The source of the error can also be in the boundary generating model or the analysis. In a real-time environment where forecasts are available every 6h, these events have a predictability of usually approximately 12h. They are dependent on the analysis fields and how fast the model system achieves a state of balance.

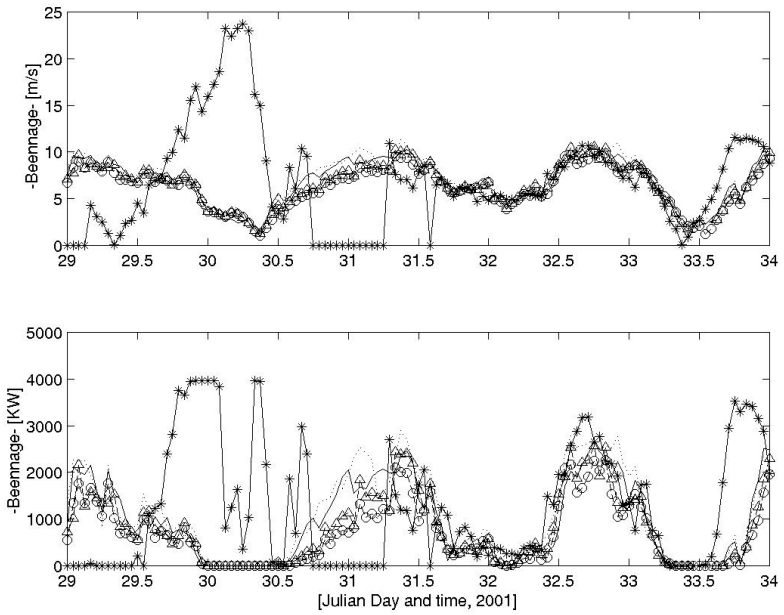

Figure 3.14: Example of predicted wind speed and wind power at Julian Day 29-34 at Beennageha Wind Farm. The line with the stars indicate the observations, the dotted line is at 0.014° (e014), the dashed line is also at 0.014° (n014), the solid line is at 0.05° (g050), the dashed line with crosses is at 0.15° (g150) and the dashed line with triangles is also at 0.30° (se300).

Figure 3.14 also shows an event, where none of the model configurations predicted the wind speed peak. In contrary, the forecasts even decreased to the threshold value (5m/s) for zero power production.

The observations in this case show an example of local extreme wind gusts that cause some of the turbines to switch off. This seems to be a very local effect, because the large scale analysis did not indicate strong winds at this day. There was however a change in wind direction within 6 hours from southerly to westerly winds.

Between Julian Day 32 midday and 33 another example of insufficient accuracy in the conversion of wind to power was observed. In other words, the power parameterisation or power curve is not site-specific enough.

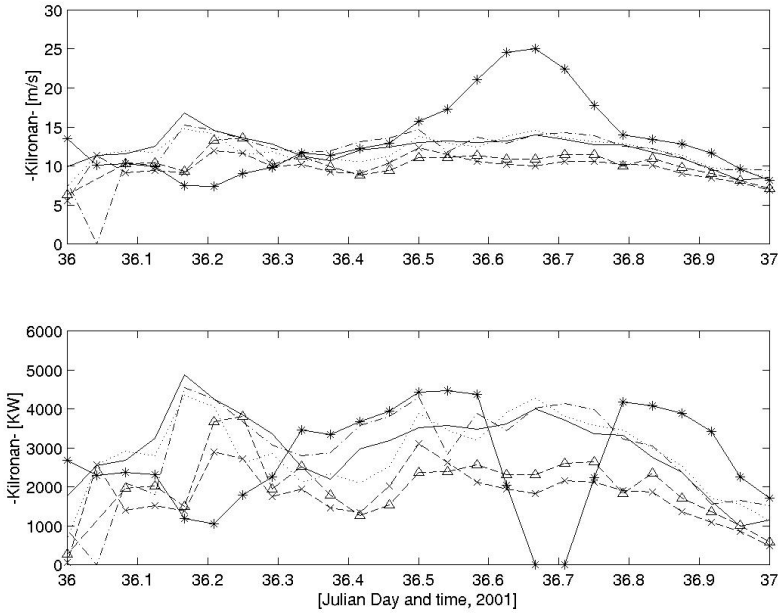

Figure 3.15: Example of predicted wind speed and wind power at Julian Day 36/37 at Kilronan Wind Farm. The line with the stars indicate the observations, the dotted line is at 0.014° (e014), the dashed line is also at 0.014° (n014), the solid line is at 0.05° (g050), the dashed line with crosses is at 0.15° (g150) and the dashed line with triangles is also at 0.30° (se300).

Figure 3.15 shows a typical example of a phase error and a local effect that could not be captured with any model resolution. It starts with a phase error at the end of day 35 of approximately 3h, which corresponds to around 2-3m/s. In power space this results in errors of up to 30% (1.5MW of 5MW installed capacity). The problem arises in the

morning of day 36, when both of the 0.014° runs (e014, n014) and the 0.05° (g050) gradually increase and reach a peak of approximately 15m/s. This corresponds to full production (5.0MW) in power space. In the same time frame the observations drop to 7m/s and 1.0MW. It is interesting to observe that the coarser resolution runs have an even stronger phase error. They peak 5h later, but with less intensity. The errors in such a case are large and can cause severe grid insecurity or economic loss.

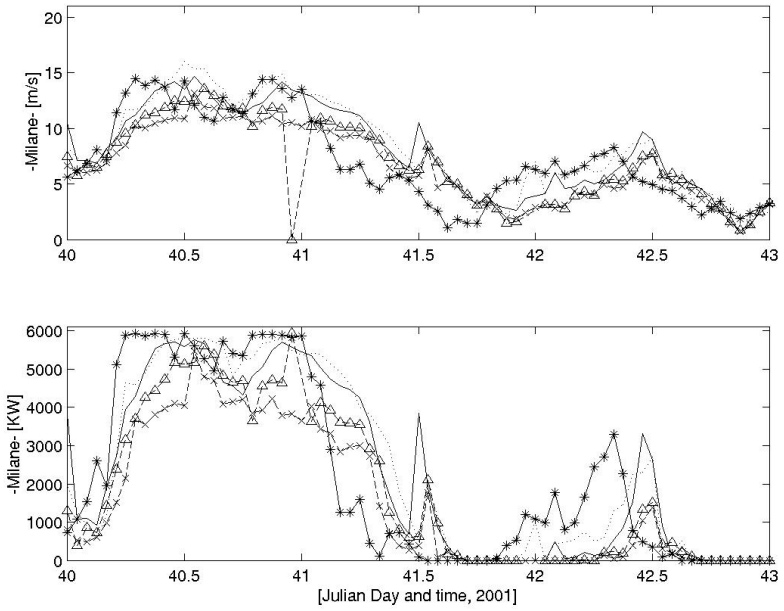

Figure 3.16: Example of predicted wind speed and wind power at Julian Day 41-43 at Milane Hill Wind Farm. The line with the stars indicate the observations, the dotted line is at 0.014° (e014), the dashed line is also at 0.014° (n014), the solid line is at 0.05° (g050), the dashed line with crosses is at 0.15° (g150) and the dashed line with triangles is also at 0.30° (se300).

The phase error example is followed by a typical case of non-predictability. The observations gradually increase up to 25m/s over a period of 5h. The peak lasts for about 2h, where the turbines switch off. This case was not predicted by any of the forecasts. An explanation is difficult, because there are many reasons why models fail. Local effects might be responsible for the errors or another reason could be unstable weather

conditions. In this case for example, the weather maps indicated that a trough went directly through the area where Kilronan wind farm is located. The wind fields became cyclonic and the atmosphere extremely unstable.

Figure 3.17 is an example of a direction dependent site that has a high variability in both wind speed and power for northerly wind directions. Changes in wind power of up to 50% of installed capacity within one hour have been observed for winds from northerly directions at that site. In the example (Julian Day 12 to 15) none of the runs, can capture the peaks measured at the site. Even though all forecasts follow the same "weather", the observations have a higher variability and thus higher peaks. The wind direction is from north-east or north-west in all cases. If the wind direction is southerly, the observations usually lie withing the spread of the forecasts.

Thus, it seems that the wind farm has a direction dependency for northerly wind directions. This phenomena is quite common for the prevailing wind direction at wind farms. Wind farm planners are in fact looking for sites, where wind speeds higher than the area average are observed. These are for example at mountain tops or valleys where lee effects enhance the average wind speed etc.

Figure 3.16 is another example of a phase error of 1-2 hours. In both cases (Julian Day 40 and 42) the higher resolutions capture the peak in wind speed and wind power, but too late. The coarser resolution runs (e300 and se300) are far below the observations. This is an examples where the subjective analysis indicates that the high resolution is of advantage in extreme events.

In all cases shown so far, the subjective analysis would give a different result than the error statistics, because the coarser resolutions are much smoother and therefore have less errors. Figure 3.18 shows an example of wind power drops from turbines. This is very pronounced at Julian Day 36. In this case there is a sudden drop in wind speed and power production followed by a gradual increase of both wind speed and power to a second peak. that experience cut-off wind speeds of more than $23 m/s$.

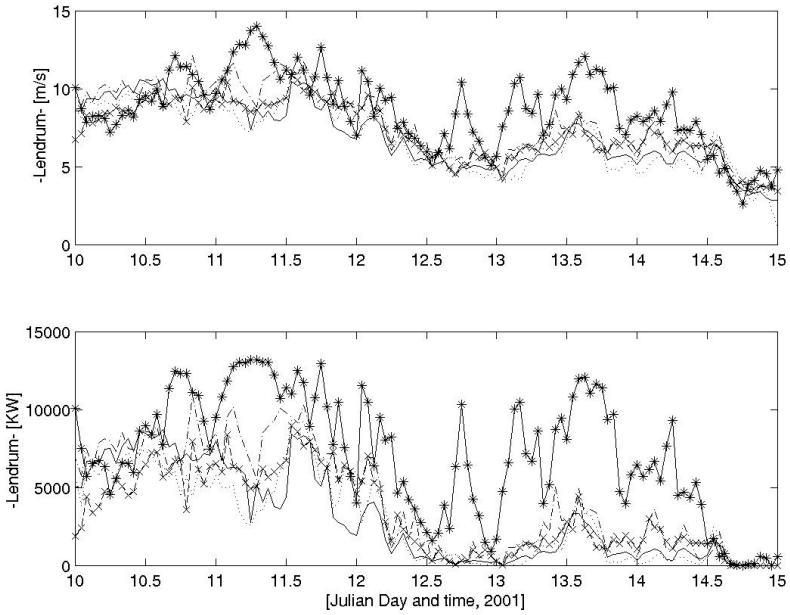

Figure 3.17: Example of predicted wind speed and wind power at Julian Day 10 to 15 at Lendrum's Bridge Wind Farm. The line with the stars indicate the observations, the dotted line is at 0.014° (e014), the dashed line is also at 0.014° (n014), the solid line is at 0.05° (g050), the dashed line with crosses is at 0.15° (g150) and the dashed line with triangles is also at 0.30° (se300).

The power production drops suddenly to only 10% of installed capacity. When analysing the data it was found that the wind speed was measured at 10m above ground.
A second wind anemometer at 45m height above ground recorded higher wind speeds of over $22m$ in these 5 hours, which is consistent with the power drop from turbines shutting down at cut-off wind speed and the hub height of the turbine. The comparison of the two recording anemometer demonstrated the increase of wind speed with height. This figure also explains why the high resolution models are not better in average than the coarser models. The 0.014° model predicted the event of the 35^{th} to the 37^{th} and also Julian Day 39 to 40 very well. At Julian Day 38 it over-predicts the wind speed strongly. This results in an over-prediction of one third of installed capacity. The coarser resolutions are much smoother and therefore have less errors.

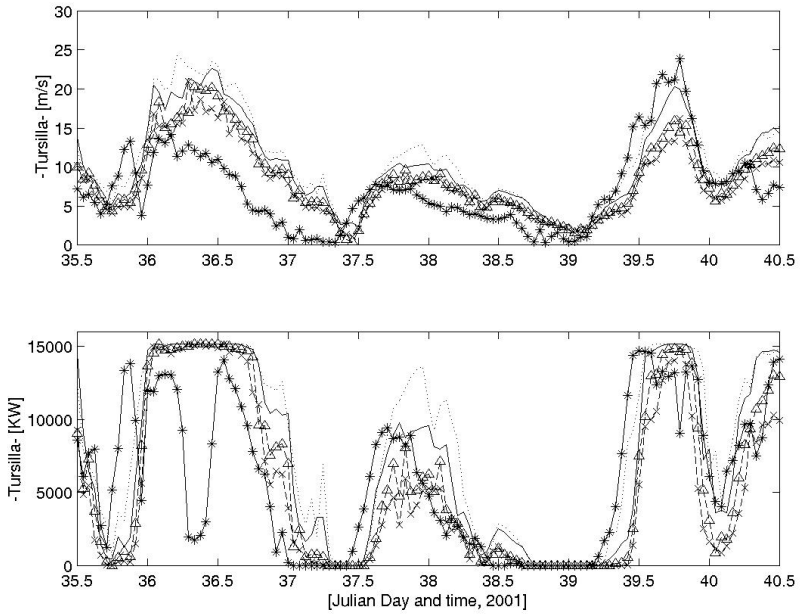

Figure 3.18: Example of predicted wind speed and wind power at Julian Day 35-40 at Tursillagh Wind Farm. The line with the stars indicate the observations, the dotted line is at 0.014° (e014), the dashed line is also at 0.014° (n014), the solid line is at 0.05° (g050), the dashed line with crosses is at 0.15° (g150) and the dashed line with triangles is also at 0.30° (se300).

Summary of the *Error Sources at a Glance*

- Truncation errors are significant if the model area is too small. If this is the case the gain of high resolution is lost.
- In many cases a more sophisticated power parameterisation is required, especially if extreme events should become more predicable.
- Phase errors of 5-6 hours usually arise when the position of a low is predicted incorrect with a few hundreds of kilometres. In this case non of the forecasts matched the observations
- Local extreme wind gusts are responsible for turbines to switch off instantaneous, which results in huge errors in the predictions and can cause severe problems in grid security
- Non-predicable extreme events are often either very local effects or non-trusted observations in the analysis that cause an underdevelopment in the forecast. It is a well-known phenomena in real-time environments and has been shown that such phenomena are mostly predictable from 12h-6h before occurrence, when new analysis fields are fed into the model.
- Phase errors of 1-2 hours are difficult to interpret. A high resolution model setup shows mostly smaller phase errors than a coarser resolution model setup. This is due to local effects and better representation of the orography.
- High variability in both wind speed and power at a site makes the prediction even with a NWP model very difficult and in some cases impossible.
- Drops in wind power can be sudden and significant and do not always correspond to the measured wind speed.
- "uncertain weather" can last for several hours. It is believed that the forecasts of such weather phenomena can only be improved by implementing such cases into a statistical correction tool.
- Direction changes within a short time can create significant discrepancy between the NWP model and the atmosphere and thus incorrect predictions

3.9 The Deficiencies and Constraints in accurately predicting Wind Power

This study revealed some of today's main deficiencies and constraints in accurately predicting wind power. In the following, the three main error sources are summarised and possible solutions are discussed to attack these errors and to improve the forecasts.

Discrepancy between the NWP model and the Atmosphere

If there is a significant discrepancy between a NWP model and the atmosphere in an ultra short range forecast or an analysis, there is usually a poorly developed low in an unstable airmass with a significant amount of humidity close to the target area. The atmospheric forcing in such a case comes from the low's cyclonic motion and latent heat release generated by the rising motion. It would require vertical soundings in a dense observational network to get hold of the flow structure in such cases. The flow structure is too complicated for the NWP model system (including the analysis) to resemble the atmosphere. The problem is that the observational network is not dense enough and observations are often randomly rejected or accepted, such that these observations cannot create enough structure in the model.

The requirement to predict such developments would include an upgrade of the observational network especially for such events and therefore seems to be unrealistic. However, it might be realistic to simulate this kind of weather in the future with a nested high resolution model system, which uses wind power observations in high time resolution to force the model. It follows the idea that, if a certain development is started in the model, it is likely that the model will keep the correct structure for a certain time. In such a case, the model system should be started in the past with wind power observations and integrate forward to create a prediction.

Lack of Accuracy of Boundary Layer Winds:

The standard deviation of the high-resolution model data was found to be closely related to the observations, while the low-resolution model data showed too little variability. However, the standard deviation of the difference between model and observations does hardly improve in the high-resolution runs compared to the low-resolution runs. This suggests to either apply a filter to smooth the high-resolution data and thereby loose variability or to introduce an ensemble of forecasts in lower resolution. In that case the introduction of direction and wind speed dependent roughness parameterisation into the model should be done to account for the lack of accuracy in the lower resolution.

Systematic Model Errors:

Systematic model errors appear in all model resolutions and have to be taken into account by local statistical corrections. It is not realistic to run a NWP model in a resolution where these errors disappear. But, the higher the resolution, the smaller the statistical corrections that need to be applied. High resolution long term statistics could therefore be used to compute statistical weight coefficients to account for systematic errors in the wind speed prediction.

Systematic Errors in the Conversion of Wind to Power

Local extreme wind gusts are often responsible for turbines to switch off instantaneous, which can result in large errors in the predictions. These can also cause instabilities in the electrical grid, if the wind farms are large. The best way of dealing with these errors is in form of efficiency based power curves. It means that an efficiency factor is computed that corrects the conversion from wind to power when the circumstances are not optimal for the turbines. This can be done with historic datasets. Such a correction is most important if the wind speed predictions are of high quality.

Phase Errors of Fronts:

Changes in wind speed on a frequency of a few hours are dependent on the area. In Ireland these are typically generated from warm fronts and cold fronts, which appear very frequent. Forecasting of those phenomena requires that the model domain covers most of the Northern Atlantic. However, the model state is not very accurate over the ocean, and therefore results in high prediction errors. The most obvious solution to solve this problem is to use an ensemble forecasting system that is capable of handling this uncertainty. This technique is already in operation in the medium time range (3-10 days) by for example the European Centre for Medium Range Weather Forecasting (ECMWF) or the National Center of Environmental Protection (NCEP). For wind energy purposes a short range ensemble system (0-48h) in higher resolution would however be required. The phase errors of small scale (1-2 hours) can only be dealt with local statistics. A way of dealing with these is by using for example a statistical tool that produces an ensemble of forecasts at extreme events for a wider area. Such a *poormans ensemble* would give the possibility of defining uncertainties in the position of the extremes. It would be a function of the probability density (pdf), the mean and standard deviation (stdev).

$$U = f_Power(pdf, mean, stdev) \tag{3.2}$$

Impact of the Results for the Prediction of Wind Power

The observational verification of five wind farms in Ireland suggested that resolution does not increase the accuracy of the forecasts over longer periods. Subjective evaluation on the other hand has identified, that high resolution is required to be able to capture all weather phenomena and especially extreme events. It has also been identified that high resolution is only beneficial over a relatively large model domain or if the model is fully nested. This is because of noise from the boundaries and imbalances that create model truncation errors.

One of the main arguments for modelling in high resolution is the bad representation

of the orography in the coarse model grids. It has been shown that the lack of small scale features can introduce errors in the forecasts, especially in coarse resolution and in complex terrain. The reason is that the NWP model uses an average orography for the grid box, which often differs from the real orography (see Figure 3.12).

This difference of the model's orography to reality is a function of resolution and implies for wind power predictions that a virtual turbine height should always to be computed at the sites of interest. Such virtual turbine heights can be identified by studying the weather pattern and orographic effects on the wind speed and direction at the area of interest.

These requirements to adjust the model's orography to reality are specific for complex terrain. In homogeneous terrain this is normally not a problem. An example for homogeneous terrain is Denmark or the northern part of Germany. These are practically flat with very few smoothly shaped hills. Thus, orographic effects play a minor role. In complex terrain (e.g. at Ireland's west coast, Spain, Italy) a flow direction dependent parameterisation might be a requirement for the computation of the virtual turbine height due to the direction dependent slope of the ground.

In general, the orographic accuracy in the model system can have effect on the accuracy of the forecasts for certain configurations of a model. This is due the parameterisation of the physical processes in a NWP model that are not equally suitable for all terrain types. The same can be applied for the requirements of resolution. In homogeneous terrain the requirements of resolution are not the same as in complex terrain. These considerations can become even more complex, if the area of interest is at a different place with totally different weather forcing such as the USA, Africa or China.

If the goal is to reduce economic risks and make wind power economically competitive within liberalised markets, the results of the *Irish Study* suggest that phase errors of frontal systems and the lack of accuracy of boundary layer winds have to be improved. Both error sources have a high degree of uncertainty from the model system itself and the initial conditions. This points towards using an ensemble of forecasts, which provides different forecasts, if the weather development is uncertain.

Chapter 4

The Benefits of an Ensemble of Predictions to forecast Wind Power

In the European Commission's Green Paper for Energy and the Environment it is envisaged that the renewable energy demand should account for 12% of the energy production in all European countries by 2010 (Commission of the European Countries, 2000). The highest potential to fulfil these requirements lies thereby within the wind energy sector, especially in large offshore wind parks. As previously discussed, it is imperative to enhance the prediction quality of especially wind velocity to assist in the realisation of these targets.

The previous two chapters described a set of experiments, which were used to identify the error sources and to develop new strategies for increasing the accuracy of today's NWP models. These experiments were necessary to find solutions that assist in understanding the uncertainty of the forecasts. The use of an ensemble of weather forecasts was found to be most suitable when dealing with the problem of forecast uncertainty.

The results of the experiments indicated the need to average the high-resolution forecasts in space and time. This however leads to the loss of variability of the wind velocity, and hence the loss of accuracy of local forecasts from the higher resolution predictions. An alternative to this strategy is to introduce an ensemble of forecasts in lower resolution. Traditional approaches in meteorology average ensembles of forecasts that are initiated from different initial conditions. In this way a deterministic model setup can

be perturbed for the purpose of reducing random errors (noise) in model predictions. The European Center of Medium Range Forecasting (ECMWF) argues that one of the requirements to be met by an ensemble forecasting system (EPS) is that the spread of the ensemble should be sufficient to cover the uncertainties in the forecast, which are due to inaccuracies in the initial conditions and also due to model imprecision (Strauss et al., 1996). Although, the strategy of ECMWF's Ensemble Prediction System (EPS) cannot be transformed directly to the short-range, the principles of the ensemble prediction hold nevertheless. The previous experiments have been examined again with this in mind and it is expected that using an ensemble of forecasts will most likely be necessary to solve the problems associated with the variability and uncertainty of forecasts for the wind energy industry.

4.1 Criteria for using an ensemble of forecasts

A set of criteria has been identified, which focus on the benefits of an ensemble of forecasts. These are weather related conditions that are mostly too difficult for deterministic models to produce reliable and correct forecasts. It is under these conditions, that the uncertainty of the forecasts is expected to be highest. The criteria are:

* Strong curvature of the isobars
* Small areas with wind extremes
* A low pressure system passing close to the target area
* Flow along target area boundaries
* Rapid changes of wind velocities in time

These criteria are thumb rules that can be used to identify subjectively when there is high uncertainty in the forecasts.

From a modelling point of view the uncertainties of the forecasts are very much related to the initial conditions (Buizza et al. 2001). In the description of the new 80km High Resolution ECMWF EPS, Buizza (2001) states, that ensemble prediction based on an appropriate probability density function (PDF) by a finite number of deterministic

integrations designed to represent both initial and model uncertainties appears to be the only feasible method to predict the PDF beyond the range of linear model error growth. In this respect ECMWF has implemented in their Strategic Plan for 1999-2008 (adopted by the Council of ECMWF in June 1999) the target to achieve a gain of one day at D+6 (forecast 6 days ahead) in the Brier-Skill-Score (Brier, 1950) of moderate 850hPa temperature anomalies (4K or larger) in Europe. In other words, ECMWF aims for a relative improvement in predictability of approximately 16.67% by 2008. Using 850hPa temperature is a useful measure in order to get an unbiased idea of the error source. This is because there are no local effects that can diffuse the error source in the free atmosphere and above the boundary layer. Mean-sea-level pressure is also often used for verification of the forecast quality my meteorologists for the same reasons (e.g. Buizza et al. 2001).

To summarise, one of the key questions is whether the ensemble technique can reduce the forecasting error growth beyond the linear error growth as descried in Chapter 2 (Figure 3.1).

4.2 State-of-the-Art in Short-Range Ensemble Prediction

Currently, there are mostly medium-range ensemble systems in operational use at the European Center for Medium Range Weather Forecasting (ECMWF), at the National Center for Environmental Prediction (NCEP), Canadian Meteorological Center (CMC). Short-range ensemble systems are only under discussion and testing in various centres such as NCEP, Meteo France, UK MetOffice, Deutscher Wetter Dienst (DWD), Norwegian Met Centre, Spanish Met Center (INM). This is because the perturbations in the initial conditions, as done for example by ECMWF with singular vectors or NCEP with breeding, are regarded as unsuitable in the short-range forecasting (Palmer, 2002). Palmer showed in his presentation time series plots of an ensemble spread and control

forecast error for a 3 month period (Jan - March 2002). These plots show the correlation between ensemble spread and control forecast error. A correlation is only visible after day 4 of the forecast, which proves that perturbations of the initial conditions with singular vectors are only feasible for the medium range. In a recent workshop on Short-Range Ensemble Prediction Systems (Quiby, 2002) these differences and possible perturbations for the short-range were discussed and it was concluded that uncertainties in the daily forecasts are the result of errors in:

1. Initial conditions
2. Model physics parameterisations
3. Lateral boundary conditions
4. Surface parameters

To tackle the uncertainties in the initial conditions so far, perturbations are done in the medium range by using the singular vector approach at ECMWF (Buizza, 1999) or error breeding in NCEP (Toth and Kalnay, 1993). In the short-range, so-called ensemble data assimilation is considered for example by Houtekamer et al. (1996) and Bishop et al, (2001), who are using a filter technique referred to as *Ensemble Transform Kalman Filter*. Mylne is using a multi-model multi-analysis technique (Mylne et al., 2000). Further plans for perturbation strategies in the short-range by Met Centres in Europe to address the uncertainties of the model physics are described in the workshop on short range ensemble prediction using limited-area models (Quiby, 2002). These are:
- using different model systems (Multi-model approach)
- Perturbing tendencies in the physics (Stochastic physics)
- using different physics schemes (Multi-Scheme approach)
- Perturbing Surface Parameters (mainly roughness)

In the Multi-scheme approach perturbations can be added effectively in the convection, cloud and micro physics, horizontal and vertical diffusion, radiation and surface roughness.

4.3 Design of an Ensemble Prediction System

It has been shown in the previous chapters that the largest errors come from phase errors in the prediction. As discussed above, there are various possibilities to deal with these errors. One possibility is to use a multi-scheme ensemble approach and perturb the NWP model in the fast physical and dynamical processes. For this reason a Multi-Scheme Ensemble System was designed to apply perturbations in the fast physical processes. The processes that are most relevant for phase errors in a NWP model are the vertical diffusion and convection (Haltinger, 1979). An ensemble system comprising 25 members was created with this strategy. In order to reflect the uncertainties in the dynamic tendencies and also tackle phase errors in the predictions, two different dynamical schemes have been applied. With this method the ensemble size was increased from 25 to 50 members.

In order to have full consistency in the model system, an individual *first guess* for each ensemble member was introduced. This can be classified as perturbations of the initial conditions. In contrast to the physical and dynamical perturbations, the *first guess* perturbations determine the smaller scales in the models initial state and are only applied in the beginning of the forecast.

The development and testing of the Multi-Scheme ensemble system for a 3-month period in the beginning of 2001 (January to March) involved three major modelling tasks and one verification task that included the development of an uncertainty estimate.

The modelling included 2 forecast series for all 50 ensemble members in coarse resolution (0.45°) and one high resolution deterministic forecast series (0.05°). Note, that the relevant starting time was 06UTC and 00UTC, and the forecast length was 42h and 48h, respectively.

This was chosen because the project was funded and designed for the Danish Transmission System Operator Eltra. In the Danish electricity market every player dealing with Renewables has to give a bid of their power production from wind by 11 GMT for the following day. For the forecasting system this means that forecasts starting from

06UTC need to be 42h and those forecasts from 00UTC need to be 48h. The study was split into 5 parts:

1. Development of the 50 member ensemble system
2. 42-hour forecasts for all 50 members starting at 06UTC
3. 48-hour forecasts for all 50 members starting at 00UTC
4. Deterministic forecast with boundary files from one selected EPS-member
5. Development of EPS verification including uncertainty estimate

The forecast spread of the EPS will grow with time. Thus, the two-day forecast based on the mean of the EPS members is often a rather conservative guess and also not necessarily the solution with the highest probability. A more advanced analysis technique is therefore applied to the ensemble to produce an estimate of forecasting uncertainty for certain variables according to their probability distribution. This includes the prediction of parameters with the highest probability. The modelling has been conducted on a LINUX-PC Cluster.

4.3.1 Model Area

The selected area for the project is shown in Figure 4.1. The area is formulated in rotated latitude/longitude coordinates.The geographical south pole is located near India at coordinate (80,0) (see also 2.7). The model grid consist of 92 longitudinal and 178 latitudinal grid points with a grid spacing of 0.45°. The model resolution is therefore under 50 km.

The area covers Europe and the Atlantic and was chosen to ensure that all large-scale phenomena arising from the North Atlantic are covered in the model grid. In other words, it is crucial that the area is large enough so that the ensemble members are not slaves of the input at the boundaries. This is especially important for the development of low pressure systems and frontal systems coming towards Europe from the Atlantic. Furthermore, the grid was tailored for Denmark and Ireland, such that only very few weather situations, that have an impact on wind energy, can reach Denmark or Ireland

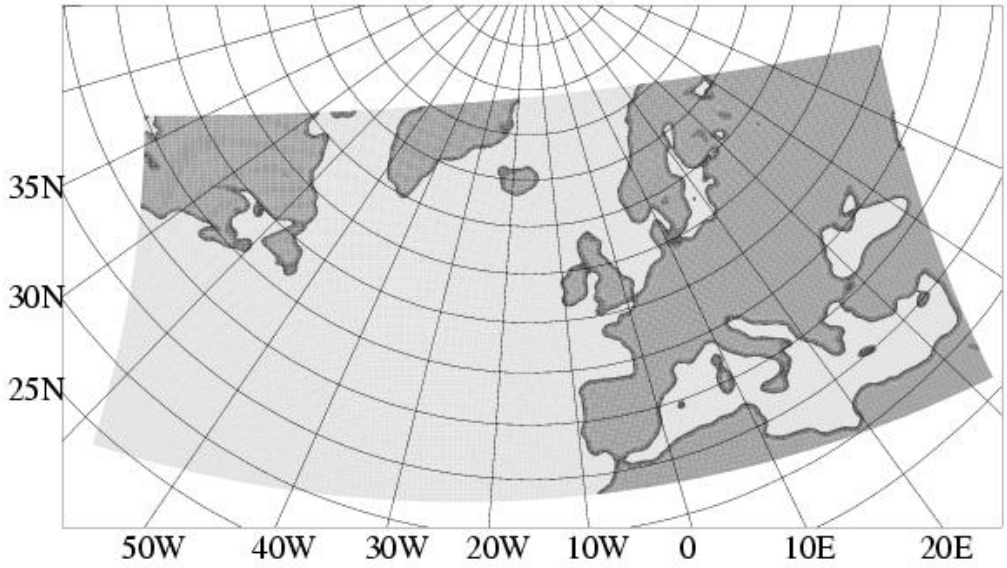

Figure 4.1: Model area for the 50-member EPS

from the boundary of this model domain in a two day period. An example would be a polar low coming from the area around Svalbart that moves southward and stays westward of Norway. This is a rare phenomena and normally only takes place when the jet stream is relatively weak at the end of March or the beginning of October.
A blocking high pressure system over the Atlantic can also cause the flow to come from that region toward Denmark. The phase speed of such a disturbance is lower than average and therefore not critical for a 48h forecast.

4.3.2 The Ensemble Prediction System

The ensemble prediction system was specifically designed to tackle the problems associated with wind energy forecasts. Problems such as very low accuracy in the lower boundary wind forecasts, phase errors of low pressure systems and frontal systems and the uncertainty of the forecast quality.
As described above an ensemble of 50 ensemble members was created for this purpose and was build by applying perturbations to:

- the initial conditions (1)

- the advection process (2)

- the fast physics processes (25)

The perturbations in the initial conditions are designed for the short-range ensemble forecasting, because the perturbations are done by preserving the smaller scales in the *first guess* for every ensemble member. Thus, only the large scale analysis increment is added to the basic prognostic model variables. This strategy ensures balance in the model system. It is a technique, which has only now become practical for ensemble forecasting, because of the reduced cost of storing data.

The use of the multi-scheme approach in the advection process was introduced due to the fact that phase errors are a very critical parameter for the requirements in wind energy. The finite differencing techniques referred to as first-order-upstream differencing and the Semi-Lagrangian technique have been used. It seems that the advection process is more accurately computed in the Semi Lagrangian scheme. On the other hand, the cyclogenisis process, that is the vorticity tendency following the motion, seems to be solved more accurately in the upstream-Eulerian scheme, presumably because of the shorter time-step.

The perturbations in the fast physical processes follow the general ideas of the multi-scheme approach (Mylne et al, 2002). The perturbed processes are the convection and vertical diffusion. The vertical diffusion simulates the mixing effects of the departure of the mean wind in space and time, which is the turbulence and boundary layer eddies in the atmosphere. These do not exist in the model and therefore have to be *parameterised*. If a process is not simulated by the prognostic equations in the model grid, the effects are described with a set of equations using the grid point averaged model variables. The process is then said to be parameterised. The vertical diffusion controls also the mixing length of the middle and upper atmosphere, which to a large extent determines the phase speed and amplification of atmospheric fronts. Furthermore, the interaction between the vertical diffusion and condensation scheme in a NWP model

is strongest near frontal systems, because these are associated with precipitation and significant amounts of vertical sub grid motion due to the condensation processes. Two forecasts with different vertical diffusion/condensation interactions typically develop slightly different with respect to frontal systems. This applies in particular when the weather pattern is not yet well developed and structured. There are parts of the condensation processes that are very uncertain because of their complexity. Both, vertical diffusion and condensation have a major impact on the development of frontal systems in the model system. There is little difference in average weather conditions, but there are significant differences between different scheme combinations at particular areas in space and time. Once there is difference in the model space, a process can grow or dampen out depending on the stability of the atmosphere. Hence, the multi-scheme EPS provides different solutions where the development is uncertain.

4.4 A new Ensemble Classification Method

The classification of the ensemble members into groups of probable outcomes of the meteorological future is not trivial. The detail of interpretation of derived probabilities from ensemble predictions depends a lot on the end users requirements. As an example, a cluster consisting of 50 PC's running the EPS system will produce 29GB data in less than 25 minutes. Only a fraction of this output is however relevant for the end-user. The analysis and presentation of the data is therefore equally important as the generation of the ensemble itself. An efficient way to reduce the information is to use the ensemble mean. However, this is also only relevant, if all ensemble members are equally good. There are two advanced methods which can be used for such a preselecting procedure. These are

1. Clustering
2. Tubing

In the Clustering procedure the selection is unbiased and groups ensemble members around hypothetical centroids. It is a basic selection procedure toward similarities in the data. Tubing on the other hand groups ensemble members if they differ similarly from the mean of the ensemble. It groups members along axes coming from the ensemble mean and reaching the extremes of the distribution. These axes represent the variation of the ensemble members deviating from the mean (Atger, 1998).

As an alternative to these classification methods a new method is proposed: *probabilistic multi-trend filter* (pmt-filter). The pmt-filter is based on the classical clustering method, but selects groups of ensemble members taking the past and future into account. In other words, it is a forward-backward clustering method that strips off those members that do not follow a group or are only temporary the most probable outcome. This algorithm is mainly designed for an operator/forecaster in an utility as a method to find a conservative guess of the most probable outcome of a certain weather situation. It should help to build up confidence for interpreting the probability distribution and estimate the risks for certain actions.

Technically, it was found that the classical clustering method produced unacceptably abrupt changes in the computations of the most likely meteorological future. In fact, it was observed that when computing the most likely outcome, computed as the group with the highest probability, the classical clustering algorithm "hopped" from one possible future to the next within one time-step. This caused the algorithm to became very unstable whenever there were two or more larger groups of members that had similar probabilities.

Therefore, a method was developed that took the past and future distribution into account as a weighting function. In the future computation those that had highest probability in the last time step start with a higher weight than the others. In that way, developing paths are followed once the selection has passed the forking point (junction).

This method will be referred to as forward-backward stepping in the following discussion. The algorithm is fed with long term statistics in the initial guess, but as the

iterations progress the selection becomes gradually more dynamic. The process can also be applied in the two dimensional space (fields).

A future version might include two horizontal dimensions and the time dimension concurrently. The potential of this method is that it allows for forecasts that are started earlier to be taken into consideration in the ensemble evaluation. However, members from such "older" forecasts can *not* take over unless they agree with the "newer" forecasts. The "older" forecasts will also only be accepted as likely, if they follow a group of fresher forecasts.

The strength of this approach is that it automatically filters out the poor forecasts and thereby provides more accurate probabilities. It is an efficient way to reduce the data. When compared to a set of static weight coefficients, it is believed that the potential improvement of the pmt-filter is higher by taking all 50 members into account with at least 1% weight.

4.4.1 The Concept of the *Probabilistic Multi-Trend Filter*

The mathematical formulation of the proposed *pmt-filter* to compute probabilities for the ensemble members can be found in Appendix~\ref{}. Note, that the probabilities are entirely computed from the density of the ensemble, while one parameter, the *best guess* is computed implicitly. This *best guess forecast* should reflect the most likely outcome of the "weather" in contrast to the ensemble mean.

In fact, the *best guess forcast* reflects the concept of the pmt-filter, namely, that it is better to rather believe in a smaller group of forecasts over longer time windows than in the mean of the entire group. The assumption follows the idea that in extreme situations the mean is biased by outliers, whereas this is not the case for the *best guess*. In longterm statistics and when considering parameter fields, the mean scores better than the best guess. However, in extreme events it was observed that the *best guess* has a clear advantage over the mean, because it does not take outliers into account. That means, the higher the spread and the higher the uncertainty of the forecast, the more

likely will the best forecast deviate from the mean and the better it scores relative to the mean.

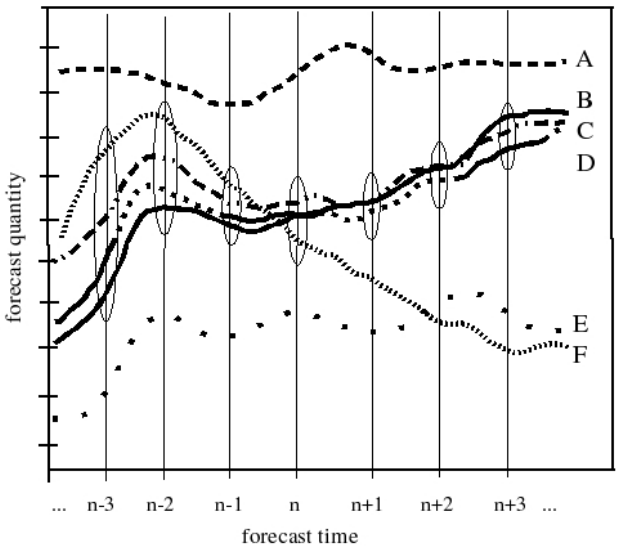

Figure 4.2: Qualitative demonstration of the pmt-filter algorithm

It has been found that the correlation between the prediction quality over a few hours is fairly high. This knowledge is used to find patterns where groups of members perform well over a certain time interval. These pattern are transformed into weights and thereby taken into account in the selection procedure of the *best guess*. In practise this means that the *best guess* is not necessarily the forecast with the highest probability, but rather the most *"reasonable of the better forecast"*.

Figure 4.2 is a graphical demonstration of the pmt-filter. In this example, the focus shall be on six ensemble members (A through F). The ensemble members could also be groups of ensemble members. These members are analysed using clustering techniques. The difference between the *pmt-filter Algorithm* and traditional cluster analysis is that the *pmt-filter* groups that persist over time. In this graphical example replicates B,C,D and F are grouped closely during the last 3 time steps (n-3 to n). In the next time

step replicate F leaves the group and forms a new group with replicate E. Over the three time windows backward (n-1..n-3), the present state n and forward (n+1..n+3) replicates B,C and D represent a clustered group and therefore they may be considered a robust and consistent forecast.

4.5 Graphical Representation of the Uncertainty

A convenient way to display the uncertainty estimate of the ensemble system at specific sites as well as averages over areas is to use contour plots or boxplots. The advantage of the contour plots to represent the probability distributions of a certain parameter is the ease of interpretation. If the forecast is rather certain, i.e. most ensemble members give a similar result, then the band width of the probability plots is also rather thin. In the case of a period of high uncertainty, the band width of the probabilities becomes large. Therefore, it is easy to gain an overview of the period of interest, e.g. low or high uncertainty. The inclusion of lines of the *best guess*, the EPS mean and the analysis complements the plot to a workable graphical interpretation tool.

Figure 4.3 shows an example of a conture probability plot. The upper and lower solid lines represent the maximum and minimum wind speeds in the ensemble. The colours of the areas are determined by the probabilities derived from the ensemble. The most likely value, the *best guess forecast*, according to the *pmt-filter*, is shown as the white dashed line. The thin black dashed line is the EPS mean, the white solid line the analysis.

In the first 24h the uncertainty of the forecast is rather small. After that, the uncertainty triples from around 2-3 m/s to over 6 m/s. At forecast hour 35 it is worth noting that the *best guess* starts following a new group, whereas the mean does not seem to be affected. The same happens in the next hours (36h-42h), when the wind speed increases again. On the development of the analysis, it can be seen that the change from one group of ensemble members to another is not due unstabilities in the algorithm. On the contrary, it confirms the theory that the *best guess forecast* is a good estimate of the uncertainty,

as it follows the ensemble spread more thoroughly than the mean and thereby gives at least an indication of the extreme changes that might occur. The mean is a more conservative estimate and probably too smooth in extreme events.

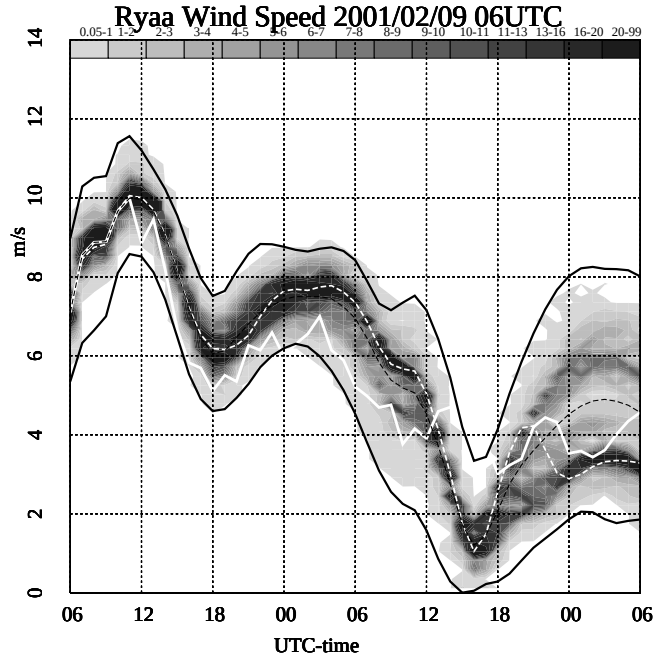

Figure 4.3: Example of a 48H forecast displayed as conture probability plot of wind speed at Ryaa (DK) with the *best guess* (dashed white line), the EPS mean (dashed blck line), Analysis (solid white line), EPS min and EPS max (solid outer lines). In the first 24 hours, where the uncertainty is low, the *best guess* is very close to the EPS mean. After 36 hours the *best guess* starts following another group of ensembles and leaves the EPS mean following closer the analysis. Approx. 6 hours later it leaves it's group again. The analysis follows and confirms that this is not a algorithm problem.

Figure 4.4 displays a box plot of the same forecast as in Figure 4.3. The boxplots are an abbreviated way to describe the statistics of a sample of data in a graphical way. These plots are a summary of the following statistical numbers:

1. Minimum
2. First (Lower) Quartile (25th percentile)

3. Median
4. *Best guess forecast*
5. Third (Upper) Quartile (75th percentile)
6. Maximum

The boxplots are a useful statistical measure of the overall uncertainty of the forecast over the forecast time. The disadvantage of the boxplots is that it is only possible to identify the defined parameters and not other "groups" of possible outcome. Nevertheless, it can be seen that the *best guess* from the pmt-filter is fairly close to the median of the EPS in times of little uncertainty (1h - 24h). When the uncertainty increases in the forecast, the *best guess* leaves the median. This can be seen most pronounced at forecast length 41h until 48h, where the *best guess* is closest to the lower quartile.

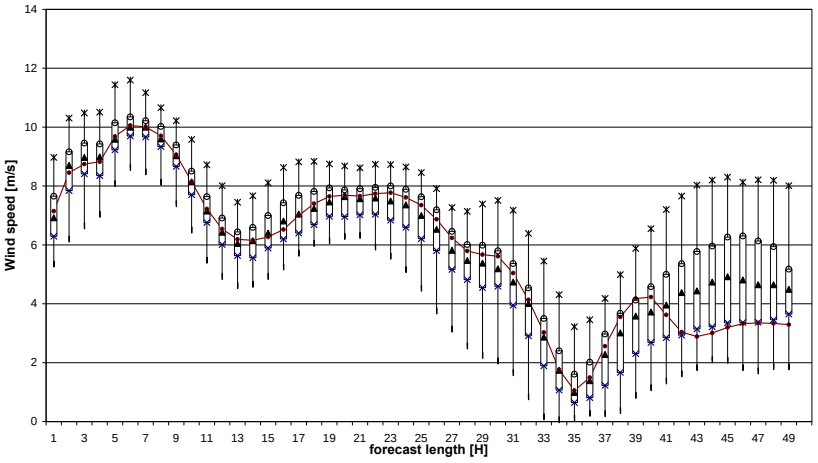

Figure 4.4: Example of a box plot of a 48H forecast at the wind farm Ryaa on the 2001/02/09 06H. The cross denote the maximum, the circle denotes the first (upper) quartile, the triangle denotes the median, the star denotes the lower quartile, the square denotes the minimum of the ensemble and the solid line denotes the *best guess*.

4.6 Verification Methods

The purpose of this study is to introduce a multi-scheme approach for predicting wind speed and wind power and verify it against the current state of the art. The approach is unique in that short-range forecasts are created with an ensemble of 50 members using an multi-scheme approach to perturb the forecast model. The 50 ensemble members are approximately of the same forecast quality. Verification of such a system is not a simple task, because of the vast output created by an ensemble of this size. However, the verification of the ensemble's forecasts can be done with observation verification and field verification.

The advantage of field verification versus observation verification has already been discussed in chapter 2 and will therefore not be discussed here. The verification of this part also focuses on observation verification. Even though field verification is necessary to estimate the full potential of the approach and to cover all error sources, it goes beyond the scope of this work. Nevertheless, it is clear that in any further analysis of the results at a later stage the field verification has to be taken into account.

It should be noted however that the observation verification results are usually a more conservative estimate of the performance than the field verification. Especially in coarse resolution, the latter gives more robust results, because it is area integrated in the model's grid space, whereas single points are only extracted from fields that can contain local errors. Point verification is therefore especially difficult to judge when the forecasts are produced with a horizontal resolution of 0.45 deg (˜45km), as it was in this project. Another point is that the uncertainty estimate of the forecasts is of major importance for system operators, such that the focal point was to investigate the benefits of probabilistic forecasts. In this study, the spread of the ensemble is defined as the standard deviation from the mean. It will be shown that the size and the spread is a parameter of importance when evaluating the sensitivity of the results.

It was found that it is not of benefit to leave out 'bad' members in the verification, because they add value to the spread of the ensemble and hence the estimate of the

uncertainty. The quality of the ensemble members is also of great importance, because of the sensitivity of the model system to the combination of the schemes and the unpredictability of the performance of the ensemble members in certain weather situations is responsible.

4.6.1 Objective Verification

As described before, a NWP model produces area averages, which are built into the equations that form the model. The model is however also fed with point observations. In some areas the density of these observational networks is significantly higher than the model can represent in its finite grid space and in other areas there are far less observations than grid points. The state of the atmosphere (analysis) from which all forecasts are started does also not always contain all available observations. Nevertheless, it is unrealistic to expect that a NWP model can do better in average than its corresponding analysis, except in areas where very few observations exist.
In the case of Denmark, the area is well covered by observations, but the analysis that was used in the experiments did not use all of them, because the analysis came from a relative coarse global model, which is not capable of using more than a fraction (in average 30%) of the available observations near Denmark (see Table 3.1 and Section 2.2.6). This means that the analysis does not contain all the local extremes in the weather over Denmark.
The analysis had in some cases quite significant errors in the observation verification for that reason. The fact that the verification of the forecasts is done directly with the observations means that the errors of the forecasts also include the error of the analysis. This needs to be taken into account when analysing the results.
The verification was done with the following parameters:

- 10m wind speed (v10s)

- model level wind speed at approx. 30m (u31,v31)

- potential wind power (pot) with a standard power curve computed from mean sea level pressure (mslp) and 10m wind speed (v10s)

- wind power pwr (pwr) with site specific power curves

The advantage of the combined mslp and v10s in the potential power is that the flat parts of the power curve contribute less to the error than the steeper parts (see Figure 2.3). An error in the predicted wind speed is very critical at 9 m/s and less critical at 18 m/s unless a major part of the turbines are in bigger farms where the power curve is rather flat. The forecast error (bias) is defined according to Figure 3.1 to the sum of a local error and the model error:

$$F - F_{obs} = (F_{ana} - F_{obs}) + (F - F_{ana}) \tag{4.1}$$

where $(F_{ana} - F_{obs})$ is the local error and $(F - F_{ana})$ is the model error.

The assumption behind this splitting is that a forecast can never be better than its corresponding analysis and that the goal is reach an accuracy close to that of the analysis. In pratice this means that it is the analysis that is measured agains the observations and the forecast is measured against its corresponding analsyis. After it was found that the local error dominates the observation verification of the 10m wind and other surface parameters, especially when modelling in the coarser resolutions (e.g. in a $0.30^{\circ} circ$ grid), this splitting was a very useful method to find and study the non-model dependent error sources. This dominance of the local error has also been shown in other studies (Moehrlen et al., 2001,2002 and Jørgensen et al. 2001, 2002). To improve the local error statistics, it was demonstrated that increased model resolution helps. The computational cost of high resolution modelling is however significant compared to the improvements that can be achieved.

On the other hand, the ultra short-range forecasts are typically close to the analysis in accuracy and considered accurate enough for wind power prediction. This is referred to as the *minimum forecast error*, and the goal is to reach this level of accuracy. The technique that is developed and applied in this work is however only the beginning

towards this target. The remaining 50% of the error has to be captured by making use of the uncertainty estimate. A reasonable strategy in a "real" environment could be to classify the periods were forecasts are reliable and periods with high uncertainty. In the periods where the forecasts are reliable, high resolution nested models can be applied to increase the accuracy of the wind parameters. In periods of high uncertainty the errors can be reduced by using the ensemble mean, which is a smoothed average. The target of reducing the mean error of forecasts by 50% toward the *minimum forecast error* by the ensemble approach can become realistic with this method and would mean a large step forward.

4.6.2 Verification Parameters for the Ensemble

Standard statistical parameters are used to verify the ensemble prediction system together with a parameter typical for ensemble prediction verification. In this development phase it was found that using standard statistical tests reduces the uncertainty in the interpretation of the data. The verification therefore took place with the following parameters;

- Bias
- Standard Deviation
- Root Mean Square error
- Variance
- Skill Score

The standard deviation, root mean square error and bias are the statistical measures for the performance of a model and will therefore not be explained in more theoretical detail. The equations can be found in the Appendix B. The variance is an ensemble spread measure. This should be closely related to the standard deviation and be of the same magnitude. The skill score is a widely used parameter to compare the skill

of different forecasts (e.g. Wilks, 1995; Mylne, 2000). It is a direct verification of a forecast against a reference forecast and a perfect forecast. The reference forecast is usually a standard forecast such as persistence or climatology. In this case, the analysis is used as the perfect forecast:

$$ss = \frac{fc_{ref} - fc}{fc_{ref} - fc_{ana}} \tag{4.2}$$

where fc_{ref} is the reference forecast, fc_{ref} is the perfect forecast.

The skill score has a maximum value of 1 (or 100%) for a perfect forecast and 0% for a performance equal to the reference forecast. The skill score has no lower limit. This means that negative values represent lower scores than the reference forecast. In this study the reference forecast is constructed to simulate the Danish Meteorological Institute's operational Hirlam setup (year 2001).

Figure 4.5: Verification Sites in Denmark

This was used to have a measure of the performance relative to the data that is used currently by Eltra. As perfect forecast a 1h to 6h forecast was chosen. In fact, verification took place with two *perfect forecasts*, where different model configurations were used.

The ensemble mean and a weighted mean are computed in the verification itself. The weight coefficients are computed as a ratio of an area averaged standard deviation over the entire period. An *best guess* and a *weighted best guess* are computed with the pmt-filter algorithm and a deterministic forecast is added. A so called *winner-of-the-day* is computed, which reflects the potential of the ensemble. This is of course only a reference and only possible in historic mode. It should give an indication of the potential accuracy, if the EPS classification was capable of choosing the best member of the ensemble. The control forecast (ctrl) is the ensemble member that provides boundary data to the deterministic forecast. The analysis is also included. The reference forecast is used to rank the ensemble members and to quantify the improvement of the approach.

The verification is conducted with and for $50 + 6 = 56$ members. Statistical output is obtained for 12 Danish wind farms (eltra), 7 synoptic stations (dk), 5 Irish wind farms (irl) and 3 Irish wind masts (ucc) (see Figure 4.5 and 3.5 in Chapter 2).

Chapter 5

A Multi-Scheme Ensemble Prediction System to forecast Wind Power

In the previous chapter the benefits of using ensemble predictions were discussed and the design of an ensemble prediction system described. In this chapter actual forecasts from that ensemble prediction system (EPS) over a three month period are presented and verified. There are large amounts of data and parameters to be evaluated from an experiment over three months with 4 times 50 forecasts per day. Therefore, only a selected fraction of the results can be presented here. The focus in this evaluation is on the wind speed and wind power at 27 stations dispersed over Denmark and Ireland. Skill score, standard deviation and variance are the statistical parameters that will be shown and discussed. The root mean square error has been neglected in this verification, because the focus of the evaluation was on a period of time and not on individual days, such that the root mean square error equals the standard deviation.

5.1 Quality of the Ensemble Predictions System

The verification of the ensemble prediction system first focused on the quality of the individual ensemble members. This is an important aspect for the applicability of the

approach and probabilistic products resulting from the ensemble prediction system. The second part of this section focuses on the performance of the ensemble system in general. One important aspect in this investigation was the implications on the size of the ensemble and the selection of the applied perturbations on the performance of the entire system.

5.1.1 Quality of the individual Ensemble Members

The quality verification of the individual ensemble members commenced by investigating how well the individual ensemble members perform. To assess this and also the performance of the approach, the best member of the period for each of the 27 stations was computed. Note, that this is only possible in historic mode, where the actual recorded values are already known.

It was found that there was no obvious pattern of best members over the period at any of the stations. In fact, when plotted against each other, the correlation of members with best forecasts was found to be a random distribution of points at all stations. It can be concluded from this investigation that the quality of the individual members can be considered as equally good in long term statistics. It should be noted however, that certain members produced better results during certain weather conditions than others.

It was also observed, and will be shown in the following paragraphs, that the extension from 50 members to 100 members by including the forecasts produced 6h earlier (at 00h UTC) did not increase the quality of the ensemble. This indicates that the quality of the ensemble is a result of the best selection of ensemble members rather than the size of the ensemble system. It will in fact be shown that the wrong selection strategy can decrease the quality of the ensemble products such as the *best guess*.

5.1.2 Overall Performance of the Ensemble Prediction System

The performance of the ensemble system has been evaluated by computing skill scores. The skill score is a measure of the gain in predictability according to Equation 4.2. The tables that contain the statistical results of the verification for the individual 27 stations can be found in Appendix E. In this chapter the focus will be on area and country averages with reference to the tables in the appendix for some selected cases. The skill scores averaged over the Danish and Irish areas are summarised in tables for wind speed and wind power. The station "denmark" is the average of the "eltra" area and the "synop-dk" area, "ireland" is the average of the Irish wind farms "windf-irl" and the UCC masts "ucc". Note, that "denmark" and "ireland" are averages of the output statistics of the areas. For the statistics of the areas "eltra", "synop-dk","windf-irl" and "ucc" the parameters (wind speed and wind power) have been averaged before the statistics are applied. These sites therefore represent upscaled values. They are referred to as area averages, whereas "denmark" and "ireland" are country averages. The column with skill scores represents the normalised error (=standard deviation/mean) for the site. Thus, high values indicate mostly erroneous observations. In a few cases the errors are also a results of systematic errors in the model system. This means that the statistical numbers presented in this work are all based on infinite error tolerance. The wind power is presented in unit kW for the Irish stations, such that the statistical parameters take on higher values. The small values in the analysis column are a quality control of the two analyses used in the computation of the skill scores (see also section 4.6.2). The threshold value for the quality check was set to 1 and was only slightly above that value for wind power at the Danish synoptic stations .

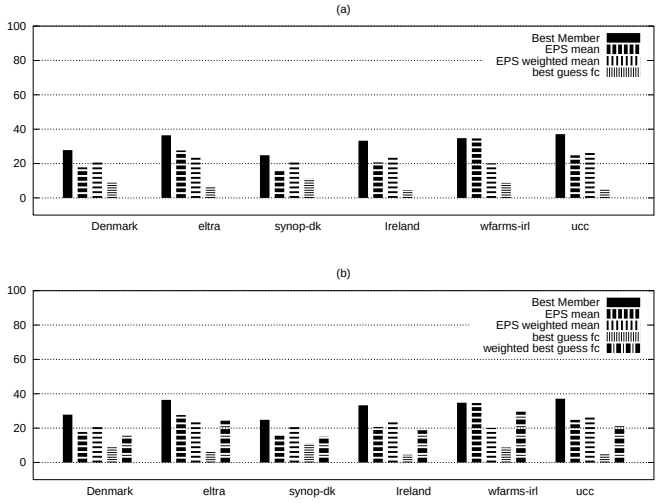

Figure 5.1: Skill Scores for 50 Member Ensemble integrated over the Danish and Irish Area. Plot (a) shows results with raw pmt-filter, plot (b) shows results with weighted parameters using the forward-backward pmt-filter

For the other statistical parameters (stdev, variance), the first column represents the results for the analysis and gives a measure of how well represented a certain station is by the model. In a few cases it was however found that the best member was superior to the analysis, the mean or the reference forecast. In these cases it is believed that the resolution of the analysis is too coarse to represent orographic features correctly, which is always a problem when verifying at specific points. The second, third and forth columns give the scores of the best member (winfc), the mean, the weighted mean, which includes long term statistical coefficients or weights for the individual members (wmean), respectively. The fifth and sixth columns (in the case of 100 members) represent the probabilistic forecasts from the ensemble computed with the *pmt-filter*, which are referred to as the *best guess* (bg), and the *weighted best guess* (wbg), which included forward-backward stepping.

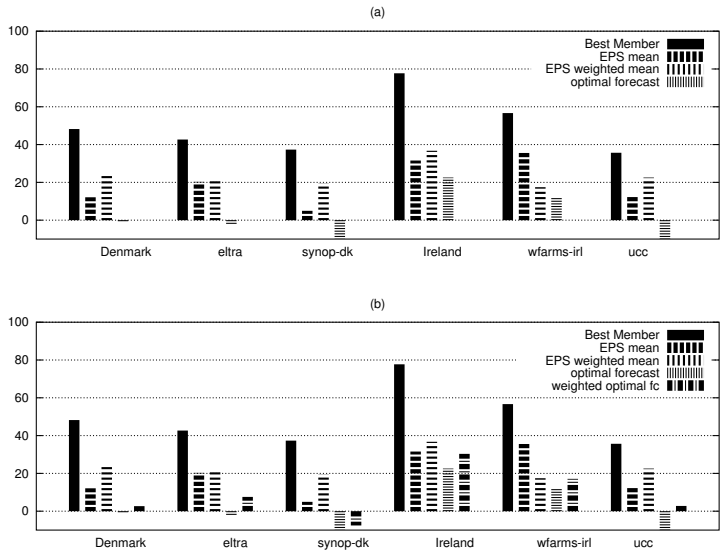

Figure 5.2: Skill Scores for 100 Member Ensemble integrated over the Danish and Irish Area. Plot (a) shows results with raw pmt-filter, plot (b) shows results with weighted parameters using the forward-backward pmt-filter

Figure 5.1 and Figure 5.2 correspond to Table 5.1 and Table 5.3, respectively. These show the area integrated skill scores for 50 Members for wind speed and wind power. It can been seen in Table 5.2 and Table 5.4, that using 100 members does not necessarily increase the skill scores. This is because the forecast error increases linear with forecast length, and hence the forecasts starting 6h earlier incorporate a larger error. This error can only be removed by applying weight coefficient from longterm statistics. The effect of these weight coefficients is reflected in the results from the weighted mean in wind speed and in wind power.

para	site	ana	winfc	mean	wmean	bg
skill	denmark	0.19	28.27	21.72	22.55	13.21
	ireland	0.23	39.76	29.62	24.55	8.42
	eltra	0.16	25.50	16.28	21.59	8.73
	synop-dk	0.22	33.39	31.76	24.33	21.49
	windf-irl	0.24	39.88	28.54	20.55	20.91
	ucc	0.21	39.72	30.06	26.20	3.27
stdev	denmark	1.22	1.47	1.49	1.49	1.52
	ireland	1.80	2.06	2.11	2.13	2.20
	eltra	1.28	1.61	1.65	1.63	1.69
	synop-dk	1.16	1.32	1.32	1.34	1.35
	windf-irl	1.85	2.01	2.04	2.06	2.05
	ucc	1.75	2.12	2.18	2.20	2.34
var	denmark	2.93	3.08	3.11	3.10	3.10
	ireland	3.80	3.72	3.93	3.93	4.02
	eltra	3.48	3.60	3.70	3.66	3.70
	synop-dk	2.38	2.56	2.52	2.54	2.49
	windf-irl	3.69	3.51	3.78	3.79	3.82
	ucc	3.91	3.93	4.07	4.08	4.21

Table 5.1: Summary of the statistics of wind speed with 50 ensemble members. The abbreviations are as follows: 'ana' is the analysis, 'winfc' is the winner of the period, 'mean' is the ensemble mean,'wmean' is the weighted mean, 'bg' is the best guess

In the Eltra area, the scores of the weighted mean are better than the mean of the ensemble in 11 out of 13 stations. In the Danish Synoptic stations the weighted mean has lower skill scores at only one station (Taasinge). In Ireland, the weighted mean has lower skill scores particularly at the wind farms, but better skill scores at the masts. In the comparison to the entire area, the skill scores of the weighted mean are lower than the skill scores for the mean.

para	site	ana	winfc	mean	wmean	bg	wbg
skill	denmark	0.19	27.81	17.80	22.22	8.82	16.45
	ireland	0.23	36.46	27.59	24.71	6.20	24.33
	eltra	0.16	24.86	16.23	20.85	11.16	15.19
	synop-dk	0.22	33.25	20.69	24.74	4.51	18.77
	windf-irl	0.24	34.79	34.63	20.13	8.72	29.57
	ucc	0.21	37.12	24.78	26.55	5.18	22.23
stdev	denmark	1.23	1.47	1.51	1.49	1.54	1.51
	ireland	1.80	2.07	2.10	2.11	2.19	2.12
	eltra	1.29	1.62	1.66	1.64	1.68	1.66
	synop-dk	1.16	1.32	1.35	1.35	1.39	1.36
	windf-irl	1.86	2.01	2.01	2.05	2.07	2.03
	ucc	1.75	2.12	2.19	2.18	2.31	2.21
var	denmark	2.94	3.10	3.10	3.12	3.08	3.10
	ireland	3.81	3.73	3.82	3.93	3.88	3.82
	eltra	3.50	3.61	3.70	3.68	3.66	3.71
	synop-dk	2.39	2.58	2.50	2.55	2.50	2.49
	windf-irl	3.70	3.52	3.65	3.79	3.71	3.66
	ucc	3.92	3.94	3.98	4.08	4.06	3.98

Table 5.2: Summary of the statistics of wind speed with 100 ensemble members. The abbreviations are as follows: 'ana' is the analysis, 'winfc' is the winner of the period, 'mean' is the ensemble mean,'wmean' is the weighted mean, 'bg' is the best guess

The reason for that seems to be the fact that the coefficients were computed as an average over the model area. In the danish areas these coefficients had positive effects, whereas in the Irish areas, these coefficients seems to be very dependent on the terrain and local effects are not captured well enough by the coarse resolution ensemble. Long term statistics might help in reducing the error at these sites.

5.1.3 Statistical Performance Tests

When summarising the statistical performance tests, it can be concluded that the skill scores for wind speed varied between 20% and 30% for the mean and weighted mean in both areas (Denmark and Ireland). This indicates a gain in predictability of approximately 10h-15h relative to the reference forecast.

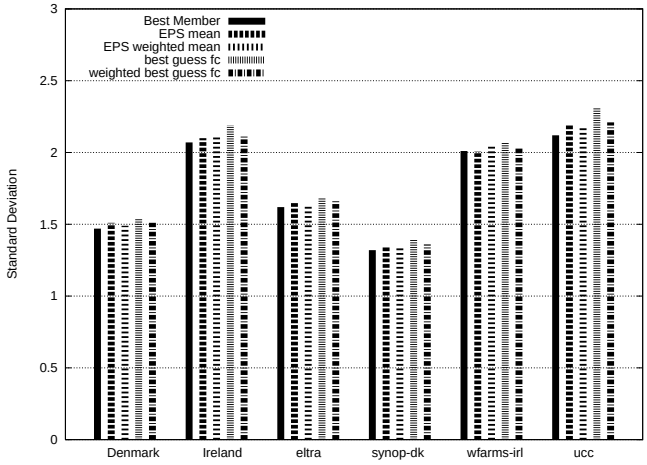

Figure 5.3: Standard Deviation of all stations for 100 members for wind speed including the weighted best guess

Expressed in standard deviation this corresponds to values ranging from 1.0 to 2.5 in average, which was found to around 1.5 in Denmark and slightly above 2.0 in Ireland. For wind power the standard deviation is slightly lower, reaching from 0.8 to 2.0 in average, whereas it is slightly over 1.0 in Denmark and close to 2.0 in Ireland. The results of standard deviation including the weighted mean can be seen in Figure 5.3 and Figure 5.4, which summarises these results.

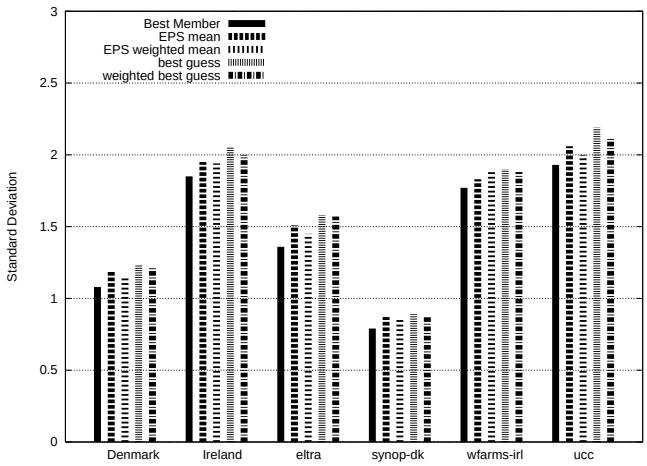

Figure 5.4: Standard Deviation of all stations for 100 members for wind power including the weighted best guess

The potential improvement of the ensemble relative to the reference forecast lies between 25% and 40%, with a maximum of 77% and minimum of 2.5%. This indicates a potential gain in predictability of 15h-20h relative to the reference forecast. The *weighted best guess* benefits from the forward-backward stepping in the pmt-filter. Whereas the *best guess* shows improvements between 8% and 20% in wind speed, the weighted mean improves between 15% and 29%. This corresponds to a gain in predictability of 7h-14h relative to the reference forecast. The standard deviation of the best member and the best guess lies within the same range as for the mean of the ensemble.
In Figure 5.5 and Figure 5.6 show the differences in standard deviation between the area average and the individual sites (Eltra area). The variance is in general higher in the Irish area than in the Danish Area. The values are in the region of two in Denmark and three in Ireland for wind speed and for wind power. This reflects the fact that the average wind speed in Ireland is almost 3m/s higher than in Denmark.

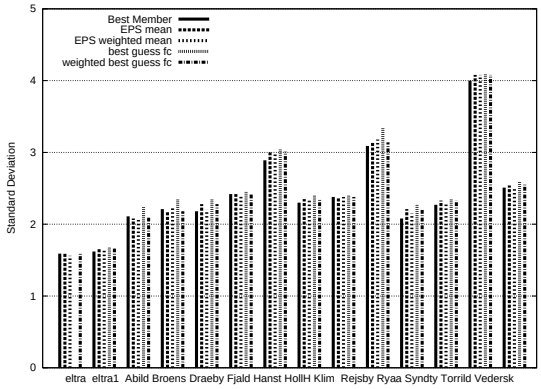

Figure 5.5: Standard Deviation of all stations for 100 members for wind speed including the weighted best guess from the pmt-filter

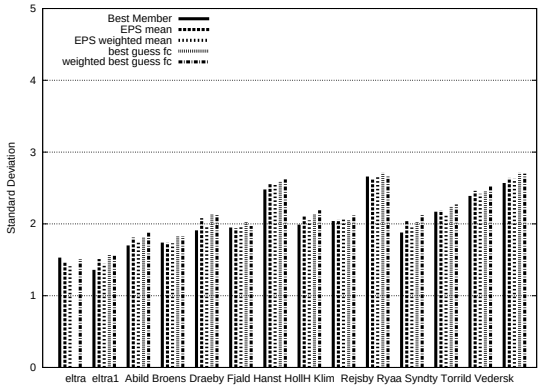

Figure 5.6: Standard Deviation of all stations for 100 members for wind power including the weighted best guess from the pmt-filter

Figure 5.7 and Figure 5.8 give a more detailed view upon the results in the Eltra area for both wind speed and wind power. Plot (a) shows the skill scores for 50 members

and plot (b) shows the skill scores for 100 members including the *weighted best guess* (wbg).

para	site	ana	winfc	mean	wmean	bg
skill	denmark	0.59	48.66	19.46	24.69	15.71
	ireland	0.62	46.22	21.67	21.07	6.32
	eltra	0.43	37.96	8.11	20.36	0.81
	synop-dk	1.21	77.60	50.17	36.40	56.02
	windf-irl	0.66	60.88	24.33	18.58	5.91
	ucc	0.58	38.68	20.30	22.35	6.54
stdev	denmark	0.91	1.07	1.17	1.15	1.18
	ireland	1.61	1.86	1.97	1.97	2.04
	eltra	1.07	1.36	1.50	1.44	1.53
	synop-dk	0.75	0.79	0.83	0.86	0.82
	windf-irl	1.65	1.77	1.88	1.90	1.94
	ucc	1.57	1.94	2.05	2.04	2.14
var	denmark	1.99	2.19	2.30	2.28	2.29
	ireland	3.14	3.20	3.33	3.33	3.41
	eltra	2.89	3.04	3.17	3.11	3.21
	synop-dk	1.10	1.34	1.43	1.44	1.37
	windf-irl	3.05	3.00	3.24	3.22	3.31
	ucc	3.22	3.40	3.43	3.44	3.50

Table 5.3: Summary of the statistics with 50 ensemble members for wind power. The abbreviations are as follows: 'ana' is the analysis, 'winfc' is the winner of the period, 'mean' is the ensemble mean,'wmean' is the weighted mean, 'bg' is the best guess

A difference between the *best guess* and the *weighted best guess* is apparent. Since the weighted best guess is computed by following trends in the forecasts, this result confirms that this method is beneficial for interpreting probabilistic forecasts. These forecasts in fact have skill scores close to those of the mean of the ensemble, which is above 20% at half of the stations.

In Figure 5.7 Hanstholmhavn however shows a negative skill score for the best member

and skill sores higher than 100% for Rejsby.

Note, that the skill score has no lower limit and takes on a negative value, if the forecast has poorer skills than the reference forecast.

Hanstholmhavn is situated directly at the sea and faces the North Sea. In the coarse resolution of the model, the accuracy of the land sea mask is very poor, which results in poor performance of the model in general. It is therefore quite possible that the reference forecast has higher skills than the forecast. In Abild, Broens, Draeby and Ryaa the skill scores for the best guess of wind speed is negative for the same reason.

para	site	ana	winfc	mean	wmean	bg	wbg
skill	denmark	0.59	48.23	12.11	24.19	-1.07	2.66
	ireland	0.62	42.68	20.26	20.87	-2.71	7.57
	eltra	0.43	37.33	4.92	19.57	-9.81	-7.57
	synop-dk	1.20	77.73	31.56	36.70	22.56	30.35
	windf-irl	0.66	56.69	36.02	17.47	12.50	17.12
	ucc	0.58	35.67	12.37	22.57	-10.32	2.80
stdev	denmark	0.91	1.08	1.19	1.15	1.23	1.22
	ireland	1.60	1.85	1.95	1.94	2.05	2.00
	eltra	1.07	1.36	1.51	1.45	1.58	1.57
	synop-dk	0.75	0.79	0.87	0.86	0.89	0.87
	windf-irl	1.65	1.77	1.83	1.88	1.90	1.88
	ucc	1.56	1.93	2.06	2.00	2.19	2.12
var	denmark	2.00	2.20	2.30	2.29	2.29	2.34
	ireland	3.14	3.20	3.23	3.32	3.33	3.34
	eltra	2.90	3.06	3.17	3.13	3.18	3.26
	synop-dk	1.10	1.35	1.42	1.45	1.41	1.41
	windf-irl	3.06	3.01	3.13	3.22	3.19	3.22
	ucc	3.22	3.40	3.33	3.42	3.47	3.47

Table 5.4: Summary of the statistics with 100 ensemble members for wind power. The abbreviations are as follows: 'ana' is the analysis, 'winfc' is the winner of the period, 'mean' is the ensemble mean,'wmean' is the weighted mean, 'bg' is the best guess

In Rejsby all variables (best member, mean, weighted mean, best guess) of the ensemble have better scores than the perfect forecast, which means that the skill score is higher than 100%. This is due to noise in the initial conditions of the perfect forecast. At station "multi" these stations are therefore excluded. Apart from this the area "multi" resembles the "eltra" area.

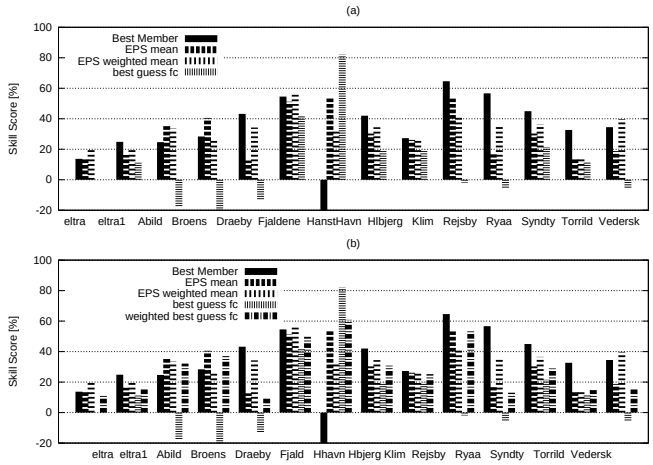

Figure 5.7: Skill Scores of wind speed for all stations in the Eltra area. Plot (a) shows results with raw pmt-filter (50 members), plot (b) shows results with weighted parameters using the forward-backward pmt-filter (100members)

Figure 5.9 gives a more detailed view upon the results in the Danish synoptic stations for both 10m-wind speed. For wind speed it shows in 5 out of 7 stations negative skill scores for the best guess. The weighted best guess on the other hand is in all tests positive and lies between 10% and 30%. As mentioned before, the skill scores are 60% for the best guess and 77% for the weighted best guess in Taasinge, which seems to be a result of instabilities in the pmt-filter under certain conditions, where it follows a wrong trend.

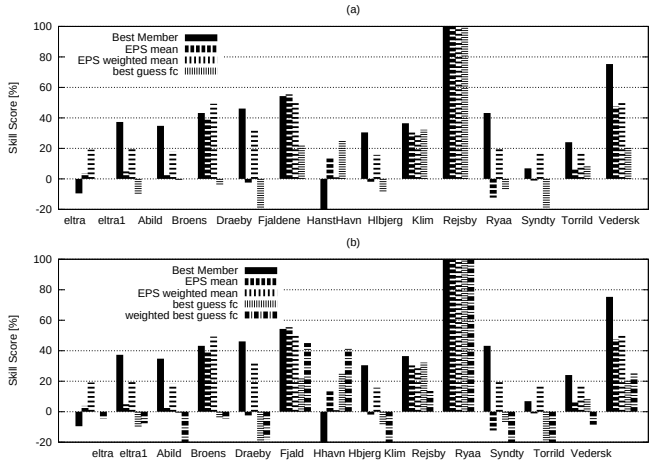

Figure 5.8: Skill Scores of wind power for all stations in the Eltra area. Plot (a) shows results with raw pmt-filter (50 members), plot (b) shows results with weighted parameters using the forward-backward pmt-filter (100members)

This problem seemed to be solved by considering the past trend with the forward-backward stepping. The function did not explode and the results are in line with the results for the ensemble mean (see graph). This was however not the case for wind power, where the weighted best guess is only superior to the best guess in two cases.
In Aarhus, Gedser and HvideSande a wind power potential was computed from 10m wind speed, where the best member of the ensemble and the reference forecast are better than the analysis and which resulted in values above 100% or below zero. There are no measurements of wind power available at these stations, such that a further analysis of the results in power space was not possible.

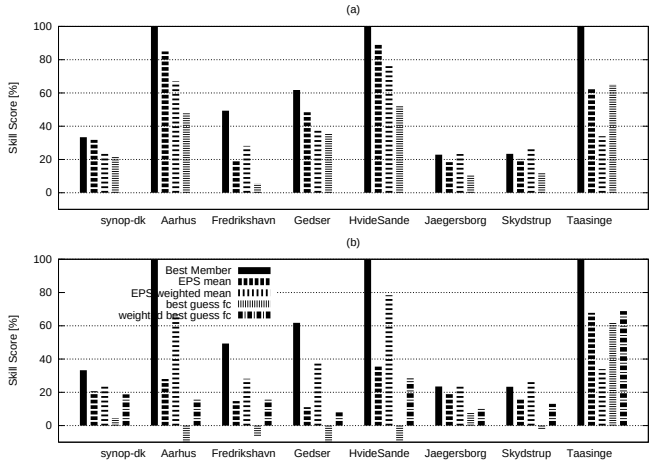

Figure 5.9: Skill Scores of wind speed for all stations at the Danish Synoptic Stations. Plot (a) shows results with raw pmt-filter (50 members), plot (b) shows results with weighted parameters using the forward-backward pmt-filter (100members)

5.2 The Uncertainty Estimate

As described in the project description, the graphical interpretation of the uncertainty estimate is a convenient way of getting overview over the forecast quality. The contour plots show the probability of the ensemble towards a certain outcome. Box plots on the other hand are a convenient way to describe the statistics of a sample of data in a graphical way. In verification mode, the observations and analysis can also be added (in both plotting techniques). In forecast mode only the EPS mean, the weighted mean and the best guess would be displayed with lines. The difference in performance of the best guess against the EPS mean, EPS weighted mean, the observations or analysis can however only be estimated with long term statistics.

As described in detail in the previous chapter, the pmt-filter takes the time development

into account, such that a trend of the most likely group over the last hours is followed. This was shown in the example Figure~\ref{ryaa}, where it was demonstrated that the forecasts actually fall into different groups, when the uncertainty is high. In these cases the groups tend to remain for a couple of hours. The curve for the 'best guess' is then following the point with the highest probability from time step to time step.

5.2.1 Interpretation of the Uncertainty Estimate

Even though Figure 4.3 and Figure 4.4 were only examples of one forecast for one site, these plots contain all necessary information about the uncertainty estimate. The graphical interpretation is useful for specific sites, but also for area integrals and for practical applications this eases the interpretation of the uncertainty significantly.

The goal of this study with regard to the quality of the ensemble was to verify, whether the present ensemble can produce enough spread to ensure that the actual occurrence of a certain weather parameter ("truth") lies within the ensemble spread. If this is the case, the ensemble fulfils the requirements, which were set in the beginning of the study.

An objective way to verify the uncertainty estimate is to measure the correlation of the spread of the ensemble with the error of the ensemble mean. This correlation has been computed for area integrated wind speed and wind power and is for both areas Denmark and Ireland 0.93. Table 5.5 gives an overview and shows the improvement and hence benefit of using a bigger area. When averaging over the North Sea the correlation increases to 0.97 for wind speed and 0.96 for wind power. The correlation is hard to interpret on a single site, because it consists of a local error and a large scale meteorological error. The local error can not be separated except with a horizontal summation over sites before computing the correlation.

This method has also been used by Stendsrud et al. (1999) and Hamill and Colucci (1998). In both studies the NCEP ensemble system with the Eta-Model and the RSM (Regional Spectral Model) for short range prediction was used. Both studies found

area	wind speed	wind power
Denmark	0.94	0.94
Ireland	0.92	0.92
North Sea	0.97	0.96

Table 5.5: Summary of the area averaged correlation of ensemble spread and ensemble error

that there was little correlation between the spread of the ensemble members and the accuracy of the ensemble. And in both cases the conclusion was that the lack of correlation between spread and forecast uncertainty presents a challenge to the production of short-range ensemble forecasts. In that respect the correlation of more than 0.93 that was achieved over the 3 months period seems to present a significant result in the area of short-range ensemble prediction. Subjective analysis of the uncertainty estimate throughout the entire period confirmed this method as a realistic measure of the EPS system's ability to predict the uncertainty of the forecasts.

5.3 Control forecast and Deterministic forecast

The deterministic forecast is a downscaling of the control forecast from 45km horizontal resolution to 5km. It was first planned to run a deterministic forecast in a fully dynamic way by choosing each day the member with the highest probability to catch the weather situation of the day. The problem associated with this procedure is that each member has a different long term bias. When using the output of the deterministic forecasts, this bias has to be subtracted. Because of the short integration period of three months the bias corrections would not have been accurate enough. Therefore, the downscaling of the control forecast took place for one selected member of the ensemble. The selection criteria included the average skill scores, stability of the model and the execution time. Results from these deterministic runs in the Eltra area and the Irish area are shown in Figure 5.10.

In average the improvement in skill scores of the deterministic forecast is only 5% for the Eltra area and the Irish masts (ucc). The small improvement is the result of averaging. It can be seen in the graphs, that there are some sites, where the deterministic forecast improves 20-30% in skill scores and other sites, where there is no or very little improvement. As mentioned before, some of the sites (e.g. Abild, Broens, Lendrum and Ringaskiddy) showed negative skill scores for the control forecast, which is also reflected in some of the deterministic forecasts.

One station (Hanstholmhavn) also had lower skill scores for the deterministic forecast than for the control forecast. All these cases are a mixture of bad observations, lack of ability of the model to resolve the terrain and local effects that are not captured by the model. These phenomena have not been studied in more detail, because these effects have been investigated in Chapter 2 and 3. It was shown that most extreme events can only be captured with a very high resolution model (e.g. 1.4km) and in some cases manual adjustment of the model's orography to account for local effects was necessary (see also Moehrlen et al, 2001, 2002).

At the Irish wind farms the analysed forecast show less accuracy than the reference forecast, ensemble mean and some of the ensemble member's forecasts. In these cases the coarse resolution of the analysis cannot resolve the complexity of the terrain, and there are too few observations in the Atlantic. Therefore, the skill scores are higher than 100% in Bessybell and in the Irish average (irl). In Kilronan, Milan Hill and Tursillagh there are improvements in skill score of approx. 30%. In Lendrum and Kilronan the model can also not resolve the complexity of the terrain at the coarse resolution and as a consequence the control forecasts are of rather poor quality.

5.4 Skill of the Multi-Scheme EPS Experiment

The goal of this experimental study was to demonstrate the benefit and improvement of the forecast quality from an ensemble prediction system in comparison to a deterministic forecast and the very short-range analysis (0-6h). It is not possible to compare the

results with those from other studies such as Mylne et al. (2000), Evans et al. (2000), Stensrud et al. (1999), Hamill et al. (1998) or Buizza et al. (2001), because in these Brier Scores on non-local fields such as 500HPa, 850HPa geopotential height, temperature, mean sea level pressure or precipitation have been used. The difference between Skill scores, which will be used n the following analysis, and Brier scores is that the Brier Scores are a measure of the mean square error of probabilities.

That is, the Brier Scores take on a value of 1, if the event occurs and a value of 0, if it does not. Hence, this method depends on the size of the bins and is therefore unsuitable as a measure of wind speed or wind power. The skill scores measure the error relative to a reference forecast and an analysis.

In this study, the skill score is based on the standard deviation. This means that in the computation of the skill sores the error of the forecast compared to the observation is measured and then compared to the corresponding error measures for the reference forecast and the analysis (see Equation 4.2). By using the skill scores, the gain in predictability was found to be 9-12 hours.

The improvement in skill scores reaches from only 8% for the best guess of the wind speed in the Irish area to up to 50% for the best guess of the power prediction averaged over the Danish Synoptic stations. The potential of the EPS measured as the best member of the ensemble is in average around 40% in skill scores. The best guess derived from the pmt-filter is in average around 20% in skill scores for the forward-backward algorithm (wbg), whereas it is almost impossible to average the plain best guess. The results showed the entire spectra of the skill scores up to 38%. This nevertheless means that a gain in predictability of at least 9h was achieved.

For stability reasons it was found to be crucial to take the past and the future into account in the selection procedure for the best guess. Since the best guess is a so-called probability product (also referred to as *uncertainty estimate* earlier in the document), it was important to derive an algorithm that is relatively stable. This meant in fact, that the dynamic selection of this product had to be limited to some extend.

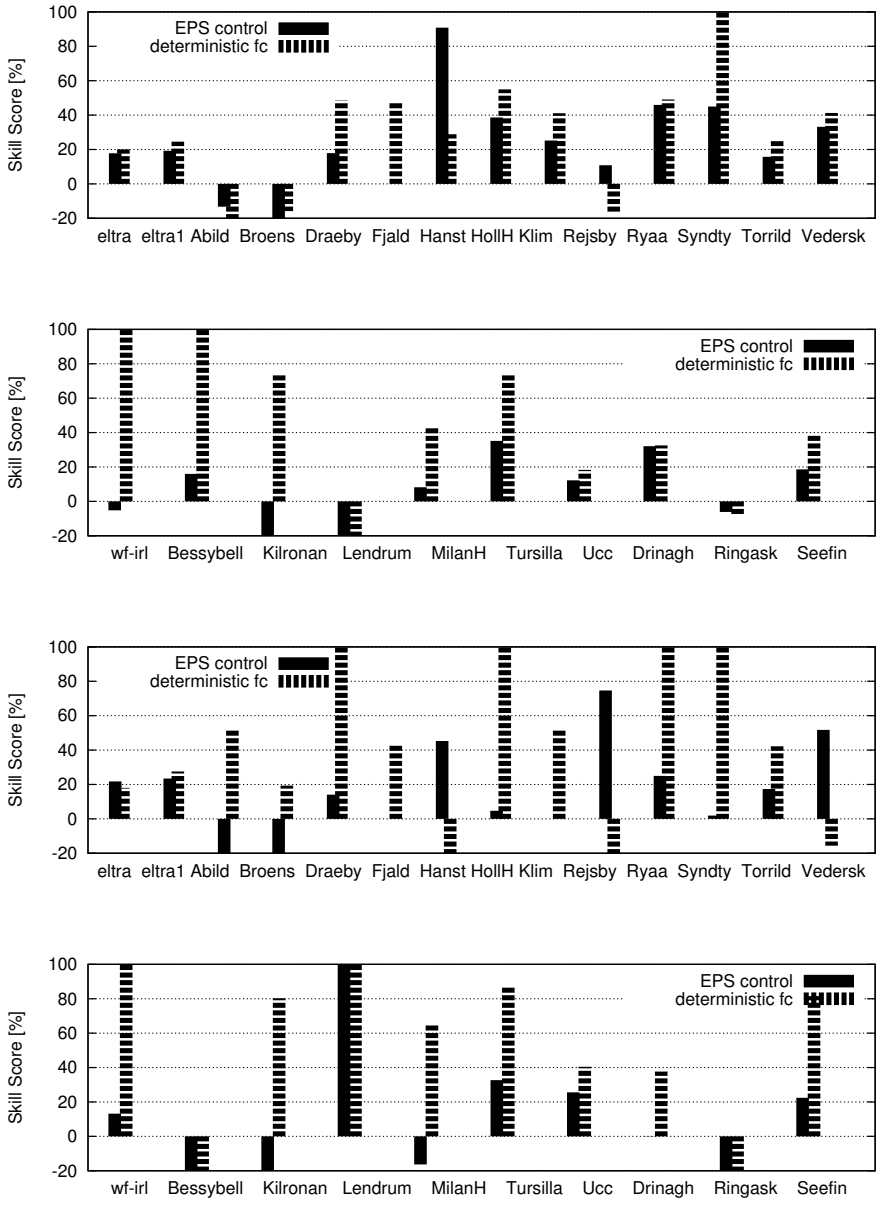

Figure 5.10: Skill scores (ss) of control forecast and deterministic forecast for 50 members. Plot (a) shows ss of wind speed for the Eltra sites, plot (b) shows ss for wind speed for the Irish sites, plot (c) shows ss of wind power for the Eltra sites and plot (d) shows ss of wind power for the Irish sites

Especially when the uncertainty of the forecast was high, such as in cases where there

are two or more clusters of members that showed a certain development, it became crucial that the selection procedure followed the trend from the previous selection. The deterministic forecast has in average around 10-20% higher skill scores than the control forecast. This can be accounted to the model resolution increase from 0.45° to 0.05°, even though it seems that the loss in accuracy is recoverable by the ensemble.

To summarise, the purpose of this study was to demonstrate the value and the benefits of a short-range ensemble system over a single deterministic forecast with respect to a very special end user. To verify a system in historic mode against an operational system can never be a fair comparison. Therefore, it should be emphasised that this study fulfilled its goal to demonstrated that the main improvements of forecasts were not achieved by only improving one individual member, but by the sum of the ensemble members and a suitable selection procedure.

Chapter 6

Conclusions

This thesis identified the main problems in wind speed and wind power forecasting and demonstrated how the current forecasting accuracy can be improved to overcome many of these problems. The research carried out in this work revealed that wind energy is such a demanding area with respect to forecast accuracy that there is an urgent need for new prediction methods to be investigated and applied. Two extensive numerical experiments with a weather prediction model have been undertaken to verify this statement:

- Deterministic Forecasts with various horizontal resolutions
- Ensemble Forecasts with a Multi-Scheme Ensemble Prediction System

The first experiments dealt with the requirements for the accuracy of wind power forecasts by applying deterministic forecasts in various horizontal resolutions. None of the applied resolutions could however satisfy the specified requirements. In other words, increasing the resolution did not reduce the forecast errors, not even at resolutions of 5km or 1.4km. This is in line with the results from Zhu et al. (2001), which indicate that using the same computational resources, potentially more economic benefit can be gained from generating an ensemble of forecasts than from increasing the horizontal resolution of the control forecast. The conclusion from these experiments was therefore that the forecast error needs to be quantified, if it is not possible to reduce it.

Knowing the uncertainty of the forecast can balance the lack of accuracy in decision making environments such as a transmission system operator. For example, it can be used to adjust the spinning reserve required to accommodate a percentage of approximately 10% and more of wind generated electricity into the grid when prediction errors occur. The required spinning reserve in an electrical market can change from 10% to 100% of installed wind energy capacity within a few hours (personal communication ELTRA 2003). Hence, there is a significant value in predicting this uncertainty. The economic value of a reduced spinning reserve is proportional to the installed wind energy capacity unless there is a good interconnection to another electricity grid, enough storage capacity or other energy sources e.g. hydro energy to match the spinning reserve requirements. In addition to the economic value of the forecast uncertainty, a grid security aspect is connected to the wind resource characteristics and the concentration of installed wind power.

To improve the wind power computation and to take advantage of all the variables predicted in the weather prediction model, the wind power prediction was integrated into the numerical model. This simplified power conversion module using standard power curves from wind turbine manufactures has been verified in this work. It was most important to proof the potential of this approach and discuss further developments into this direction. The EU 5th Framework project HONEYMOON [1] is using this approach as a basis for further development of the initial power prediction tool with an efficiency based power prediction and a statistical power curve analysis tool.

In the first experiment campaign, three major error sources have been identified. These are:

1. Lack of Accuracy of Boundary Layer Winds
2. Random Model Errors
3. Phase Errors of Lows and Fronts

[1] HONEYMOON stands for "a High resOlution Numerical wind EnergY Model for On- and Offshore predictions using eNsemble predictions". It is a 2 year CORDIS FP5 project (2003-2004) with contract No. ENK5-CT-2002-00606.

A possible solution to these problems was suggested by using ensemble predictions. Another aspect that pointed strongly towards using an ensemble of forecasts, is the goal to reduce economic risks in resource studies and to assist wind power to become economically competitive within liberalised markets.

Such an ensemble of forecasts naturally offers a multitude of decision levels compared to a single decision based on a control forecast. In statistical terms this means that an ensemble of forecasts provides detailed probability distributions instead of only two levels of probabilities. It is known that a multiple value probability forecast can be constructed based on a single deterministic forecast, using past verification statistics (Toth and Kalnay 1997, Zhu et al. 2001). Such a system can produce statistically post-processed, bias free probabilistic forecasts, but only on a single decision level. Toth et al. 1998 even argues that statistical post-processing of some sophistication applied on a control forecast system may be able to capture part of the day to day variations in predictability, but it is not likely that all information that affects predictability (i.e. case dependent initial errors and their evolution in the forecast) could be captured through statistical approaches. Zhu et al. (2001) conclude in their study on the economic value of ensemble based weather forecasts that the reason for the ensemble to perform better, even though a control forecast was supplemented by a detailed probability distribution, must be due to some genuine information contained in the ensemble but not in the control based distributions. Smith et al. (2001) came to similar conclusions in their complex economic value analysis addressing hypothetical applications in the electricity sector.

With this background a 50-member Multi-Scheme Ensemble Prediction System (EPS) was developed and verified over a 3 month period against 12 Danish wind farms, 7 Danish synoptic stations, 5 Irish wind farms and 3 Irish wind masts. This multi-scheme approach was however especially designed for the wind energy market. The basis in the design of the ensemble members was the fact that atmospheric processes, which involve condensation and turbulence, contribute significantly to the error in the wind power predictions. Additionally, the difference of the ensemble members was designed

to attack the models inaccuracy regarding simulation of fronts and the friction between the air and the surface. In that way it could be demonstrated that the ensemble system provides a range of possible forecasts, if the weather development is uncertain. An implicit forward-backward stepping algorithm, the *pmt-filter*, was also developed in this work to analyse the ensemble members and to compute an uncertainty estimate for the forecasts.

Toth and Kalnay argued already in 1997 that the ensemble distribution may be centred closer to the truth than the distribution based on a single forecast due to nonlinear effects. This statement can be confirmed with the Multi-Scheme Ensemble, where it was demonstrated that an improvement in forecast skill from 8%-20% for the optimal forecast of wind speed could be achieved with the ensemble system in the Irish area. Around 20% was achieved for the optimal power prediction averaged over the Danish synoptic stations. This means that a gain in predictability of 9-12h in a 48 hour forecast was achieved.

The goal of this work was to demonstrate the benefit and improvement with respect to a control forecast and the very short-range analysis (0-6h). This goal was achieved as gain in predictability of at least 9h and confirms again Toth and Kalnay's statement (1997) that an ensemble distribution may be centred closer to truth than a distribution based on a single forecast.

An objective way to verify the ensemble system in its capability to predict the uncertainty of the forecasts is to measure the correlation of the spread of the ensemble with the error of the ensemble mean. This correlation has been found to reach a correlation of 93% for Denmark and Ireland and a correlation of 97% for wind speed and 96% for wind power when averaging over the entire North Sea area. According to the studies carried out by Stendsrud et al. (1999) and Hamill and Colucci (1998) the lack of correlation between spread and forecast uncertainty presents a challenge to the production of short-range ensemble forecasts. Both studies found that there was little correlation between the spread of the ensemble members and the accuracy of the ensemble. Even though these studies have already been carried out in 1998 and 1999, no

other publications of similar contents in the short-range forecasting area that indicated further development has been found since. Therefore, it is believed that the results of the multi-scheme ensemble presents a large step forward in the area of short-range ensemble forecasting.

The presented work has also shown events that were not predicted very well. There are many possibilities to test the ensemble system and potential improvements by, for example, adding more perturbations to the initial conditions. The implementation of the system into a daily schedule to gain more experience in end-users operational environment could also be beneficial.

The main conclusion from this work and recommendation for further studies is to concentrate the forecasting of wind speed and wind power in first instance on the predictability of the weather situation. If the uncertainty of the forecast can be quantified with a certain accuracy, an end-user can take advantage of that knowledge, such that further steps to increase the accuracy of an individual prediction is then of second order, even though it was demonstrated in this work that the ensemble in fact improved the accuracy of the forecasts.

These findings are in line with the conclusion of Zhu et al. (2001), that the added benefits of an ensemble of forecasts is derived from (1) the fact that the ensemble provides a more detailed forecast probability distribution, allowing the users to tailor their weather forecast related actions to their particular cost/loss situation, and (2) the ensemble's ability to differentiate between high and low predictability cases, which has also been discussed in Section 1.2 in this work.

To link these two tasks dynamically can provide a realistic way forward to meet the accuracy requirements of wind energy forecasting in the future, thereby assist in increased deployment of wind energy worldwide and in the competitiveness of wind as a *green energy source*.

6.1 Recommendation for future Research

The following is a list of possible research topics for the future.

- Development of the pmt-filter into the third dimension (space) to adopt the algorithm for parameter fields from the NWP output
- Verifying the pmt-filter with Medium Range Ensembles (e.g. ECMWF, NCEP)
- Testing the performance of the EPS in higher resolution for improved accuracy of the surface winds
- Developing efficiency based power curves for the wind power module
- Developing a wind farm deployment index from the EPS data for sites with good wind resources that are also predictable
- Developing and/or linking a decision making model for the electricity market to the ensemble predictions and verifying it with the produces EPS data
- Developing and linking a decision making model for a system operator to the ensemble predictions and verifying it with the produces EPS data
- Use the ensemble data to investigate the predictability of other Renewable Energies (Solar, Hydro, etc.) and the possibilities of linking these to wind energy
- Use the short-range ensemble data to verify, whether the method can also be used as hydrological forecasts for emergency management and water resources decision making
- Developing a safety index for offshore wind farms for the installation and maintenance phases

Bibliography

[1] Atger, F., *Tubing: an alternative to clustering for EPS classification*, ECMWF *Newsletter No. 79*, 7-14, (1998).

[2] Arakawa, A., *Design of the UCLA general circulation model. Numerical Simulation of Weather and Climate*, Dept. of Meteorology, University of California, Los Angeles, Tech. Rept. 7, 116pp, (1972).

[3] Barkmeijer, J. Buizza, R., Palmer, T.N., Puri, K., Mahfouf, J.-F., *Tropical Singular Vectors computed with linearized diabatic physics*, Q.J.R. Meteorol. Soc., 127, 685-708, (2001).

[4] Bouttier, F., Rabier, F, *The operational implementation of 4DVAR*, ECMWF Newsletter No. 78 ,72-76 (1998).

[5] Buizza, R.,Petroliagis, T.,Palmer, T.N.,Barkmeijer, J.,Hamrud, M., Hollingsworth, A., Simmons, A.,Wedi, N., *Impact of model resolution and ensemble size on the performance of an Ensemble Prediction System*, Q.J.R.Meteorol. Soc., 124, 1935-1960, (1998).

[6] Buizza, R., Miller, M., Palmer, T.N., *Stochastic representation of model uncertainties in the ECMWF Ensemble Prediction System*, Q.J.R.Meteorol. Soc., 125, 2887-2908, (1999).

[7] Black, T.L., *The new NMC mesoscale ETA model: Description and forecast examples*, Weather. Forecasting, 9, 265-278, 1994.

[8] Commission of the European Countries, *Green Paper - Towards a European strategy for the security of energy supply*, Commission of the European Countries COM(2000) 769, (2000).

[9] Buizza, R., Richardson, D.S., Palmer, T.N., *The new 80-km High-Resolution ECMWF EPS*, ECMWF *Newsletter No. 90*, 2-9, (2001).

[10] Buizza, R., Hollingsworth, A., *Severe weather prediction using ECMWF EPS: The European storms of 1999*, ECMWF *Newsletter No. 89*, 2-12, (2001).

[11] Courant, R., Friedrichs, K.O., Lewi, H., *Über die partiellen Diferenzengleichungen der mathematischen Physik*, Math. Annalen, 100, 32-74, (1928).

[12] Courtier, P., Thépaut, J.-N., Hollingsworth, A., *A strategy for implementation of 4DVAR using an incremental approach*, Quart. Journ. of Roy. Meteor. Soc., Vol. 120, 1367-1388, (1994).

[13] Cuxart, J, Bougeault, P., Redelsperger, J.-L., *A turbulence scheme allowing for mesoscale and large-eddy simulations*, Q. J. R. Meteorol. Soc. 126, 1-30, (2000).

[14] Database on Wind Characteristics, *http://www.afm.dtu.dk/wind/database*, EU-DG XII Joule Project, (1996).

[15] Fast, J.D., Takle, E.S., *Application of a quasi non-hydrostatic parameterisation for numerical modelling neutral flow over an isolated hill*, Boudary Layer Meteorology, 44, 285-304, (1988).

[16] Garratt, J.R., *The Atmpspheric Bounday Layer*, Cambridge University Press, (1992).

[17] Giebel, G., *On the benefits of Distributed Generation of Wind Energy in Europe*, Fortschritt-Berichte VDI, Reihe 6 Energietechnik, No. 444, (2001).

[18] Giebel, G., Brownsword, A., Kariniotakis, G., *State of the art on short-term wind prediction*, Technical Report, EU 5th Framework ANEMOS Project, (2003).

[19] GLCC, *The Global Land Characteristics Data Base. U.S. Geological Survey*, http://edcdaac.usgs.gov/glcc/glcc.html, USGS (1997).

[20] Gustafsson, N., *HIRLAM Final Report*, HIRLAM Tech. Report 9, (1993).

[21] Gustafsson, N., Berre, L., Hörnquist, S., Huang, X.-Y., Lindskog, M., Navascués, B., Mogensen, K.S., Thornsteinsson, S., *Three-dimensional variational data assimilation for a limited area model. Part I: General formulation and the background error constraint*, Tellus, 53A, (2001).

[22] GTOPO30, *Global 30 Arc Second Elevation data Set. U.S. Geological Survey*, http://edcdaac.usgs.gov/gtopo30/gtopo30.html, USGS, (1998).

[23] Haltiner, G.J., *Numerical Weather Prediction*, Wiley (Publisher), (1971).

[24] Haltiner, G.J., Williams, R.T. *Numerical Prediction and Dynamic Meteorology*, John Wiley & Sons (Publisher), (1980).

[25] Hamill, T.M., Colucci, S.J., *Verification of the Eta-RSM short-range ensemble forecasts*, Mon. Wea.Rev., 125, 1312-1327, (1997). Houtekamer et al, 1996

[26] Hatziargyriou, N., G. Contaxis, M. Matos, J.A. Pecas Lopes, G. Kariniotakis, D. Meyer, J. Halliday, G. Dutton, P. Dokopoulos, A. Bakirtzis J. Stefanakis, A. Gigantidou, Ph.O'Donnell, D. McCoy, M.J. Fernandes, J.M.S. Cotrim, A.P.Figueira, *"MORE CARE" Advice for Secure Operation of Isolated Power Systems with Increased Renewable Energy Penetration and Storage"*, Proc. European Wind Energy Conference, Copenhagen. 2001.

[27] Holton, J.R., *An Introduction to Dynamic Meteorlogy*, Int. Geophysics Series, Academic Press, Vol. 23, (1979).

[28] Jackson, J., *A cry for better forecasts in Denmark*, Wind Power Monthly, 40-42, (2003).

[29] Jackson, J., *What the weather man says*, Wind Power Monthly, p.42, (2003a).

[30] Järvinen, H., Undén, P., *Observation sreening and background quality control in the ECMWF 3D-VAR data assimilation system*, ECMWF Research Department Technical Memorandum No. 236, (1997).

[31] Jørgensen,J.U., *Application of Plug and Play FORTRAN at the Danish Meteorological Institute*, *Towards Terra Computing*, Proc. of the Super Computer Conference in ECMWF, (1999).

[32] Jørgensen,J.U., Moehrlen, C., Gallachir, B., McKeogh, E.J., *HIRPOM: Description of an operational numerical wind power prediction model for large scale integration of on- and offshore wind power in Denmark*, Proc. 2002 Global Wind power Conference and Exhibition, Paris, (2002).

[33] Jørgensen,J.U., Moehrlen, C., Sattler, K.,*HIRPOM-WAM: An on - and offshore prediction system for real-time prediction and climatic studies, Offshore Wind Energy*, Proc. EWEA Special Topic Conference, Brussels, (2001).

[34] Källén, E. *HIRLAM Documentation Manual. System 2.5.* SMHI, Norrköping, Sweden, (1996).

[35] Klinker, E., Rabier, F., Kelly, G., Mahfouf, J.-F., *The ECMWF operational implementation of the four dimensional data assimilation. Part III: Experimental results and diagnostics with operational configurations*, Q.J.R. Meteor. Soc., Vol. 126, 1191-1215, (2000).

[36] Knight, S., *Balancing cost halved by forecast program*, Windpower Monthly, 42-43, (2003).

[37] Krishnamurti, T.N., Bounoua, L., *An Introduction to Numerical Weather Prediction Techniques.* CRC Press, Inc., (1996).

[38] Lönnberg, P., Shaw, D.,*ECMWF data assimilation: Scientific Documentation*, ECMWF Research Manual, second revised edition 1, (1987).

[39] Lorenc, A.C., *A Global Three-Dimensional Multivariate Statistical Interpolation Scheme*, Mon. Weather Rev., 109, 701-721, (1981).

[40] Landberg, L., *Short-term prediction of the power production of wind farms.* J. Wind Eng. Ind. Aerodyn., 80, 207-220, 1999.

[41] Landberg, L., Joensen, A., Giebel, G., Madsen, H., Nielsen, T.S., *Short Term prediction towards the 21st Century*, In Wind Forecasting Techniques, 33 Meeting of Experts, Technical Report from the International Energy Agency, R&D Wind, Ed. S.-E. Thor, FFA, Sweden, 77-85, 2000.

[42] Lorenz, E.N. Energy and numerical weather prediction, Tellus, 12, 364-373, (1960).

[43] Mesinger F., and Z. I. Janji'c, *Problems and numerical methods of the incorporation of mountains in atmospheric models*, Large-scale Computations in Fluid Mechanics, Part 2. Lect. Appl. Math, Vol. 22, American Mathematical Society, Providence, Rhode Island, 81-120, 1985.

[44] Machenhauer,B. *HIRLAM Final Report*, HIRLAM Tech. Report 5, 1-116, (1988).

[45] Madsen, H., *Wind Power Prediction Tool in Control Dispatch Centres.*, ELSAM, Skaerbaek, Denmark, ISBN:87-87090-25-2, 1995.

[46] Madsen, H., *Models and Methods for Predicting Wind Power.*, ELSAM , Skaerbaek, Denmark, ISBN:87-87090-29-5, 1996.

[47] Mahfouf, J.-F.,Rabier, F.,*The ECMWF operational implementation of the four dimensional data assimilation. Part II: Experimental results with improved physics*, Q.J.R. Meteor. Soc., Vol. 126, 1171-1190, (2000).

[48] Massey, J., *Worst Fears Realised in Britain*, Windpower Monthly, 17 No 5, 26-27, 2001.

[49] Mathur, M.B., *A note on an improved quasi-Lagrangian advective scheme for primitive equations*, Mon. Wea. Rev.,98, 214-219, (1970).

[50] McGovern, M., *Forecasting focus on who pays in Spain*, Windpower Monthly, 45-46, 2003.

[51] Mengelkamp, H.-T., *On the Energy Output Estimation of Wind Turbines*, International Journal of Energy Research, Vol. 12, 113-123, 1988.

[52] Mesinger, F., Arakawa, A., *Numerical Methods used in Atmospheric Models*, GARP Publication Series No. 17, Vol. 1, 47-53, (1978)

[53] Moehrlen, C., Jørgensen, J.U., McKeogh, E.J.,*Power Predictions in complex terrain with an Operational Numerical Weather Prediction Model in Ireland including Ensemble forecasting*, Proc. Clean Power for the World, World Wind Energy Conference and Exhibition, Berlin, Germany, (2002).

[54] Moehrlen, C.,*On the Benefits of and Approaches to Wind Energy Forecasting*, Presentation at Irish Wind Energy Association Annual Conference "Towards 500MW", Ennis, (2001); submitted to Wind Engineering and Industrial Aerodynamics (2001).

[55] Moehrlen, C., Jørgensen, J. U. , Sattler,K., McKeogh, E.J.,*On the accuracy of land cover data in NWP forecasts for high resolution wind energy prediction*, Proc. European Wind Energy Conference and Exhibition, Copenhagen, Denmark, 2-6 July (2001).

[56] Mönnig, K. Vorhersage zur Leistungsabgabe netzeinspeissender Windkraftanlagen zur Unterstuetzung der Kraftwerkseinsatzplanung, PhD thesis at the Faculty of Physics at the university of Oldenburg, Germany, (2000).

[57] Molteni, F., Buizza, R., Parlmer, T.N., Petroliagis, T., *The ECMWF Ensemble Prediction System: Methodology and validation*, Q.J.R. Meteorol. Soc., 122, 73-119, (1996).

[58] Mylne,K., Evans, R.E., Clark, R.T.,*Multi Model Multi-Analysis Ensembles in Quasi-Operational Medium Range Forecasting*, Numerical Weather Prediction, Forecasting Research Scientific Paper No. 60, UK Met Office, Nov. (2000).

[59] Mylne,K. and Robertson,K., *Poor Man's EPS experiments and LAMEPS plans at the Met Office*, Presentation in the LAM EPS Workshop Madrid, Oct. (2002).

[60] Nielsen, T.S., *using Meteorological Forecast in On-line Prediction of wind Power*, Technical Report IMM-ELTRA-ELSAM, Sept. 1999.

[61] Nielsen, T.S., Madsen, H., Tofting, T., *WPPT, A Tool for On-Line Wind Power Prediction*. In Wind Forecasting Techniques, 33 Meeting of Experts, Technical Report from the International Energy Agency, R&D Wind, Ed. S.-E. Thor, FFA, Sweden, 93-116, July (2000).

[62] Orlanski, I. *The quasi hydrostatic approximation*, J. Atmos. Sci, 38, 572-582, (1981).

[63] Palmer, T.N., *Ensemble Forecasting - An Introduction*, Proc. First SRNWP Workshop on Short-Range Ensemble Prediction Systems (EPS), SRNWP Network, Madrid, (2002).

[64] Persson, A., *User Guide to ECMWF forecast products*, Meteorological Bulletin M3.2, (2001).

[65] Physick, W.L., *Review: Mesoscale modelling in Complex Terrain*, Earth-Science Reviews, 25, 199-235, (1988).

[66] Pileke, R.A., *Comparison of a Hydrostratic and an Anelastic Dry Shallow Primitive Equation Model*, NOOA Technical emorandum ERL OD-13, Boulder Colorado, (1972).

[67] Pielke, R.A., *Mesoscale Meteorological Modelling*, Academic Press New York, pp.612, (1994).

[68] Quiby, J. *Proc. First SRNWP Workshop on Short-Range Ensemble Prediction Systems (EPS)*, SRNWP Network, Madrid, (2002).

[69] Rabier, F., Järvinen, H., Klinker, E., Mahfouf, J.-F., Simmons, A., *The ECMWF operational implementation of the four dimensional data assimilation. Part I: Experimental results with simplyfied physics*, Q.J.R. Meteor. Soc., Vol. 119, 845-880, (2000).

[70] Rohrig, K., *Online Monitoring and Short Term Prediction of 2400MW Wind Capacity in an Utility Supply Area.*, Wind Forecasting Techniques, 33 Meeting of Experts, Technical Report from the International Energy Agency, R&D Wind, Ed. S.-E. Thor, FFA, Sweden, 117-119, 2000.

[71] Saas, B.H., Rontu, L., Räisänen, P., *HIRLAM-2 Radiation Scheme:Documentation and Tests*, HIRLAM Tech. Report 16, 1-43, (1994).

[72] Sass, B. H., *STRACO - Soft Transition Condensation scheme*, HIRLAM Newsletter, 29, (1997).

[73] Sass, B. H., Nielsen, N. W., Jørgensen, J. U. , Amstrup, B., Kmit, M., *The operational DMI-HIRLAM system* Technical Report 00-26, Danish Meteorological Institute, (2000).

[74] Smith, L. A., M. S. Roulston, and J. Hardenberg, *End to End Ensemble Forecasting: Towards Evaluating the Economic Value of the Ensemble Prediction System.*, ECMWF Technical Memorandum No. 336, (2001).

[75] Stensrud, D.J., Brooks, H.E., Du, J., Tracton, M.S., Rogers, E., *Using Ensembles for Short-Range Forecasting*, Mon. Wea. Rev., 127, 433-446, (1999).

[76] Toth, Z., Y. Zhu, T. Marchok, S. Tracton, and E. Kalnay, *Verification of the NCEP glob-al ensemble forecasts.* Preprints of the 12th Conference on Numerical Weather Predic-tion, 11-16 January 1998, Phoenix, Arizona, 286-289, (1998).

[77] Toth, Z., and E. Kalnay, *Ensemble forecasting at NCEP and the breeding method*. Mon. Wea. Rev, 125, 3297-3319, (1997).

[78] Toth, Z., Kalnay, E., *Ensemble Forecasting at NMC: the generation of perturbations*, Bull. Am. Meteorol. Soc., 74, 2317-233-, (1993).

[79] Wilks, D.S., *Statistical Methods in the Atmospheric Science - An Introduction*, International Geophysics Series Vol59, Academic Press, (1995).

[80] Zhu, Y. ,Toth, Z., Wobus,R., Richardson, D., Mylne, K., *On the Economic Value of Ensemble based Weather Forecasts*, Submitted to the Bulletin of American Meteorological Society, Second revised version September 7, (2001).

Appendix A

Mathematical Formulation of the *Probabilistic Multi-Trend Filter*

In the first step the vectors fc (forecasted values) and c_w (weigth coefficient) are coupled in time-space to take the past and future development into account. The coupled terms are solved in an implicit iteration process and then decoupled again. The iteration algorithm uses forward-backward stepping. At present a filter is applied that iterates three times to smooth the function. The width of the time window is from -k to +k.

$$fc_p(i,j) = \widetilde{fc}(i,j) - \frac{1}{n_{eps}} \cdot \sum_{m=1}^{neps} fc(m,j) \tag{A.1}$$

where $i = 1, 2, ...n_{eps}$ is the number of ensemble members, j is the time step variable or data dimension of each ensemble member, $\widetilde{fc}(i,j)$ is updated after each iteration process of the pmt-filter algorithm.

The deviation of the ensemble to the mean is computed as

$$\Delta fc(i,j) = \sum_{l=-k}^{k} (\Delta fc_p(i, j+l) \cdot A(l)) \tag{A.2}$$

$i = 1, 2, ...n_{eps}$ and $j = 1, ...fclen$ (fclen is the forecast length) and $l = -k, (-k+1), ...k$, A(l) is a weight function in the interval -k to k.

As mentioned before, the weight function c_w is also coupled in time and a time-integrated ensemble deviation from -k to +k steps is computed. It is decoupled after

the integration process to the actual time step. The coupling of the weight functions is done by

$$c_w(i,j,k) = \sum_{l=-k}^{k} (c_{wp}(i,j+l,k) \cdot A(l)) \tag{A.3}$$

where $i = 1, 2, ...n_{eps}$, $j = 1, ...k$ and $l = -k, (-k+1), ...k$, $A(l)$ is a weight function in the interval -k to k.

The two parameter Δfc_p and c_{wp} are passed into the implicit algorithm to compute the probability distribution and the best member ($fc_{optimal}$). Note, that the weighting factor c_{wp} was in the first step estimated from a long-term statistical coefficient. If this is unknown the coefficient can be set to 1. After the first iteration process c_{wp} is updated with $\widetilde{c_w}$ over the full forecast length and decoupled by inverting the weight function $A(l)$.

$$c_{wp}(i,j,k+1) = \sum_{l=0}^{fclen} (\widetilde{c_{wp}}(i,j+l,k) \cdot A^{-1}(l)) \tag{A.4}$$

where fclen is the forecast length.

The optimal forecast $f_{optimal}$ is computed inside the pmt-filter algorithm. The weighted optimal forecast is also computed inside the pmt-filter algorithm, but from the updated $\widetilde{\Delta fc_p}$:

$$\widetilde{fc_{opt}}(j) = fc_{optimal}(j) + \frac{1}{n_{eps}} \cdot \sum_{m=1}^{n_{eps}} fc(m,j) \tag{A.5}$$

and

$$\widetilde{fc_{wopt}}(j) = \widetilde{\Delta fc_p(j)} + \frac{1}{n_{eps}} \cdot \sum_{m=1}^{n_{eps}} fc(m,j) \tag{A.6}$$

In the algorithm, the ensemble forecasts are first evaluated according to their probability density. The sums, minimum, maximum and the mean of the forecasts is initialised:

$$w_{min} = min[fc_{eps}(i)] \qquad\qquad i = 1, 2, ..n_{eps} \tag{A.7}$$

$$w_{max} = max[fc_{eps}(i)] \qquad i = 1, 2, ..n_{eps} \tag{A.8}$$

$$fc_{mean} = \frac{1}{n_{eps}} \cdot \sum_{i=1}^{n_{eps}} f_{eps}(i) \qquad i = 1, 2, ..n_{eps} \tag{A.9}$$

$$c_{sum}(n) = \sum_{i=1}^{n_{eps}} (c_{wp}(i) \cdot B(n, i)) \tag{A.10}$$

$$fc_{sum}(n) = \sum_{i=1}^{n_{eps}} (c_{wp}(i) \cdot fc_{eps}(i) \cdot B(n, i)) \tag{A.11}$$

The index n corresponds to the number of intervals or bins in the probability distribution, $B(n, i)$ is the bin-matrix that defines, which members are in the n bins b. It is defined as

$$B(i, n) = \begin{cases} 1 & \text{for } \; b(n+1) > n > b(n) \\ \\ 0 & \text{otherwise} \end{cases} \tag{A.12}$$

where the bin b(i,n) is defined as

$$b(i, n) = \frac{w_{max} - w_{min})}{n_y} \cdot n + w_{min} \tag{A.13}$$

with n_y being the number of bins. The probability density p_{eps} can be calculated as

$$p_{eps}(n) = 100 \cdot \frac{c_{sum}(i_1)}{sum_{cw}} \qquad \text{for} \quad n = 1, 2, ...ny \tag{A.14}$$

where sum_cw is the sum of the weight coefficients

$$sum_{cw} = \sum_{i=1}^{n_{eps}} c_{wp}(i) \tag{A.15}$$

The *pmt-filter function* f_{strip} is used for the selection procedure of the optimal forecast. The intervals for the integration of the probability density function p_{eps} are defined by f_{strip}. In other words, if f_{eps} is within the interval z_{min1} and z_{max1}, j=1 and f_{strip} is the

sum of all weights in this interval. If f_{eps} lies within the interval z_{min2},z_{max2}, j=2 and f_{strip} is the sum of all weights in this interval.

$$f_{strip}(j) = \sum_{i=1}^{n_y} c_{wp}(i) \begin{cases} j = 1 \quad \text{for} \quad z_{min1} < f_{eps}(i) > z_{max1} \\ \\ j = 2 \quad \text{for} \quad z_{min2} < f_{eps}(i) > z_{max2} \end{cases} \tag{A.16}$$

where $i = 1, 2, ...n_{eps}$.

The intervals are renewed in each iteration step and parts of the intervals *"stripped off"* until the function converges to the optimal value of $f_{optimal}$.

The minima and maxima z_{min1}, z_{max1}, z_{min2},z_{max2} define two intervals in the probability function and thereby reduce the iteration process. The pmt-filter function has therefore a second implicit level. The definition of the minima and maxima are:

$$\begin{aligned} z_{min1} &= w_{min} \\ \\ z_{max1} &= 0.25 \cdot w_{min} + 0.75 \cdot w_{max} \\ \\ z_{min2} &= 0.75 \cdot w_{min} + 0.25 \cdot w_{max} \\ \\ z_{max2} &= w_{max} \end{aligned} \tag{A.17}$$

The *pmt-filter function* is now used to define the boundaries of the intervals. After some testing, it was found that if $f_{strip}(1) = f_{strip}(2)$, the coefficients $a_1 = 0.875$ and $b_1 = 0.125$ have proved to be a good estimate.

$$\text{for} \quad f_{strip}(1) = f_{strip}(2) \begin{cases} z^*_{min_1} = a_1 \cdot z_{min_1} + b_1 \cdot z_{max_1} \\ \\ z^*_{max_2} = a_1 \cdot z_{max_2} + b_1 \cdot z_{min_2} \end{cases} \tag{A.18}$$

and

$$\text{for} \quad f_{strip}(1) > f_{strip}(2) \begin{cases} z^*_{max_2} = a_2 \cdot z_{max_2} + b_2 \cdot z_{max_1} \\ z^*_{max_1} = a_2 \cdot z_{min_1} + b_2 \cdot z_{max_2} \\ z^*_{min_2} = a_2 \cdot z_{min_1} + b_2 \cdot z_{max_1} \end{cases} \tag{A.19}$$

and

$$\text{for} \quad f_{strip}(1) < f_{strip}(2) \begin{cases} z^*_{max_1} = a_2 \cdot z_{min_2} + b_2 \cdot z_{min_2} \\ z^*_{min_2} = a_2 \cdot z_{min_1} + b_2 \cdot z_{max_2} \\ z^*_{max_1} = a_2 \cdot z_{min_2} + b_2 \cdot z_{max_1} \end{cases} \tag{A.20}$$

For the second and third set of boundaries, tests have shown that a good approximation for these coefficients is to use $a_2 = 0.75$ and $b_2 = 0.25$.

Then the maximum probability p_{max} is updated by updating the intervals/bins of the probability distribution with the new z_{min} and z_{max}

$$p_{max} = p_{eps}(n) \tag{A.21}$$

The interval/bins n for which p_{max} is computed are

$$n = (n_y \cdot \frac{z_{mean} - w_{min}}{w_{max} - w_{min}} + 1) \tag{A.22}$$

where $n = 1, 2, ...n_y$ and

$$z_{mean} = \frac{1}{2} \cdot (z_{min_1} + z_{max_2}) \tag{A.23}$$

The optimal forecast with the highest probability is then

$$\text{for} \quad c_{sum}(n) = 0 \begin{cases} fc_{max} = fc_{mean} \\ p_{eps}(n) = 100 \end{cases} \tag{A.24}$$

or

$$\text{for} \quad c_{sum}(n) \neq 0 \begin{cases} fc_{max} = \frac{fc_{sum}(n)}{sum(n)} \\ P_{eps}(n) = 0 \end{cases} \tag{A.25}$$

where $P_{eps}(n)$ is the integrated probability that is zero when the sum of the coefficients $c_{sum}(n)$ has a value different from zero.

$$c_{sum}(n) = \sum_{1}^{n} c_{wp} \tag{A.26}$$

The computation of the distribution of the remaining probabilities is split into an upper and a lower part. The upper part is defined as

$$p_{max} < n_{yu} \leq 100 \tag{A.27}$$

and the lower part is defined as

$$0 < n_{yl} \leq p_{max} \tag{A.28}$$

The probability distribution computation for both upper and lower part is done by initialising

$$sum_w = \frac{1}{2} \cdot p_{eps}(n) \tag{A.29}$$

and summing it up over n_y

$$sum_w = \begin{cases} \frac{100}{\sum_{i=1}^{n-1} p_{eps}(i)} \text{ for } & 1 < n_y \leq n-1 \\ \frac{100}{\sum_{i=n+1}^{n_y} p_{eps}(i)} \text{ for } & n+1 < n_y \leq 100 \end{cases} \tag{A.30}$$

In this case the index n from Equ. A.22 is again used to reduce the boundaries according to the intervals for which p_{max} was computed.
The integrated probability

$$P_{eps}(i) = \sum_{0}^{n_y} p_{eps}(i) \tag{A.31}$$

is now, as mentioned above, split up into an upper and lower part and is 100% when it reaches its maximum and minimum. Therefore the integration of p_{eps} is done from half-levels (middle points).

$$p^*_{eps}(i,2) = p_{eps}(i,2) + \frac{1}{2} \cdot p_{eps}(i,1) \cdot sum_w, \left.\begin{array}{l} \imath = n-1, n-2, ..., 1 \\ \imath = n+1, n+2, ...n_y \end{array}\right. \tag{A.32}$$

and

$$p_{eps}(i,2) = \begin{cases} p^*_{eps}(i,2) & \text{for } \; p^*_{eps}(i,2) < 100 \\ 100 & \text{otherwise} \end{cases} \tag{A.33}$$

The last step is the decoupling in time of the weight function from the time window 2k to the actual time step according to Equation A.4. The optimal and weighted optimal forecast are calculated according to Equation A.5 and Equation A.6 by using

$$fc_{optimal} = min(|(f_{eps}(i) - fc_{max}(i)|) \quad \text{for} \quad 1 \leq i \leq n_{eps} \tag{A.34}$$

The other parameters w_{min}, w_{max}, fc_{max}, fc_{min} fc_{mean}, p_{max} are then recalculated according to Equation A.7 to Equation A.11.

If the algorithm is run for a single site, the output contains a series of tables of probabilities for each bin with maximum and minimum percentages. The tables are created for each hour of the forecast length of 42h. The values for the optimal forecast, the minimum and maximum, the mean and the weighted mean are also printed.

If the pmt-filter algorithm should be applied for paramter fields, the iteration needs to be conducted in space rather than in the time level or in both. This means that the algorithm has to be applied in a 2-dimensional or 3-dimensional way. When dealing with fields the uncertainty of the forecast needs to be extended into the horizontal space, i.e. if one member is best at one grid point, it "needs" to be best at the next one as well. The principle is however the same.

Appendix B

Statistical Parameters used in the Verification

The verification took place with the following standard statistical parameters:

- mean:

$$mean = \frac{1}{n}\sum(fc) \tag{B.1}$$

- mean absolut error (mae):

$$mae = \frac{1}{n}\sum|fc - obs| \tag{B.2}$$

- bias:

$$bias = \frac{1}{n}\sum(fc - obs) \tag{B.3}$$

- Variance:

$$var = (\frac{1}{n}\sum(fc - mean)^2 \tag{B.4}$$

- Standard Deviation:

$$stdev = \sqrt{(\frac{1}{n}\sum(fc - obs)^2) - bias^2} \tag{B.5}$$

- Root Mean Square error:

$$rms = \sqrt{(\sum(bias^2)} \tag{B.6}$$

- skill score:

The skill scores are a direct verification of a forecast against a reference forecast and a perfect forecast. The reference forecast is usually a standard forecast such as persistence or climatology. The skill scores are computed as:

$$ss = \frac{fc_{reference} - fc}{fc_{reference} - fc_{perfect}} \tag{B.7}$$

The skill score has a maximum value of 1 or 100\% respectively for a perfect forecast and 0 for a performance equal to the reference forecast.

Appendix C

Observational Data Information

The table gives an overview of the Irish and Danish observational measurements. All observations have been averaged to hourly values for the statistical tests.

Site	Wind Speed	[unit]	Wind Power	[unit]
Beenaghe	Mast(45m)	10min	SCADA system	10min
BessyBell	Turbine	1h	Turbine Metering	1h
Kilronan	Turbine	1h	Turbine Metering	1h
Lendrum	Mast(45m)	10min	SCADA system	10min
MilaneHill	Mast(45m)	10min	SCADA system	10min
Tursillagh	Mast(10m/45m)	30min	PowerMetering	1h
Drinagh	Mast(30m)	10min	-	-
Ringaskiddy	Mast(30m)	10min	-	-
Seefin	Mast(30m)	10min	-	-
Abild	Mast(32m)	10min	PowerMetering	1h
Broens	Mast(32m)	10min	PowerMetering	10min
Draeby	Mast(32m)	10min	PowerMetering	1h
Fjaldene	Mast(32m)	10min	PowerMetering	10min
HanstholmHavn	Mast(32m)	10min	PowerMetering	10min
Hollandsbjaerg	Mast(32m)	10min	PowerMetering	10min
Klim	Mast(32m)	10min	PowerMetering	10min
Ryaa	Mast(32m)	10min	PowerMetering	10min
Rejsby	Mast(32m)	10min	PowerMetering	10min
Sydthy	Mast(32m)	10min	PowerMetering	10min
Torrild	Mast(32m)	10min	PowerMetering	10min
VedersoeKaer	Mast(32m)	10min	PowerMetering	10min
Aarhus	Mast(10m)	15min	-	-
Blaavand	Mast(10m)	15min	-	-
Fredrikshavn	Mast(10m)	15min	-	-
Gedser	Mast(10m)	15min	-	-
HvideSande	Mast(10m)	15min	-	-
Jaegersborg	Mast(10m)	15min	-	-
Skrydstrup	Mast(10m)	15min	-	-
Taasinge	Mast(10m)	15min	-	-

Table C.1: Information of the Irish and Danish observational data

Appendix D

Wind Farm Verification

The following tables are complementary to the verification discussion in Chapter 3.7. The variables are in rows and the experiments in columns. The variables are named *pwrobs* and *wsobs* for observed power and observed wind speed, respectively. The modelled variables are*ws* and *pwr* and indicate average wind speed over one hour and average power production over one hour, respectively. Missing data was excluded in the statistical computations. Each table contains statistical tests for one farm.

cases	1417	1434	1411	1440	1422	1422
mean:	e014	g014	n014	g050	e300	se300
pwrobs	1626.33	1658.38	1653.08	1651.49	1636.59	1636.59
pwr	1261.94	1174.24	1154.24	1183.14	800.27	966.34
wsobs	7.86	7.94	7.94	7.92	7.88	7.88
ws	7.96	7.7	7.6	7.69	6.69	7.18
var:	e014	g014	n014	g050	e300	se300
pwrobs	1503.87	1512.29	1512.33	1512.82	1508.15	1508.15
pwr	1441.71	1438.16	1434.21	1440.23	1125.94	1261.34
wsobs	3.61	3.62	3.63	3.63	3.61	3.61
ws	3.97	3.87	3.94	3.88	3.25	3.46
max:	e014	g014	n014	g050	e300	se300
pwrobs	4978	4978	4978	4978	4978	4978
pwr	4988.31	4976.32	4976.32	4979.33	4980.76	4972.42
wsobs	25.07	25.07	25.07	25.07	25.07	25.07
ws	23.86	20.02	20.02	20.99	21.44	18.77
MAE:	e014	g014	n014	g050	e300	se300
maepwr	665.61	777.78	784.11	743.91	991.01	876
maews	1.45	1.59	1.66	1.52	1.77	1.56
BIAS:	e014	g014	n014	g050	e300	se300
biaspwr	-398.02	-520.36	-535.86	-503.68	-868.83	-704.93
biasws	-0.01	-0.34	-0.44	-0.33	-1.27	-0.78
STDEV:	e014	g014	n014	g050	e300	se300
stdpwr	925.03	1043.29	1052.37	986.96	1081.56	1060.21
stdws	2.01	2.15	2.3	2.06	2.1	2.12
RMS:	e014	g014	n014	g050	e300	se300
rmspwr	1006.72	1165.53	1180.61	1107.74	1387.02	1272.86
rmsws	2.01	2.17	2.34	2.09	2.45	2.26
COR:	e014	g014	n014	g050	e300	se300
corpwr	0.8	0.75	0.74	0.77	0.7	0.72
corws	0.86	0.83	0.81	0.85	0.82	0.82
SKEW:	e014	g014	n014	g050	e300	se300
pwrobs	0.683	0.64	0.65	0.65	0.6689	0.6689
pwr	1.0669	1.15	1.18	1.13	1.627	1.4339
wsobs	1.0502	1.01	1.02	1.01	1.03	1.0332
ws	0.6967	0.62	0.57	0.61	0.71	0.6601
KURT:	e014	g014	n014	g050	e300	se300
pwrobs	-0.7749	-0.83	-0.82	-0.83	-0.8	-0.805
pwr	0.0366	0.1929	0.25	0.09	2.06	1.2346
wsobs	1.6922	1.5424	1.57	1.53	1.63	1.6351
ws	0.4032	-0.17	-0.14	-0.18	0.25	0.0181
P25:	e014	g014	n014	g050	e300	se300
pwrobs	264	280	273.75	269.5	264.5	264.5
pwr	19.56	15.83	11.94	17.02	0	9.0225
wsobs	5.26	5.31	5.29	5.275	5.2625	5.2625
ws	4.7775	4.72	4.635	4.705	4.16	4.52
P50:	e014	g014	n014	g050	e300	se300
pwrobs	1171	1215	1200.5	1196	1178	1178
pwr	755.56	492.65	461.7	503.61	211.28	345.975
wsobs	7.27	7.35	7.33	7.33	7.295	7.295
ws	7.56	6.93	6.885	6.935	6.085	6.56
P75:	e014	g014	n014	g050	e300	se300
pwrobs	2736	2796	2790.75	2789.5	2752.5	2752.5
pwr	2113.22	1945.48	1898.23	1991.87	1301.9	1572.885
wsobs	9.74	9.91	9.91	9.905	9.8375	9.8375
ws	10.5475	10.27	10.19	10.32	8.9125	9.49

Table D.1: Statistics for Kilronan

cases	1403	1420	1398	1426	1409	1409
MEAN:	e014	g014	n014	g050	e300	se300
pwrobs	1801.073	1849.40	1845.886	1841.14	13.265	1813.26
pwr	1531.582	1539.05	1530.373	1373.82	990.508	1169.86
wsobs	7.921	8.0333	8.0333	8.0045	7.9421	7.94
wd	8.640	8.6829	8.6654	8.2468	7.3007	7.78
VARIAB:	e014	g014	n014	g050	e300	se300
pwrobs	1611.452	1633.88	1631.366	1634.89	1617.981	1617.981
pwr	1631.241	1641.69	1639.471	1569.07	1261.193	1378.074
wsobs	3.818	3.839	3.837	3.855	3.821	3.821
wd	4.428	4.342	4.335	4.182	3.405	3.611
MAX:	e014	g014	n014	g050	e300	se300
pwrobs	4996	4996	4996	4996	4996	4996
pwr	4984.88	4979.48	4979.48	4980.8	4979.46	5000
wsobs	25.83	25.83	25.83	25.83	25.83	25.83
ws	22.76	21.04	21.04	21.48	21.03	18.82
wd	270	270	270	270	270	270
MAE:	e014	g014	n014	g050	e300	se300
mae.pwr	782.680	894.370	889.4484	851.02	1027.72	917.27
mae.ws	1.996	2.1648	2.1532	1.8304	1.74	1.70
BIAS:	e014	g014	n014	g050	e300	se300
biaspwr	-332.67	-371.45	-374.10	-528.66	-882.56	-703.73
biasws	0.535	0.474	0.4601	0.0707	-0.7803	-0.3042
RMS:	e014	g014	n014	g050	e300	se300
rmspwr	1154.18	1284.31	1278.488	1251.06	1453.433	1330.68
rmsws	2.60	2.84	2.83	2.44	2.464	2.39
COR:	e014	g014	n014	g050	e300	se300
corpwr	0.76	0.71	0.71	0.74	0.70	0.72
corws	0.80	0.75	0.76	0.80	0.79	0.79
SKEW:	e014	g014	n014	g050	e300	se300
pwrobs	0.5912	0.55	0.56	0.5648	0.5799	0.5799
pwr	0.8315	0.81	0.82	0.973	1.4028	1.2128
wsobs	1.0229	0.99	1.00	0.9776	1.0072	1.0072
ws	0.5546	0.48	0.49	0.6469	0.665	0.607
KURT:	e014	g014	n014	g050	e300	se300
pwrobs	-0.9791	-1.04	-1.03	-1.03	-1.0028	-1.0028
pwr	-0.671	-0.68	-0.67	-0.35	1.1287	0.4658
wsobs	1.546	1.35	1.38	1.336	1.4973	1.4973
ws	-0.1236	-0.42	-0.40	-0.09	0.087	-0.0436
P25:	e014	g014	n014	g050	e300	se300
pwrobs	371.5	385	385.7	379	373.75	373.75
pwr	44.43	38.69	38.47	33.16	13.225	27.835
wsobs	5.27	5.29	5.297	5.29	5.2775	5.2775
ws	5.33	5.26	5.24	5.09	4.62	4.9625
P50:	e014	g014	n014	g050	e300	se300
pwrobs	1324	1392	1383.5	1374	1342.5	1342.5
pwr	916.71	930.29	923.785	673.87	404.81	623.15
wsobs	7.24	7.32	7.315	7.31	7.26	7.26
ws	7.97	8.06	8.01	7.36	6.69	7.225
P75:	e014	g014	n014	g050	e300	se300
pwrobs	3109.75	3165	3163.5	3163	3133.25	3133.25
pwr	2655.88	2678.29	2664.1	2325.06	1630.655	1918.57
wsobs	10.02	10.18	10.18	10.18	10.0525	10.0525
ws	11.52	11.57	11.56	10.93	9.605	10.1775

Table D.2: Statistics for Bessybell

cases	888	3187	3130	3115	726	726
MEAN:	e014	g014	n014	g050	e300	se300
pwrobs	5422.65	5741.62	5737.29	5725.98	5572.47	5572.47
pwr	3276.72	4344.91	4339.20	4620.09	3295.39	3661.79
wsobs	7.8141	8.2226	8.2171	8.2167	7.9826	7.9826
ws	7.1777	7.8667	7.8604	7.9529	6.7303	7.0415
wd	93.726	103.482	103.18	103.25	80.166	78.436
VARIAB:	e014	g014	n014	g050	e300	se300
pwrobs	4515.04	4432.88	4432.22	4455.79	4606.81	4606.81
pwr	4299.49	4306.37	4312.83	4410.73	3893.03	4149.231
wsobs	3.381	3.452	3.448	3.489	3.484	3.484
ws	4.007	3.504	3.512	3.582	3.287	3.483
wd	64.332	83.244	83.41	84.75	71.457	71.707
MAX:	e014	g014	n014	g050	e300	se300
pwrobs	13194	13196	13196	13196	13194	13194
pwr	13200	13200	13200	13200	13184.86	13165.62
wsobs	18.36	22.67	22.67	22.67	18.36	18.36
ws	19.16	20.73	20.73	19.37	18.32	18.09
wd	259	270	270	270	266.31	266.22
MAE:	e014	g014	n014	g050	e300	se300
mae.pwr	3032.11	2141.07	2158.65	2208.79	2549.41	2348.235
mae.ws	2.1065	1.5087	1.505	1.6826	1.7118	1.5866
BIAS:	e014	g014	n014	g050	e300	se300
bias.pwr	-2214.69	-1365.32	-1396.56	-1128.86	-2263.54	-1898.982
bias.ws	-0.8183	-0.3567	-0.3585	-0.281	-1.25	-0.9492
RMS:	e014	g014	n014	g050	e300	se300
rms.pwr	4289.47	3007.49	3046.31	3107.42	3496.10	3243.085
rms.ws	2.54	1.9481	1.94	2.128	2.1403	2.0024
COR:	e014	g014	n014	g050	e300	se300
cor(p):	0.6509	0.8125	0.808	0.787	0.8162	0.8249
cor(w):	0.8018	0.849	0.849	0.8228	0.8712	0.8726
SKEW:	e014	g014	n014	g050	e300	se300
pwrobs	0.3087	0.3061	0.3056	0.3116	0.3009	0.3009
pwr	0.9963	0.6323	0.6347	0.5	0.931	0.8035
wsobs	0.4374	0.8254	0.8259	0.8146	0.4666	0.4666
ws	0.4321	0.5601	0.5575	0.4155	0.5609	0.5389
KURT:	e014	g014	n014	g050	e300	se300
pwrobs	-1.338	-1.317	-1.32	-1.320	-1.370	-1.3703
pwr	-0.5096	-1.0049	-1.00	-1.20	-0.40	-0.7414
wsobs	-0.2449	0.7685	0.77	0.71	-0.33	-0.3334
ws	-0.49	0.0106	0.00	-0.33	-0.25	-0.3788
P25:	e014	g014	n014	g050	e300	se300
pwrobs	911.5	1669	1665	1627	1068	1068
pwr	0	311.77	306.98	331.21	0	0
wsobs	5.095	5.73	5.73	5.7	5.31	5.31
ws	3.7975	5.14	5.14	5.09	3.9675	4.0725
P50:	e014	g014	n014	g050	e300	se300
pwrobs	4756	4916	4916.5	4883	4913	4913
pwr	531.6	2859.17	2828.85	3287.59	1227.12	1589.405
wsobs	7.56	7.6	7.6	7.59	7.62	7.62
ws	6.745	7.48	7.47	7.73	6.14	6.505
P75:	e014	g014	n014	g050	e300	se300
hline pwrobs	9590	9820	9817	9847	10025	10025
pwr	6770.42	8040.07	8040.20	8515.13	6334.74	7061.8325
wsobs	10.165	10.35	10.34	10.37	10.51	10.51
ws	10.175	10.1975	10.2	10.51	9.2	9.6

Table D.3: Statistics for Lendrum

cases	937	1386	1371	1392	943	943
MEAN:	e014	g014	n014	g050	e300	se300
pwrobs	2048.262	2433.27	2432.25	2423.30	2075.68	2075.683
pwr	1879.496	2470.00	2468.64	1964.22	1212.71	1424.456
wsobs	8.0451	8.4199	8.4066	8.4032	8.0928	8.0928
ws	8.0756	9.1127	9.1048	7.9749	6.4313	6.9141
wd	102.509	88.462	88.251	97.979	112.917	114.926
VARIAB:	e014	g014	n014	g050	e300	se300
pwrobs	2066.578	2179.36	2178.15	2179.21	2084.46	2084.468
pwr	2085.303	2284.06	2283.53	2076.21	1794.89	1909.957
wsobs	5.069	4.936	4.923	4.93	5.083	5.083
ws	4.479	5.343	5.329	4.05	3.482	3.753
wd	105.853	95.369	95.656	95.871	96.843	97.623
MAX:	e014	g014	n014	g050	e300	se300
pwrobs	5938	5939	5939	5939	5938	5938
pwr	5940	5940	5940	5940	5940	5940
wsobs	28.98	28.98	28.98	28.98	28.98	28.98
ws	24.63	27.56	27.56	23.6	21.67	20.81
wd	270	269.22	269.22	270	270	270
MAE:	e014	g014	n014	g050	e300	se300
mae.pwr	969.0259	1534.66	1533.39	1079.95	1251.67	1168.915
mae.ws	1.7917	3.374	3.3798	1.9003	2.2668	2.1088
BIAS:	e014	g014	n014	g050	e300	se300
bias.pwr	-124.474	82.9031	82.226	-407.92	-787.09	-580.2241
bias.ws	0.1715	0.8447	0.8497	-0.3173	-1.5356	-1.0427
RMS:	e014	g014	n014	g050	e300	se300
rms.pwr	1602.653	2196.45	2193.35	1635.12	1879.51	1803.145
rms.ws	2.5686	4.5058	4.5066	2.6253	3.2482	3.0209
CORREL:	e014	g014	n014	g050	e300	se300
cor(p):	0.711	0.5234	0.5241	0.7278	0.6317	0.6482
cor(w):	0.8639	0.6411	0.6388	0.8489	0.8358	0.8326
SKEW:	e014	g014	n014	g050	e300	se300
pwrobs	0.7802	0.4588	0.4597	0.4659	0.7602	0.7602
pwr	0.9093	0.3432	0.3437	0.7512	1.5231	1.312
wsobs	1.5943	1.2231	1.217	1.2294	1.5589	1.5589
ws	1.3279	0.9026	0.8993	0.9493	1.266	1.1857
KURT:	e014	g014	n014	g050	e300	se300
pwrobs	-0.8665	-1.3139	-1.3109	-1.308	-0.9121	-0.9121
pwr	-0.7003	-1.5021	-1.5032	-0.947	0.9444	0.3092
wsobs	2.8431	1.8157	1.7965	1.8318	2.7034	2.7034
ws	1.6168	0.57	0.5697	0.8032	1.4242	1.1526
P25:	e014	g014	n014	g050	e300	se300
pwrobs	281	362	359	358.5	281	281
pwr	162.08	159.555	160.43	158.13	0	0
wsobs	4.92	5.13	5.1175	5.125	4.935	4.935
ws	5.165	5.21	5.21	5.14	3.95	4.26
P50:	e014	g014	n014	g050	e300	se300
pwrobs	1273	1814	1817.5	1799	1285	1285
pwr	882.77	1772.22	1768.65	1010.21	252.96	473.37
wsobs	6.67	7.28	7.275	7.26	6.7	6.7
ws	6.8	8.1	8.1	7	5.47	5.97
P75:	e014	g014	n014	g050	e300	se300
pwrobs	3486	4666	4653.25	4638	3611.5	3611.5
pwr	3353.865	4798.52	4795.96	3643.71	1487.84	2042.93
wsobs	9.92	10.82	10.7875	10.795	10.02	10.02
ws	9.81	11.995	11.99	10.2	7.74	8.355

Table D.4: Statistics for Milane Hill

cases	1584	2587	2560	2515	1422	1422
MEAN:	e014	g014	n014	g050	e300	se300
pwrobs	5305.36	5462.79	5434.81	5505.62	5423.29	5423.298
pwr	5599.31	6732.83	6637.23	5526.37	3200.31	3797.667
wsobs	7.6975	7.6907	7.6749	7.7111	7.8743	7.8743
ws	8.9778	9.2888	9.2665	8.2316	6.4284	6.9343
dir.obs	217.633	208.359	208.20	208.71	217.83	217.836
wd	92.688	97.442	96.764	113.96	96.304	98.377
VARIAB:	e014	g014	n014	g050	e300	se300
pwrobs	4761.02	4962.52	4951.56	4988.96	4827.59	4827.595
pwr	5653.59	5813.73	5823.95	5369.93	4447.11	4844.119
wsobs	4.419	4.355	4.34	4.394	4.468	4.468
ws	4.449	4.975	4.976	3.911	3.288	3.576
dir.obs	9.175	14.205	14.198	14.243	9.452	9.452
wd	86.316	92.133	92.11	85.236	91.231	91.623
MAX:	e014	g014	n014	g050	e300	se300
pwrobs	14759	14780	14780	14780	14759	14759
pwr	15180	15180	15180	15180	15180	15180
wsobs	25.6	25.6	25.6	25.6	25.6	25.6
ws	24.31	27.58	27.58	22.64	20.99	20.28
dir.obs	248	248	248	248	248	248
wd	270	270	270	270	270	270
MAE:	e014	g014	n014	g050	e300	se300
mae.pwr	2620.39	4243.46	4234.10	2106.95	3018.03	2816.106
mae.ws	2.1421	3.9604	3.9577	2.0076	2.3768	2.2448
BIAS:	e014	g014	n014	g050	e300	se300
bias.pwr	293.950	1270.03	1202.42	20.753	-2222.98	-1625.631
bias.ws	1.1163	1.5943	1.5776	0.5205	-1.4459	-0.9372
RMS:	e014	g014	n014	g050	e300	se300
rms.pwr	3893.56	5701.37	5690.85	3123.60	4384.21	4137.582
rms.ws	2.8405	5.0054	5.0064	2.5713	3.2098	3.0032
CORREL:	e014	g014	n014	g050	e300	se300
cor(p):	0.7346	0.477	0.4765	0.8205	0.6706	0.6903
cor(w):	0.8285	0.4901	0.4889	0.8222	0.7677	0.77
SKEW:	e014	g014	n014	g050	e300	se300
pwrobs	0.5591	0.5148	0.5286	0.4966	0.5366	0.5366
pwr	0.5345	0.2094	0.2344	0.5357	1.3519	1.1328
wsobs	1.0252	0.8294	0.8334	0.8208	1.0559	1.0559
ws	0.7966	0.6748	0.6802	0.6748	1.0268	0.9658
KURT:	e014	g014	n014	g050	e300	se300
pwrobs	-1.0459	-1.1653	-1.1461	-1.1897	-1.1076	-1.1076
pwr	-1.3033	-1.5685	-1.5626	-1.2305	0.5363	-0.1288
wsobs	1.2973	0.7335	0.7527	0.6798	1.2394	1.2394
ws	0.2475	0.2593	0.2621	0.0477	0.7651	0.5477
P25:	e014	g014	n014	g050	e300	se300
pwrobs	864.75	764	769.5	745	963.25	963.25
pwr	173.337	719	606.012	411.66	0	0
wsobs	4.8	4.6	4.6	4.5	4.8	4.8
ws	5.63	5.58	5.5675	5.16	3.87	4.21
P50:	e014	g014	n014	g050	e300	se300
pwrobs	4058.5	4087	4062.5	4155	4132.5	4132.5
pwr	3310.97	5928.99	5500.65	3413.94	801.5	1280.385
wsobs	6.9	7	7.05	7.1	7	7
ws	8.12	8.7	8.66	7.51	5.615	6.03
P75:	e014	g014	n014	g050	e300	se300
pwrobs	9022.75	9779	9719.25	9922	9549.75	9549.75
pwr	10986.16	12742.64	12666.61	9969.2	5165.54	6346.7575
wsobs	9.9	10.2	10.2	10.2	10.1	10.1
ws	11.6475	12.275	12.26	10.62	8.345	8.84

Table D.5: Statistics for Tursillagh

Appendix E

Statistics of Multi-Scheme Experiment

The performance of the ensemble system has been evaluated by computing skill scores. The following tables are complementary to the statistics shown in Chapter 5, where only area and country averages were presented. These tables show the results of the individual 27 stations. Note, in the following tables, the first column ("ana") refers to the analysis, which takes the value 100% in the skill scores.

site	ana	winfc	mean	wmean	bg
eltra	0.16	26.81	13.71	19.83	9.60
multi	0.16	25.50	16.28	21.59	8.73
Abild	0.23	26.23	38.62	34.66	25.51
Broens	0.24	28.20	33.48	26.48	27.50
Draeby	0.25	44.28	26.03	33.65	5.85
Fjaldene	0.29	55.65	51.10	56.76	37.02
HanstholmHavn	0.37	-57.64	46.21	29.85	98.03
Hollandsbjaerg	0.26	41.17	28.34	34.18	28.66
Klim	0.27	30.79	26.70	28.77	7.59
Rejsby	0.36	50.47	45.23	43.66	46.62
Ryaa	0.25	55.61	27.10	33.25	-1.67
Sydthy	0.25	46.25	28.81	37.43	20.30
Torrild	0.48	33.79	8.14	14.37	-0.55
VedersoeKaer	0.28	34.44	43.01	40.50	13.26
dk	0.22	33.39	31.76	24.33	21.49
Aarhus	0.39	110.70	84.93	66.98	47.72
Fredrikshavn	0.31	49.35	19.48	28.16	5.63
Gedser	0.38	61.78	48.37	37.91	36.08
HvideSande	0.27	107.17	89.61	76.81	51.93
Jaegersborg	0.28	22.90	18.39	23.26	10.96
Skrydstrup	0.29	23.39	20.31	27.13	12.01
Taasinge	0.45	104.44	62.30	34.00	65.33
irl	0.24	39.88	28.54	20.55	20.91
Bessybel	0.35	81.76	22.15	21.37	7.42
Kilronan	0.30	2.55	-10.27	3.94	-6.98
Lendrum	0.26	9.30	-16.89	2.63	-55.46
Milane	0.34	80.47	50.32	42.33	38.92
Tursilla	0.34	50.12	44.76	36.07	27.66
ucc	0.21	39.72	30.06	26.20	3.27
Drinagh	0.20	54.88	50.36	44.15	42.47
Ringaski	0.26	49.29	40.18	25.97	25.82
Seefin	0.60	30.26	17.77	17.35	12.78
denmark	0.19	28.27	21.72	22.55	13.21
ireland	0.23	39.76	29.62	24.55	8.42

Table E.1: Results of the skill score with 50 ensemble members. The abbreviations are as follows: 'ana' is the analysis, 'winfc' is the winner of the period, 'mean' is the ensemble mean,'wmean' is the weighted mean, 'bg' is the best guess, 'ctrl' is the control forecast for the high resolution deterministic forecast 'dfc'

site	ana	winfc	mean	wmean	bg	wbg
eltra	0.16	13.67	14.12	20.91	11.12	12.10
multi	0.16	24.86	16.23	20.85	11.16	15.19
Abild	0.23	24.64	35.72	33.60	-18.08	32.11
Broens	0.24	28.36	40.55	25.67	-20.54	37.02
Draeby	0.25	43.22	12.61	34.27	-13.32	9.99
Fjaldene	0.29	54.52	51.19	55.68	41.90	49.67
HanstholmHavn	0.37	-43.96	53.29	33.21	81.97	60.83
Hollandsbjaerg	0.26	42.03	30.29	34.44	19.73	30.77
Klim	0.27	27.25	26.12	25.99	19.77	25.22
Rejsby	0.36	64.58	53.24	42.28	-1.90	53.29
Ryaa	0.25	56.64	16.64	34.82	-5.50	13.00
Sydthy	0.25	44.97	30.30	36.57	21.51	28.97
Torrild	0.49	32.66	13.48	13.50	11.90	14.75
VedersoeKaer	0.28	34.50	18.81	39.84	-5.51	16.32
dk	0.22	33.25	20.69	24.74	4.51	18.77
Aarhus	0.39	110.70	28.00	66.98	-29.86	15.91
Fredrikshavn	0.31	49.35	14.72	28.16	-6.47	16.62
Gedser	0.38	61.78	11.04	37.91	-12.56	7.96
HvideSande	0.27	109.25	35.47	78.41	-9.74	28.41
Jaegersborg	0.28	23.48	19.82	23.62	8.06	11.08
Skrydstrup	0.29	23.34	16.23	27.08	-2.19	13.04
Taasinge	0.45	104.20	67.80	33.97	62.12	68.83
irl	0.24	34.79	34.63	20.13	8.72	29.57
Bessybel	0.35	88.36	36.41	20.40	63.41	32.39
Kilronan	0.30	2.55	-36.81	3.94	-29.01	-54.97
Lendrum	0.26	10.47	-130.72	-29.89	-242.56	-158.54
Milane	0.34	80.47	30.52	42.33	5.08	26.65
Tursilla	0.33	50.02	42.82	35.95	9.06	39.51
ucc	0.21	37.12	24.78	26.55	5.18	22.23
Drinagh	0.20	54.88	40.67	44.15	21.01	40.00
Ringaski	0.26	49.29	36.46	25.97	3.27	35.95
Seefin	0.59	28.69	9.80	17.14	-7.48	8.42
denmark	0.19	27.81	17.80	22.22	8.82	16.45
ireland	0.23	36.46	27.59	24.71	6.20	24.33

Table E.2: Results of skill score with 100 ensemble members. The abbreviations are as follows: 'ana' is the analysis, 'winfc' is the winner of the period, 'mean' is the ensemble mean,'wmean' is the weighted mean, 'bg' is the best guess, 'ctrl' is the control forecast for the high resolution deterministic forecast 'dfc'

site	ana	winfc	mean	wmean	bg
eltra	0.42	38.39	6.81	19.96	1.09
multi	0.43	37.96	8.11	20.36	0.81
Abild	0.55	35.64	0.33	19.30	2.67
Broens	0.56	44.54	30.47	50.76	2.21
Draeby	0.69	46.84	20.24	32.74	1.30
Fjaldene	0.72	56.46	51.06	52.61	40.38
HanstholmHavn	0.94	-41.47	17.12	0.35	50.43
Hollandsbjaerg	0.69	30.76	-6.46	15.37	-0.80
Klim	0.72	40.79	32.61	33.33	18.19
Rejsby	0.96	154.71	150.35	120.32	129.96
Ryaa	0.67	42.64	-1.03	18.59	-8.54
Sydthy	0.64	5.38	-2.71	16.92	-35.53
Torrild	0.90	23.50	8.56	18.00	1.39
VedersoeKaer	0.82	75.14	60.70	50.36	45.71
dk	1.21	77.60	50.17	36.40	56.02
Aarhus	2.90	395.01	252.15	186.39	266.89
Fredrikshavn	1.04	43.79	10.70	28.04	12.93
Gedser	1.84	-199.54	-105.34	-33.13	-97.10
HvideSande	1.30	183.23	150.20	112.08	128.64
Jaegersborg	1.38	50.66	30.78	32.85	45.57
Skrydstrup	2.25	43.09	27.31	37.41	18.68
Taasinge	1.37	59.98	19.45	17.81	26.94
irl	0.66	60.88	24.33	18.58	5.91
Bessybel	0.56	52.11	32.96	18.44	-7.53
Kilronan	0.51	46.24	41.58	17.30	17.93
Lendrum	0.42	100.86	104.09	103.48	109.12
Milane	0.54	68.09	64.86	65.89	42.18
Tursilla	0.51	51.36	49.00	40.84	37.39
ucc	0.58	38.68	20.30	22.35	6.54
Drinagh	0.57	54.39	23.26	26.42	20.18
Ringaski	0.71	72.42	17.78	9.52	-14.50
Seefin	1.52	24.49	16.53	15.62	9.93
denmark	0.59	48.66	19.46	24.69	15.71
ireland	0.62	46.22	21.67	21.07	6.32
multi	0.43	37.96	8.11	20.36	0.81
dk	1.21	77.60	50.17	36.40	56.02
irl	0.66	60.88	24.33	18.58	5.91
ucc	0.58	38.68	20.30	22.35	6.54

Table E.3: Summary of skill scores with 50 ensemble members for wind power. The abbreviations are as follows: 'ana' is the analysis, 'winfc' is the winner of the period, 'mean' is the ensemble mean,'wmean' is the weighted mean, 'bg' is the best guess

site	ana	winfc	mean	wmean	bg	wbg
eltra	0.42	-9.51	3.79	19.18	0.00	-4.49
multi	0.43	37.33	4.92	19.57	-9.81	-7.57
Abild	0.56	34.77	2.50	18.26	-0.96	-21.99
Broens	0.56	43.23	39.65	49.28	-4.23	-4.55
Draeby	0.69	46.12	-2.71	33.26	-19.53	-18.29
Fjaldene	0.72	54.33	55.48	50.39	21.96	45.00
HanstholmHavn	0.94	-42.31	14.05	1.04	25.03	41.68
Hollandsbjaerg	0.69	30.47	-1.89	15.73	-8.49	-23.15
Klim	0.71	36.51	30.37	29.59	32.23	13.56
Rejsby	0.96	146.02	178.41	124.11	105.28	139.37
Ryaa	0.67	43.21	-12.28	19.83	-6.72	-45.76
Sydthy	0.64	6.89	-1.08	16.78	-18.71	-26.98
Torrild	0.90	24.07	7.05	18.09	8.18	-8.49
VedersoeKaer	0.83	75.35	47.60	50.17	21.00	25.07
dk	1.20	77.73	31.56	36.70	22.56	30.35
Aarhus	2.90	395.01	138.78	186.39	1.81	123.36
Fredrikshavn	1.04	43.79	-1.10	28.04	-5.91	-6.77
Gedser	1.84	-199.54	-6.26	-33.13	72.82	36.03
HvideSande	1.30	182.90	67.99	111.83	22.96	57.85
Jaegersborg	1.37	50.69	36.64	32.87	56.38	41.19
Skrydstrup	2.25	43.11	8.39	37.44	-11.99	1.31
Taasinge	1.37	60.82	32.41	17.82	28.84	35.92
irl	0.66	56.69	36.02	17.47	12.50	17.12
Bessybel	0.56	47.98	56.92	15.12	36.08	8.45
Kilronan	0.51	46.24	-6.23	17.30	-130.41	-169.69
Lendrum	0.42	98.87	105.05	102.22	113.65	110.67
Milane	0.54	68.09	46.59	65.89	6.88	-2.23
Tursilla	0.50	51.59	53.06	40.92	2.25	25.71
ucc	0.58	35.67	12.37	22.57	-10.32	2.80
Drinagh	0.57	54.39	15.35	26.42	-2.17	-14.76
Ringaski	0.71	72.42	17.18	9.52	-54.28	2.32
Seefin	1.51	24.72	11.86	16.04	-11.13	-7.30
denmark	0.59	48.23	12.11	24.19	-1.07	2.66
ireland	0.62	42.68	20.26	20.87	-2.71	7.57

Table E.4: Summary of the skill score with 100 ensemble members for wind power. The abbreviations are as follows: 'ana' is the analysis, 'winfc' is the winner of the period, 'mean' is the ensemble mean,'wmean' is the weighted mean, 'bg' is the best guess

site	ana	winfc	mean	wmean	bg
eltra	1.26	1.55	1.67	1.62	1.68
multi	1.29	1.62	1.75	1.70	1.78
Abild	2.12	2.38	2.65	2.58	2.65
Broens	1.98	2.24	2.27	2.26	2.27
Draeby	2.02	2.35	2.49	2.42	2.54
Fjaldene	2.28	2.45	2.48	2.45	2.52
HanstholmHavn	3.41	3.02	3.09	3.09	3.13
Hollandsbjaerg	2.33	2.80	3.05	2.97	3.05
Klim	2.20	2.37	2.41	2.39	2.49
Rejsby	3.49	3.33	3.40	3.46	3.41
Ryaa	2.10	2.66	2.78	2.70	2.87
Sydthy	2.20	2.76	2.88	2.80	2.94
Torrild	4.29	4.72	5.01	4.93	5.05
VedersoeKaer	3.71	3.73	3.40	3.47	3.44
dk	1.17	1.35	1.35	1.38	1.37
Aarhus	2.09	2.03	2.05	2.06	2.09
Fredrikshavn	1.95	2.31	2.41	2.37	2.43
Gedser	2.63	2.45	2.46	2.47	2.49
HvideSande	1.90	1.88	1.82	1.82	1.88
Jaegersborg	1.49	2.13	2.06	2.07	2.04
Skrydstrup	1.37	1.64	1.67	1.67	1.69
Taasinge	2.97	3.20	3.29	3.35	3.26
irl	1.88	2.06	2.20	2.19	2.25
Bessybel	3.06	3.10	3.44	3.41	3.50
Kilronan	2.71	3.12	3.06	3.00	3.08
Lendrum	2.07	2.20	2.33	2.27	2.38
Milane	3.40	3.73	3.99	3.97	4.03
Tursilla	2.75	3.16	3.29	3.31	3.41
ucc	1.84	2.32	2.58	2.55	2.74
Drinagh	2.30	3.09	3.29	3.23	3.39
Ringaski	2.65	3.00	3.29	3.26	3.33
Seefin	4.87	4.96	5.04	5.06	5.07
denmark	1.23	1.48	1.55	1.54	1.58
ireland	1.86	2.19	2.39	2.37	2.49

Table E.5: Summary of standard deviation with 50 ensemble members for wind speed. The abbreviations are as follows: 'ana' is the analysis, 'winfc' is the winner of the period, 'mean' is the ensemble mean,'wmean' is the weighted mean, 'bg' is the best guess

site	ana	winfc	mean	wmean	bg	wbg
eltra	1.25	1.66	1.66	1.61	0.00	1.67
multi	1.30	1.63	1.75	1.71	1.76	1.75
Abild	2.13	2.40	2.66	2.59	2.76	2.68
Broens	1.99	2.25	2.25	2.27	2.42	2.26
Draeby	2.01	2.35	2.52	2.42	2.57	2.54
Fjaldene	2.29	2.46	2.48	2.46	2.50	2.49
HanstholmHavn	3.43	3.03	3.11	3.11	3.13	3.11
Hollandsbjaerg	2.33	2.80	3.05	2.97	3.07	3.06
Klim	2.18	2.38	2.41	2.40	2.43	2.41
Rejsby	3.48	3.23	3.36	3.45	3.58	3.36
Ryaa	2.10	2.66	2.80	2.70	2.86	2.82
Sydthy	2.19	2.76	2.87	2.81	2.89	2.88
Torrild	4.31	4.74	5.00	4.95	5.01	5.01
VedersoeKaer	3.73	3.74	3.47	3.48	3.51	3.47
dk	1.18	1.35	1.38	1.38	1.41	1.38
Aarhus	2.09	2.03	2.11	2.06	2.17	2.12
Fredrikshavn	1.95	2.31	2.43	2.37	2.50	2.42
Gedser	2.63	2.45	2.54	2.47	2.60	2.55
HvideSande	1.89	1.87	1.89	1.82	1.95	1.90
Jaegersborg	1.50	2.13	2.06	2.07	2.04	2.10
Skrydstrup	1.37	1.64	1.68	1.67	1.72	1.69
Taasinge	2.97	3.19	3.27	3.34	3.29	3.27
irl	1.88	2.07	2.19	2.18	2.24	2.21
Bessybel	3.06	3.14	3.40	3.42	3.34	3.43
Kilronan	2.71	3.12	3.11	3.00	3.12	3.15
Lendrum	2.08	2.15	2.34	2.24	2.43	2.37
Milane	3.40	3.73	4.03	3.97	4.12	4.05
Tursilla	2.75	3.16	3.31	3.31	3.53	3.34
ucc	1.83	2.31	2.58	2.52	2.68	2.61
Drinagh	2.30	3.09	3.35	3.23	3.53	3.37
Ringaski	2.65	3.00	3.31	3.26	3.42	3.33
Seefin	4.84	4.95	5.05	5.04	5.13	5.05
denmark	1.24	1.49	1.56	1.54	1.59	1.57
ireland	1.85	2.19	2.38	2.35	2.46	2.41

Table E.6: Summary of standard deviation with 100 ensemble members for wind speed. The abbreviations are as follows: 'ana' is the analysis, 'winfc' is the winner of the period, 'mean' is the ensemble mean,'wmean' is the weighted mean, 'bg' is the best guess, 'wbg' is the weighted best guess

site	ana	winfc	mean	wmean	bg
eltra	1.05	1.32	1.53	1.43	1.55
multi	1.07	1.37	1.59	1.48	1.61
Abild	1.56	1.80	2.10	1.95	2.06
Broens	1.63	1.75	1.84	1.75	1.88
Draeby	1.73	1.96	2.13	2.03	2.17
Fjaldene	1.83	1.96	1.99	1.96	2.01
HanstholmHavn	2.92	2.53	2.60	2.61	2.66
Hollandsbjaerg	1.82	2.22	2.45	2.29	2.41
Klim	1.90	2.05	2.09	2.07	2.15
Rejsby	3.01	2.70	2.76	2.86	2.80
Ryaa	1.78	2.19	2.38	2.24	2.38
Sydthy	1.97	2.37	2.55	2.42	2.64
Torrild	2.12	2.53	2.70	2.59	2.72
VedersoeKaer	3.36	3.02	3.18	3.32	3.23
dk	0.75	0.80	0.85	0.88	0.83
Aarhus	1.61	1.44	1.50	1.52	1.51
Fredrikshavn	1.47	1.77	1.90	1.83	1.86
Gedser	2.31	1.95	2.01	2.05	2.03
HvideSande	1.66	1.56	1.55	1.58	1.60
Jaegersborg	0.40	0.70	0.80	0.79	0.72
Skrydstrup	0.89	0.97	1.00	0.98	1.02
Taasinge	1.13	1.29	1.44	1.46	1.40
irl	1.70	1.84	2.08	2.05	2.14
Bessybel	1215.67	1308.85	1315.70	1300.67	1352.07
Kilronan	1094.92	1198.77	1195.72	1157.01	1203.24
Lendrum	2863.23	2873.65	3234.31	3072.44	3379.94
Milane	2045.98	2219.15	2248.78	2213.10	2311.28
Tursilla	4089.59	5005.18	4914.70	4838.14	5014.18
ucc	1.68	2.12	2.37	2.31	2.45
Drinagh	1.90	2.38	2.73	2.64	2.74
Ringaski	2.11	2.31	2.54	2.50	2.61
Seefin	3.86	4.01	3.99	4.02	4.02
denmark	0.91	1.08	1.22	1.18	1.22
ireland	1.69	1.98	2.22	2.18	2.30

Table E.7: Summary of standard deviation with 50 ensemble members for wind power. The abbreviations are as follows: 'ana' is the analysis, 'winfc' is the winner of the period, 'mean' is the ensemble mean,'wmean' is the weighted mean, 'bg' is the best guess

site	ana	winfc	mean	wmean	bg	wbg
eltra	1.06	1.60	1.55	1.44	0.00	1.57
multi	1.07	1.37	1.60	1.49	1.65	1.65
Abild	1.57	1.81	2.10	1.95	2.04	2.15
Broens	1.63	1.75	1.82	1.76	1.87	1.89
Draeby	1.73	1.97	2.21	2.03	2.22	2.25
Fjaldene	1.83	1.96	1.98	1.97	2.05	2.00
HanstholmHavn	2.94	2.54	2.61	2.63	2.64	2.67
Hollandsbjaerg	1.83	2.23	2.45	2.29	2.42	2.51
Klim	1.87	2.05	2.09	2.07	2.07	2.15
Rejsby	2.98	2.70	2.71	2.84	2.83	2.77
Ryaa	1.79	2.19	2.42	2.24	2.38	2.49
Sydthy	1.97	2.37	2.55	2.43	2.56	2.60
Torrild	2.13	2.53	2.72	2.60	2.68	2.77
VedersoeKaer	3.37	3.03	3.21	3.31	3.32	3.28
dk	0.76	0.80	0.89	0.88	0.90	0.88
Aarhus	1.61	1.44	1.54	1.52	1.62	1.56
Fredrikshavn	1.47	1.77	1.95	1.83	1.95	1.95
Gedser	2.31	1.95	2.07	2.05	2.16	2.12
HvideSande	1.66	1.56	1.63	1.58	1.70	1.66
Jaegersborg	0.40	0.70	0.78	0.80	0.66	0.75
Skrydstrup	0.89	0.97	1.04	0.98	1.08	1.05
Taasinge	1.14	1.28	1.41	1.46	1.39	1.37
irl	1.69	1.83	2.02	2.02	2.06	2.05
Bessybel	1212.03	1310.31	1298.12	1302.31	1323.82	1333.60
Kilronan	1094.92	1198.77	1209.63	1157.01	1242.72	1238.61
Lendrum	2839.71	2804.69	3236.67	3024.40	3488.95	3405.12
Milane	2045.98	2219.15	2244.81	2213.10	2330.93	2336.43
Tursilla	4095.50	5012.41	4902.61	4845.13	5310.45	5112.87
ucc	1.66	2.10	2.37	2.26	2.47	2.41
Drinagh	1.90	2.38	2.80	2.64	2.93	2.94
Ringaski	2.11	2.31	2.55	2.50	2.69	2.56
Seefin	3.84	3.99	3.99	4.00	4.08	4.06
denmark	0.91	1.09	1.25	1.18	1.27	1.27
ireland	1.68	1.97	2.19	2.14	2.27	2.23

Table E.8: Summary of standard deviation with 100 ensemble members for wind power. The abbreviations are as follows: 'ana' is the analysis, 'winfc' is the winner of the period, 'mean' is the ensemble mean,'wmean' is the weighted mean, 'bg' is the best guess

site	obs	ana1	winfc	mean	wmean	bg
eltra	3.74	3.49	3.61	3.71	3.68	3.70
multi	3.72	3.48	3.60	3.70	3.66	3.70
Abild	3.76	3.51	3.54	3.61	3.61	3.60
Broens	3.73	3.65	3.87	3.75	3.73	3.74
Draeby	3.67	3.46	3.58	3.60	3.59	3.59
Fjaldene	3.66	3.44	3.49	3.54	3.51	3.52
HanstholmHavn	3.80	3.67	3.92	3.87	3.84	3.82
Hollandsbjaerg	3.79	3.52	3.64	3.75	3.73	3.72
Klim	3.89	3.58	4.00	3.87	3.86	3.91
Rejsby	3.83	3.61	3.94	3.71	3.69	3.71
Ryaa	3.94	3.61	3.93	3.94	3.91	3.93
Sydthy	4.07	3.77	4.00	4.02	4.00	3.96
Torrild	3.61	3.32	3.49	3.51	3.49	3.52
VedersoeKaer	3.89	3.70	3.69	3.79	3.76	3.76
dk	2.59	2.38	2.56	2.52	2.54	2.49
Aarhus	2.41	2.19	2.34	2.32	2.35	2.26
Fredrikshavn	3.19	3.12	3.15	3.20	3.22	3.16
Gedser	3.04	2.81	3.10	2.96	2.97	2.96
HvideSande	2.81	2.65	2.67	2.70	2.71	2.65
Jaegersborg	2.28	1.97	2.20	2.18	2.20	2.14
Skrydstrup	2.41	2.09	2.44	2.28	2.31	2.25
Taasinge	2.57	2.48	2.38	2.49	2.53	2.46
irl	3.94	3.69	3.51	3.78	3.79	3.82
Bessybel	4.25	3.97	3.98	4.07	4.06	4.11
Kilronan	3.97	3.90	3.73	3.81	3.80	3.85
Lendrum	3.95	3.76	3.74	3.78	3.76	3.75
Milane	5.04	4.40	4.50	4.70	4.71	4.69
Tursilla	4.29	3.84	3.94	3.99	4.02	4.05
ucc	4.34	3.91	3.93	4.07	4.08	4.21
Drinagh	4.73	4.07	4.20	4.35	4.38	4.40
Ringaski	4.42	4.04	4.08	4.18	4.19	4.24
Seefin	4.17	3.76	3.93	3.89	3.91	3.96
denmark	3.16	2.93	3.08	3.11	3.10	3.10
ireland	4.14	3.80	3.72	3.93	3.93	4.02

Table E.9: Summary of variance with 50 ensemble members for wind speed. The abbreviations are as follows: 'ana' is the analysis, 'winfc' is the winner of the period, 'mean' is the ensemble mean,'wmean' is the weighted mean, 'bg' is the best guess, 'wbg' is the weighted best guess

site	obs	ana	winfc	mean	wmean	bg	wbg
eltra	3.72	3.49	3.69	3.68	3.66	0.00	3.63
multi	3.74	3.50	3.61	3.70	3.68	3.66	3.71
Abild	3.78	3.53	3.56	3.57	3.63	3.50	3.58
Broens	3.87	3.66	3.89	3.71	3.75	3.62	3.72
Draeby	3.69	3.47	3.60	3.56	3.61	3.55	3.57
Fjaldene	3.68	3.45	3.51	3.55	3.53	3.52	3.57
HanstholmHavn	4.03	3.69	3.94	3.87	3.85	3.77	3.87
Hollandsbjaerg	3.81	3.54	3.65	3.76	3.74	3.71	3.78
Klim	3.91	3.59	4.02	3.87	3.88	3.87	3.88
Rejsby	3.84	3.61	4.02	3.65	3.70	3.58	3.66
Ryaa	3.95	3.62	3.95	3.95	3.93	3.95	3.96
Sydthy	4.10	3.78	4.02	4.01	4.02	3.96	4.01
Torrild	3.63	3.34	3.51	3.50	3.51	3.48	3.51
VedersoeKaer	3.91	3.71	3.70	3.81	3.78	3.78	3.82
dk	2.60	2.39	2.58	2.50	2.55	2.50	2.49
Aarhus	2.41	2.19	2.34	2.31	2.35	2.27	2.31
Fredrikshavn	3.19	3.12	3.15	3.17	3.22	3.20	3.16
Gedser	3.04	2.81	3.10	2.86	2.97	2.79	2.85
HvideSande	2.80	2.64	2.66	2.69	2.69	2.64	2.68
Jaegersborg	2.28	1.97	2.20	2.14	2.19	2.07	2.14
Skrydstrup	2.41	2.08	2.44	2.25	2.31	2.21	2.25
Taasinge	2.57	2.48	2.39	2.42	2.53	2.39	2.41
irl	3.93	3.70	3.52	3.65	3.79	3.71	3.66
Bessybel	4.25	3.98	3.95	3.94	4.07	3.92	3.94
Kilronan	3.97	3.90	3.73	3.69	3.80	3.73	3.70
Lendrum	3.96	3.78	3.74	3.76	3.77	3.74	3.78
Milane	5.04	4.40	4.50	4.60	4.71	4.65	4.60
Tursilla	4.29	3.84	3.93	3.85	4.01	3.90	3.83
ucc	4.34	3.92	3.94	3.98	4.08	4.06	3.98
Drinagh	4.73	4.07	4.20	4.22	4.38	4.23	4.22
Ringaski	4.42	4.04	4.08	4.10	4.19	4.13	4.10
Seefin	4.17	3.75	3.93	3.78	3.91	3.80	3.79
denmark	3.17	2.94	3.10	3.10	3.12	0.00	3.10
ireland	4.13	3.81	3.73	3.82	3.93	0.00	3.82

Table E.10: Summary of variance with 100 ensemble members for wind speed. The abbreviations are as follows: 'ana' is the analysis, 'winfc' is the winner of the period, 'mean' is the ensemble mean,'wmean' is the weighted mean, 'bg' is the best guess, 'wbg' is the weighted best guess

site	obs	ana1	winfc	mean	wmean	bg
eltra	3.16	2.90	3.06	3.18	3.12	3.21
multi	3.16	2.89	3.04	3.17	3.11	3.21
Abild	3.25	3.01	3.03	3.19	3.13	3.20
Broens	3.35	3.15	3.27	3.30	3.24	3.33
Draeby	3.18	2.97	3.08	3.13	3.08	3.15
Fjaldene	3.07	2.90	3.08	3.07	3.02	3.05
HanstholmHavn	3.28	3.11	3.35	3.33	3.27	3.34
Hollandsbjaerg	3.15	2.96	3.12	3.17	3.13	3.17
Klim	3.31	2.90	3.31	3.31	3.27	3.36
Rejsby	3.31	3.12	3.38	3.26	3.21	3.29
Ryaa	3.32	2.97	3.31	3.34	3.31	3.34
Sydthy	3.46	3.14	3.39	3.43	3.39	3.46
Torrild	3.04	2.80	2.93	3.02	2.97	3.07
VedersoeKaer	3.31	3.19	3.42	3.30	3.24	3.30
dk	1.49	1.10	1.34	1.43	1.44	1.37
Aarhus	1.33	0.93	1.19	1.23	1.28	1.13
Fredrikshavn	2.23	1.99	2.23	2.29	2.26	2.22
Gedser	2.27	1.80	2.29	2.21	2.19	2.17
HvideSande	1.95	1.60	1.71	1.84	1.87	1.78
Jaegersborg	1.11	0.64	0.92	1.03	1.02	0.92
Skrydstrup	1.18	0.74	1.20	1.06	1.08	1.03
Taasinge	1.60	1.31	1.44	1.58	1.58	1.51
irl	3.35	3.05	3.00	3.24	3.22	3.31
Bessybel	3.66	3.59	3.61	3.53	3.56	3.60
Kilronan	3.52	3.50	3.47	3.39	3.41	3.46
Lendrum	3.95	3.93	3.88	3.76	3.84	3.80
Milane	3.74	3.70	3.58	3.49	3.55	3.57
Tursilla	3.74	3.67	3.67	3.55	3.63	3.60
ucc	3.59	3.22	3.40	3.43	3.44	3.50
Drinagh	3.63	3.28	3.49	3.49	3.48	3.52
Ringaski	3.60	3.31	3.40	3.47	3.49	3.53
Seefin	3.45	3.04	3.19	3.29	3.30	3.36
denmark	2.32	1.99	2.19	2.30	2.28	2.29
ireland	3.47	3.14	3.20	3.33	3.33	3.41

Table E.11: Summary of variance with 50 ensemble members for wind power. The abbreviations are as follows: 'ana' is the analysis, 'winfc' is the winner of the period, 'mean' is the ensemble mean,'wmean' is the weighted mean, 'bg' is the best guess

site	obs	ana1	winfc	mean	wmean	bg	wbg
eltra	3.18	2.92	3.27	3.18	3.14	0.00	3.19
multi	3.17	2.90	3.06	3.17	3.13	3.18	3.26
Abild	3.27	3.03	3.05	3.16	3.15	3.11	3.27
Broens	3.37	3.17	3.29	3.26	3.26	3.22	3.37
Draeby	3.20	2.99	3.09	3.10	3.10	3.10	3.22
Fjaldene	3.09	2.91	3.09	3.06	3.03	3.10	3.17
HanstholmHavn	3.37	3.12	3.36	3.32	3.28	3.33	3.43
Hollandsbjaerg	3.16	2.98	3.14	3.17	3.14	3.17	3.27
Klim	3.32	2.91	3.32	3.30	3.29	3.30	3.42
Rejsby	3.33	3.13	3.34	3.23	3.23	3.22	3.35
Ryaa	3.33	2.98	3.32	3.33	3.32	3.32	3.44
Sydthy	3.47	3.15	3.41	3.42	3.40	3.44	3.55
Torrild	3.05	2.81	2.95	3.01	2.99	3.02	3.13
VedersoeKaer	3.33	3.21	3.42	3.28	3.25	3.32	3.40
dk	1.50	1.10	1.35	1.42	1.45	1.41	1.41
Aarhus	1.33	0.93	1.19	1.23	1.28	1.14	1.20
Fredrikshavn	2.23	1.99	2.23	2.29	2.26	2.29	2.31
Gedser	2.27	1.80	2.29	2.15	2.19	2.07	2.16
HvideSande	1.96	1.60	1.71	1.86	1.87	1.79	1.85
Jaegersborg	1.11	0.64	0.93	1.00	1.02	0.87	0.97
Skrydstrup	1.18	0.74	1.20	1.05	1.08	1.03	1.03
Taasinge	1.60	1.31	1.33	1.51	1.58	1.47	1.49
irl	3.35	3.06	3.01	3.13	3.22	3.19	3.22
Bessybel	3.66	3.59	3.61	3.41	3.56	3.53	3.55
Kilronan	3.52	3.50	3.47	3.28	3.41	3.44	3.42
Lendrum	3.95	3.94	3.88	3.68	3.84	3.79	3.84
Milane	3.74	3.70	3.58	3.39	3.55	3.55	3.66
Tursilla	3.74	3.67	3.66	3.43	3.63	3.59	3.62
ucc	3.57	3.22	3.40	3.33	3.42	3.47	3.47
Drinagh	3.63	3.28	3.49	3.40	3.48	3.53	3.60
Ringaski	3.60	3.31	3.40	3.38	3.49	3.49	3.51
Seefin	3.45	3.04	3.19	3.20	3.30	3.27	3.31
denmark	2.34	2.00	2.20	2.30	2.29	0.00	2.34
ireland	3.46	3.14	3.20	3.23	3.32	0.00	3.34

Table E.12: Summary of variance with 100 ensemble members for wind power. The abbreviations are as follows: 'ana' is the analysis, 'winfc' is the winner of the period, 'mean' is the ensemble mean,'wmean' is the weighted mean, 'bg' is the best guess

Appendix F

Glossary

F.1 Symbols

Symbol		Unit
g	gravity	m/s^2
dZ	Gradient of the geopotential	m
E	Energy Output	J
F	Forecast Error (unit is dependent on the paramter)	-
p	Pressure	Pa
U	Uncertainty Estimate of a Forecast	-
u	velocity	m/s
R	Universal Gas constant (287)	J/kgK
T	Temerature	K
η	general pressure based and terrain following vertical coordinate system	-
ϕ	geopotential height	m^2/s^2
λ	Longitudinal axis in the spherical coordinate system	rad
ρ	density	kg/m^3
θ	Latitudinal axis in the spherical coordinate system	rad
v_c	Phase speed of the fastest propagating perturbation	m/s

F.2 Abbreviations

Abbreviation	Explanation
CFL	Courant, Friedrichs, and Lewy criterion
3DVAR	Three-Dimensional Variational Data Assimilation
4DVAR	Four-Dimensional Variational Data Assimilation
DMI	Danish Meteorological Institute
ECMWF	European Center for Medium range Weather Forecasting
EPS	Ensemble Prediction System
GTS	Global Telecommunication System, a global onetwork for atmspheric data
GLCC,	The Global Land Characteristics Data Base. U.S. Geological Survey
GTOPO30	Global 30 Arc Second Elevation data Set. U.S. Geological Survey
HIRLAM	High Resolution Limited Area Model
mae	mean absolut error
mslp	mean sea level pressure
NOAA	National Oceanic And Atmospheric Administration
NWP	Numerical Weather Prediciton
OI	Optimal Interpolation
pdf	Probability density function
pmt	probabilistic multi-trend filter
rms	root mean square error
ss	skill scores - verification method used for ensemble predictions
stdev	Strandard Deviation
TSO	Transmission System Operator
UCC	University College Cork
UTC	Universal Time Coordinated
var	Variance

F.3 Glossary of Meteorological Terms

Most of the following terms are from the electronic version of the American Meteorological Society's Meteorological Glossary, which is a copy of the second edition of the Glossary (http://amsglossary.allenpress.com/glossary).

Adiabatic process: deals with the changing temperature of a parcel of air due to the air rising or sinking. An adiabatic process assumes no heat, mass or momentum pass across the air parcel boundary.

Analysis: is the production of an accurate image of the true state of the atmosphere at a given time, represented by a collection of numbers, usually on regular model grids. Objective analysis is an automated procedure for performing such analysis versus subjective, hand analysis. See also Data Assimilation.

CFL criterion: The three mathematicians named Courant, Friedrichs, and Lewy created a criterion which imposes a restriction on the size of the integration time step based on the reciprocal of the smallest spatial step. Because of the CFL criterion, a modeller cannot arbitrarily choose a horizontal grid spacing without also taking into account the time step of the model.

Cyclogenisis: Process of initiation or intensification of a cyclonic circulation in the atmosphere; the opposite to cyclolysis.

Cyclolysis: Process of weakening or terminating of a cyclonic circulation in the atmosphere;the opposite of cyclogenesis.

Cyclonic circulation: Atmospheric circulation associated with a cyclone (depression, low pressure area). It is counterclockwise in the Northern Hemisphere and clockwise in the Southern Hemisphere.

Data Assimilation: Data assimilation is an analysis technique in which the observed information is accumulated into the model state by taking advantage of consistency constraints with laws of time evolution and physical properties. It is the

process of combining observations and short- range forecasts to obtain an initial condition for NWP. The purpose of data assimilation is to determine as accurately as possible the state of the atmospheric flow by using all the available information.

Diabatic process: Process where any temperature change of air is not related to an air parcels adiabatic vertical displacement. The prime contributor to diabatic heating is the sun.

First Guess: The use of short-range forecasts as a first guess has been universally adopted in operational systems into what is called an "analysis cycle". Initially climatology, or a combination of climatology and a short forecast were used as a first guess. The first guess or background field is our best estimate of the state of the atmosphere prior to the use of the observations.

Forecast: is a scientific predictions about future states of the atmpsphere made with a numerical model or method. A forecast incorporates meteorological, oceanographic, and/or river flow rate forecasts; makes predictions for locations where observational data will not be available; and is usually initialized by the results of a nowcast. see also *Numerical Forecasting*.

Front: In meteorology, generally, the interface or transition zone between two air masses of different density.

Frontal System: The orientation and nature of the fronts within the circulation of a frontal cyclone (cyclonic circulation).

Hindcast: is a scientific predictions about past states of the atmpsphere made with a numerical model or method. These predictions rely on either observed or forecast data, not on hypothetical data. A hindcast incorporates past or historical observational data.

Hydrostatic Approximation: An approximation in geophysical fluid dynamics that is based on the assumption that the horizontal scale is large compared to the

vertical scale, such that the vertical pressure gradient may be given as the product of density times the gravitational acceleration.

Initial Conditions: Initial conditions in a global model are prepared by making a synthesis of observed values of atmospheric fields taken over a for example 24 hour period and short-range forecasts provided by the global model itself. This synthesis is a process of assimilating observed values into a model. The use of both observations and model forecasts in the construction of initial values is required. High quality data are sparsely and irregularly distributed over the globe. Short-range model forecasts carry knowledge forward in time of earlier observations and also provide a crucial background for extracting useful information from expensive satellite observations.

Isopleth: An isopleth is a line of equal value (a Greek word iso - equal; pleth - value). A weather map contains isopleths of different weather parameters.

Isobar: Isopleth of Pressure

Isotherm: Isopleth of Temperature

Isotach: Isopleth of Wind Speed

Jet Stream: A jet stream is a narrow stream of relatively strong winds. The existence of the polar front jet streams is tied to the presence of horizontal temperature gradients. If temperature gradients exist through a deep layer of the troposphere, a pressure gradient force increases with height throughout the layer, and so does the wind.

Mesosphere: The mesosphere starts just above the stratosphere and extends to 85 kilometers (53 miles) high. In this region, the temperatures again fall as low as -93 degrees Celsius as you increase in altitude. The chemicals are in an excited state, as they absorb energy from the Sun. The mesopause separates the mesophere from the thermosphere.

Nowcast: is a scientific predictions about the present states of the atmpsphere made with a numerical model or method. A nowcast incorporates recent (and often near real-time) observed meteorological, oceanographic, and/or river flow rate data; covers the period of time from the recent past (up to a few days) to the present; and makes predictions for locations where observational data are not available. The present is the time at which the nowcast is made, and at which the most recent observations are from a few minutes to an hour old.

Numerical Weather Prediction: NWP is an initial- boundary value problem: given an estimate of the present state of the atmosphere (initial conditions), and appropriate surface and lateral boundary conditions, the model simulates (forecasts) the atmospheric evolution.

Numerical Integration: A solution of the governing equations of hydrodynamics by numerical methods. The numerical solutions are carried out with the aid of computers ranging from desktop workstations to the most powerful computers available.

Numerical Forecasting: (Also called mathematical forecasting, dynamical forecasting, physical forecasting, numerical weather prediction.) The integration of the governing equations of hydrodynamics by numerical methods subject to specified initial conditions. Numerical approximations are fundamental to almost all dynamical weather prediction schemes since the complexity and nonlinearity of the hydrodynamic equations do not allow exact solutions of the continuous equations.

Mesoscale: Pertaining to atmospheric phenomena having horizontal scales ranging from a few to several hundred kilometers. From a dynamical perspective, this term pertains to processes encompassing deep moist convection and the full spectrum of inertio-gravity waves but stopping short of synoptic-scale phenomena, which have Rossby numbers less than 1.

Parameterisation: The representation of physical effects in a dynamic model in terms

of simplified parameters, which represent a series of simplifications of the full turbulence model to remove complex terms and form a closed set of equations that lead to a hierarchy of so-called closure models of decreasing complexity.

Primitive Equations: The Eulerian equations of motion of a fluid in which the primary dependent variables are the fluid's velocity components. These equations govern a wide variety of fluid motions and form the basis of most hydrodynamical analysis. In meteorology, these equations are frequently specialized to apply directly to the cyclonic-scale motions.

Spherical coordinates: A system of curvilinear coordinates which is natural for describing positions on a sphere or spheroid.

Stratosphere: The stratosphere starts just above the troposphere and extends to 50 kilometers (31 miles) high. Compared to the troposphere, this part of the atmosphere is dry and less dense. The stratopause separates the stratosphere from the next layer.

Synoptic Scale: Used with respect to weather systems ranging in size from several hundred kilometers to several thousand kilometers, the scale of migratory high and low pressure systems (frontal cyclones) of the lower troposphere.

Thermosphere: The thermosphere starts just above the mesosphere and extends to 600 kilometers (372 miles) height. The temperatures go up with increasing altitude due to the Sun's energy. This layer is known as the upper atmosphere.

Troposphere: The troposphere starts at the Earth's surface and extends 8 to 14.5 kilometers high (5 to 9 miles). This part of the atmosphere is the most dense. Almost all weather is in this region. The tropopause separates the troposphere from the next layer. The tropopause and the troposphere are known as the lower atmosphere.